

Haptic Sensory Feedback for Improved Interface to Smart Prosthetics

by

Jeremy DeLaine Brown

A dissertation submitted in partial fulfillment
of the requirements for the degree of
Doctor of Philosophy
(Mechanical Engineering)
in The University of Michigan
2014

Doctoral Committee:

Associate Professor R. Brent Gillespie, Chair
Assistant Professor Cynthia Chestek
Certified Orthotist and Prosthetist Sr Alicia Davis, UMH Orthotics and
Prosthetics Center
Professor Arthur D. Kuo

© Jeremy DeLaine Brown 2014

All Rights Reserved

This dissertation is dedicated to my great uncle, the Reverend Joseph Armstrong DeLaine, whose tireless efforts in the fight for educational equality helped bring about the Brown v. Board of Education decision that has afforded me the opportunity to pursue this prestigious degree.

ACKNOWLEDGEMENTS

I am honored and humbled to have the opportunity to thank those who have made this dissertation possible.

I would like to first thank my committee for all their guidance and advice in this process. Brent, thanks for being willing to take a bet on me and always pushing me to stretch and grow as a scholar. Thank you also for instilling trust in me as a leader in our lab group and standing behind me whenever things got rough during this process. I have been able to get to know you as well as your family over these years, and I am truly fortunate for both. I can say, without a doubt, that you are one of the best advisors walking the halls of any university.

Art, thank for you for showing me that the really cool engineering goes on in the research laboratory. Although I probably aggravated you to no end, you welcomed me into your research group during my undergraduate years here and helped develop a passion for discovery and understanding that burns strong to this very day. Thank you for supporting me and the work I have done throughout this process, as well as challenging me to develop an appreciation for the science.

Alicia, thank you for being so willing to help connect me to the prosthetics community. Your wisdom and insight have helped me see what the true reason for my graduate school toils have been. Thank you for all you have done in helping me carry out my various experiments and being willing to serve on my committee.

Cindy, I really appreciate the conversations we have had over the last few years about both my dissertation as well as the career path I want to pursue. Your insight has been very helpful, and I hope to be able to lean on you as I continue to pursue an academic career.

I would also like to thank my collaborators at Rice University, The University of Houston, and Drexel University for all their hard work on our collaborative NSF project. It has been great working with each and every one of you, and I hope that we can continue to build on the work already done.

I would like to thank my fellow HaptiX lab mates for all their continued support through the years, both inside the lab and out. You have been a constant source of

encouragement and support and have provided the comic relief needed to make this journey that much easier. Thank you also to the members of the Neuromechanics Group for your advice on ways to enhance my scholarship.

Thank you to all of my research assistants. This work would not be possible without your help. Thank you especially to Mackenzie Shelley, Duane Gardner, and Timothy Kunz for all the work you put in during this last year. I am still amazed as to what we were able to accomplish in such a short period of time.

Thank you to all of my various mentors. Dr. Rockward, thank you for being the first person to tell me I had what it takes to pursue a PhD and inviting me into your research lab. Dr. Gallimore, thank you for all the work you did in helping me get into graduate school and all of the advice you have given me along the way. Dr. Thompson, thank you as well of all the help along way, including being willing to provide support for me to do research both in China and after finishing my undergraduate education.

Thank you to all the support staff. Debby Mitchell, Sharon Burch, and Elaine Dowell, each of you holds a special place in my heart. Thank you for all that you have done over the years to help make this journey easier.

Thank you to all of my financial supporters including the National Science Foundation, Rackham Graduate School, and the Alliance for Graduate Education and the Professoriate (AGEP). You have provided me with the financial freedom to pursue the research that I am truly passionate about, without the worry of how I am going to make a living. In addition to financials, I have gained much more from the communities that each of these organizations helped establish. Graduate school can sometimes be an isolating experience and having these communities has helped to alleviate that as much as possible.

Thank you to all of the friends and colleagues I have made along the way. Being able to step away from the work and just have fun has provided the balance I have needed. Thank you especially to Mike, Gbenga, Davin, and Brandon for encouraging me in the last year to keep pressing forward. Thank you also to Brian Burt for checking in on me to make sure I'm still moving forward. I look forward to maintaining our friendship as we each finish this journey and move on to the next stages of our lives.

Thank you to my family, through both blood and by marriage. Not a day has gone by where I doubt your support of me in this journey. Mah and Dad, thanks for encouraging me to pursue those things which truly bring me happiness and championing me along the way. Thanks for picking up when I've been knocked down and continually encouraging me to press ahead. Grandma, you are truly an inspiration to

me. The love you have for me and this family is without compare. Thank you for all the valuable life lessons along the way and always reminding me of the giants whose shoulders I stand upon. To Momma Reid, Daddy Reid, Pam, Paula, Gary, Big Jules, Little Jules, and Reid, thank you for welcoming me into your family with open arms and showing me that 'in-law' has no bearing on the love you share. Thank you to my church family across the country for showing me that this journey is a part of God's plan, and that I have to stay the course and continue to trust Him to finish it.

Finally, thank you to my wife, partner, other half, and best friend Ashley. Words alone cannot describe what you mean to me. You have been with me at every step during my journey and have had to carry me at many points along the way. You have seen me at my best and at my worst, and for some reason have decided to stick by my side. I would not be here if it were not for you. I truly believe that God brought you into my life for a reason, and every day we have together I realize more and more what that reason is. You are awesome and amazing, and I thank God for you.

TABLE OF CONTENTS

DEDICATION	ii
ACKNOWLEDGEMENTS	iii
LIST OF FIGURES	ix
LIST OF TABLES	xiv
ABSTRACT	xv
CHAPTER	
I. Introduction	1
1.1 Dissertation Outline and Contributions	5
1.1.1 Contributions	9
II. The Effect of Haptic Feedback on Teleoperated Grasp and Lift Performance for Amputees and Non-amputees	10
2.1 Introduction	10
2.2 Methods	13
2.2.1 Experimental Setup	13
2.2.2 Experimental Protocol	16
2.2.3 Metrics	19
2.2.4 Statistical Analysis	19
2.3 Results	20
2.3.1 Grip Force by Weight	22
2.3.2 Grip Force by Condition	24
2.3.3 Slip by Weight, Condition, and Participant Group	25
2.4 Discussion	26
2.4.1 Grip/Load Force Coordination	27
2.4.2 Grip Force Scaling with Object Weight	28
2.4.3 Effect of Haptic Feedback on Grip Force	29
2.4.4 Object Slip	31

2.4.5	Final Considerations	31
III. Colocation of Action and Re-action Improves Task Performance and Psychometric Sensitivity		
3.1	Introduction	33
3.1.1	Perception Through Action Response Relationships	33
3.1.2	Haptic Exploration Through an Interface	34
3.1.3	Haptic Perception of Stiffness Through an Interface	35
3.2	Experiment 1 Methods	36
3.2.1	Participants	36
3.2.2	Experimental Apparatus	37
3.2.3	Stimuli	37
3.2.4	Setup and Training	38
3.2.5	Testing	39
3.2.6	Metrics and Data Analysis	40
3.2.7	Statistical Analysis	40
3.3	Results: Experiment 1	41
3.3.1	Object Identification Accuracy	41
3.3.2	Trial Duration	41
3.3.3	Object Exploration	43
3.4	Experiment Two: Methods	44
3.4.1	Participants	44
3.4.2	Apparatus and Stimuli	44
3.4.3	Training	48
3.4.4	Testing	49
3.4.5	Metrics and Data Analysis	50
3.4.6	Statistical Analysis	52
3.5	Results: Experiment 2	52
3.5.1	Survey Results	54
3.6	Discussion	56
3.6.1	Task Performance	57
3.6.2	Psychometric Performance	58
3.6.3	Haptic Display Considerations	60
IV. [Characterizing the Gold Standard:] Assessing the Impact of Vision and Force Feedback in a Body-Powered Prosthesis		
4.1	Introduction	62
4.2	Methods	65
4.2.1	Participants	65
4.2.2	Experimental Apparatus	65
4.2.3	Stimuli	70
4.2.4	Setup and Training	70
4.2.5	Testing	71

4.2.6	Metrics and Data Analysis	72
4.3	Results	73
4.3.1	Object Identification Accuracy	75
4.3.2	Object Identification Duration	77
4.3.3	Object Exploration	79
4.4	Discussion	80
APPENDIX		84
BIBLIOGRAPHY		90

LIST OF FIGURES

<u>Figure</u>		
2.1	Motorized elbow brace with right-handed elbow brace and motorized capstan drive. The brace produced an extension moment about the elbow proportional to force measured by the gripper.	14
2.2	Motorized gripper with motorized capstan drive and load cell. . . .	14
2.3	C2 tactor inside mp3 sports band.	16
2.4	Instrumented object with attached distance sensor and removable weight drawer atop a force plate. The card stock and force plate constitute the “table”.	17
2.5	Testing setup. (a) Able-bodied participants hold the gripper in hand. (b) Amputee participants wear the gripper attached to the motorized elbow brace. In addition to the motorized elbow brace and gripper, participants are wearing the vibrotactile display, and brain imaging (EEG and fNIR) sensors.	18
2.6	Time-domain plots for a representative able-bodied participant: (A) EMG, (B) Gripper Aperture, (C) Grip Force, (D) Load Force, (E) Normalized Object Position. All traces are for successful (no-slip) trials with the heavy object in blocks one and two (trials 1-72). Time has been scaled to object lift-off using a 99% threshold on the maximum load force, and scaled to object set-down using a 98% threshold on the maximum force for each trial.	20
2.7	Grip force vs. load force trajectory for able-bodied and amputee participants for the (A) Heavy object and (B) Light object. Solid lines represent mean phase trajectory for all successful (no-slip) trials in the first two blocks (trials 1-72). Shaded regions represent the 95% confidence interval of the mean. Purple traces represent able-bodied participants. Cyan traces represent amputee participants. Dashed line represents the slip threshold.	22

2.8	Grip force trajectory by object weight: (A) Able-bodied (C) Amputee participant. Solid lines represent the mean of all successful (no-slip) trials in the first two block (trials 1-72). Shading represents the 95% confidence intervals of the mean. Brown traces represent the light object and orange traces represent the heavy object. The mean grip force for each weight just before lift-off <i>GripT-10</i> is shown in the accompanying bar plots: (B) Able-bodied, (D) Amputee participants. Error bars represent 1 standard error	23
2.9	Grip force trajectory by feedback condition for the heavy object: (A) Able-bodied (C) Amputee participant. Solid lines represent the mean of all successful (no-slip) trials in the first two block (trials 1-72). Shading represents the 95% confidence intervals of the mean. Blue traces represent force feedback, green traces represent vibrotactile feedback, and red traces represent no feedback. The mean grip force for each condition with the heavy weight just before lift-off <i>GripT-10</i> is shown in the accompanying bar plots: (B) Able-bodied, (D) Amputee participant. Error bars represent 1 standard error.	24
2.10	Odds ratio for object slip by (A) object weight, (B) participant group, and (C) feedback condition. An odds ratio of or 1.0 represents an equal odds of slipping. Error bars represent the 95% confidence interval.	26
3.1	Testing Setup showing two linear voice-coil motors with loadcells attached. Yellow arrows indicate axis of motion.	37
3.2	Virtual Springs (Black, Orange, Green)	38
3.3	Sample force/displacement relationship displayed to participants prior to testing. Used to familiarize participants with the motor operation.	39
3.4	Object identification accuracy by feedback condition for the normal group of participants (N=11): (A) Average identification accuracy across participants for trials 1-60. (B) Average identification accuracy for the last 30 trials (31-60). Red traces represent the collocated condition. Blue traces represent the non-collocated condition. Error bars represent 1 standard error.	42
3.5	Trial duration by feedback condition for all subjects in the normal group (N=11): (A) Average trial duration for trials 1-60. (B) Average trial duration for the last 30 trials (31-60). Red traces represent the collocated condition. Blue traces represent the non-collocated condition. Error bars represent 1 standard error.	43

3.6 Object probe characteristics by feedback condition for all subjects in the normal group: (A) Average number of probes across participants for trials 1-60. (B) Average probe rate for trials 1-60. Red traces represent the colocated condition. Blue traces represent the non-colocated condition. 45

3.7 Two single-axis linear voice-coil motors lying in the horizontal plane. Yellow arrows indicate axis of motion. A stimuli adjustment knob contains a rotary knob with a position indicator. Inset figure shows grip attached to motor. 46

3.8 Tactile array with five tactors attached to volar surface of the forearm with elastic straps. 47

3.9 Sample virtual springs. Springs each have a parabolic force/displacement relationship. Linear spring (Black, Solid) corresponds to $\alpha = 0$. Springs above the linear spring (Magenta, Dotted) correspond to $+\alpha$ and are ‘softening’ springs. Springs below linear line (Cyan, Dashed) correspond to $-\alpha$ and are ‘hardening’ springs. 48

3.10 Time-domain trajectory of α for a representative participant. Solid red traces represent the colocated condition. Dotted blue traces represent the non-colocated condition. Dashed brown traces represent the vibrotactile condition. Solid circles represent the end of each stage. This particular participant caused a reset of α in both the colocated and vibrotactile conditions by turning past $\alpha = 0, \theta = \theta_n$ 53

3.11 Average trajectory of α for all participants in the three conditions. Time has been scaled and normalized to the completion of each stage prior to averaging. Solid red traces represent the colocated condition. Dotted blue traces represent the non-colocated condition. Dashed brown traces represent the vibrotactile condition. Solid circles represent the end of each stage. The large jumps in the trajectory are due to a reset in θ_n or large adjustments by certain participants. 54

3.12 Psychometric Measures. (A) Mean Absolute Threshold (AT) for all 10 participants in each of the three conditions. (B) Mean Separation Threshold (ST) for all 10 participants in each of the three conditions. Error bars represent 1 Standard Error. 56

4.1 Linear actuator drive featuring rotational motor, encoder, ballscrew, beam loadcell carriage, loadcell carriage, Bowden cable anchor and housing mount, and linear slide. In operation, the motor, ballscrew, and carriage tracked a desired position to generate no force on cable, or produced a pulling force on the cable. 66

4.2	Mock prosthesis featuring a thermoplastic shell with accommodations for the fist of an able-bodied participant, a voluntary-closing terminal device, and anchor and mount points for a Bowden cable and housing. To ensure a snug fit, participants were required to wear prosthetic socks. In operation, pulling on the cable closed the terminal device.	67
4.3	Cable-driven exoskeleton featuring an encoder and thermoplastic cuffs with velcro straps, and anchor and mount for Bowden cable and housing. In operation, pulling on the cable would produce and extension moment about the elbow.	67
4.4	Schematic of mock body-powered prosthesis for able-bodied participants.	68
4.5	Block diagrams of exoskeleton actuator with force feedback on and off, and prosthesis actuator.	69
4.6	Foam testing blocks in three different stiffnesses. The names in quotes are the identifiers used during testing. Black athletic socks were used to hide the color of the blocks.	70
4.7	Testing setup for trials with vision feedback.	72
4.8	Testing setup for trials without vision feedback.	72
4.9	Exoskeleton actuator and prosthesis actuator kinematics with force feedback ‘off’ for a sample probe of a medium foam block: (A) Exoskeleton actuator cable displacement, (B) Prosthesis actuator cable displacement, (C) Exoskeleton actuator and prosthesis actuator loadcells, (D) Exoskeleton actuator and prosthesis actuator command voltage. Green traces refer to the exoskeleton actuator. Blue traces refer to the prosthesis actuator. Dashed traces represent the desired position as commanded by the exoskeleton.	74
4.10	Exoskeleton actuator and prosthesis actuator kinematics with force feedback ‘on’ for a sample probe of a medium foam block: (A) Exoskeleton actuator cable displacement, (B) Prosthesis actuator cable displacement, (C) Exoskeleton actuator and prosthesis actuator loadcells, (D) Exoskeleton actuator and prosthesis actuator command voltage. Green traces refer to the exoskeleton actuator. Blue traces refer to the prosthesis actuator. Dashed traces represent the desired position as commanded by the exoskeleton.	75

4.11 Sample stiffness (force/displacement) profiles generated by the (A) Prosthesis actuator and (B) exoskeleton actuator, with force feedback ‘off.’ Blue dotted traces refer to the ‘hard’ block. Pink solid traces refer to the ‘medium’ block. Yellow dashed traces refer to the ‘soft’ block. 76

4.12 Sample stiffness (force/displacement) profiles generated by the (A) Prosthesis actuator and (B) exoskeleton actuator, with force feedback ‘on.’ Blue dotted traces refer to the ‘hard’ block. Pink solid traces refer to the ‘medium’ block. Yellow dashed traces refer to the ‘soft’ block. 76

4.13 Average identification accuracy for all nine normal participants in all five trials of the four conditions. Error bars represent 1 standard error. 77

4.14 Average identification duration for all nine normal participants in all five trials of the four conditions. Note that the first object exploration for each condition is excluded. Error bars represent 1 standard error. 78

LIST OF TABLES

Table

1.1	Comparison of Force and Vibrotactile Display	8
1.2	Comparison of Body-Powered and Myoelectric Prostheses	8
2.1	Slip Descriptives (#slips/total)	26
3.1	Post-Test Survey Results (# responses)	55

ABSTRACT

Haptic Sensory Feedback for Improved Interface to Smart Prosthetics

by

Jeremy DeLaine Brown

Chair: R. Brent Gillespie

Grip force feedback is not available in modern myoelectric upper-limb prostheses, yet its benefits are well known in object manipulation tasks performed through cable-driven body-powered prostheses. To evaluate the efficacy of grip force feedback in a myoelectric prosthesis, direct head-to-head comparisons should be made with body-powered prostheses, as well as with proposed designs that provide grip force feedback through haptic displays such as vibrotactile arrays. Direct comparisons, however, are difficult because myoelectric control for a trans-radial amputee uses residual muscles in the forearm, body-power generally refers interaction to the shoulder, and haptic displays often involve additional information encoding transformations. Currently, no unifying theory exists to cover both information encoding as well as the body part used for control or display. The work developed in this dissertation presents a systematic hypothesis-driven approach to evaluating both information encoding and body part used in the display of grip force feedback. Drawing upon principles from psychophysics, teleoperation, and sensory substitution, we use a series of human subject experiments to quantify the value of grip force feedback for an amputee wearing a trans-radial myoelectric prosthesis. First, using a custom prototype prosthesis, we compare the ability of able-bodied and amputee participants to grasp and lift an object with changeable mass. We assess whether grip force feedback referred to the elbow or vibrotactile feedback on the upper arm is better than vision alone. Second, we assess whether certain haptic displays filter out valuable cues pertaining to the stiffness properties of objects. We develop a new experimental paradigm that changes the body site at which information is presented in a haptic display without changing the haptic modality itself. We assess the impact of both the change in presentation

site and haptic modality on performance in a manual task as well as on psychometric sensitivity. Third, we experimentally evaluate the relative value of vision and grip force feedback in a body-powered prosthesis. We develop a custom prosthesis that can be used by able-bodied individuals and features removable force feedback. We assess the impact of vision and force feedback on performance in an object identification experiment based on stiffness. Our findings demonstrate that both able-bodied individuals and amputees scale and coordinate their grip force for the anticipated weight of an object, that control and grip force feedback should be located on the same body site to improve stiffness recognition, and that grip force feedback is more useful than vision feedback in stiffness recognition through a prosthesis.

CHAPTER I

Introduction

In everyday life, we use our arms and our hands to interact with (grab, rotate, squeeze, lift, hold) objects in our environment. These objects range from fruit in a grocery store, to our cell phones, to a child's hand. Each one of these objects has unique mechanical properties, such as stiffness, surface texture, and weight, which are important for correctly manipulating the object, and can only be elucidated by actively touching and exploring the object. For a healthy individual, our central/peripheral nervous systems along with our neuromuscular system are designed to accomplish these activities. When we actively touch these objects, an efferent command originates in the motor system of the brain pertaining to the volitional action we desire (squeezing the hand for example). The efferent nerves that originate in the central nervous system carry this efferent command out to the muscles of the periphery. These electrical signals then trigger the conversion of chemical energy into mechanical work by our muscles, causing them to contract, and thus our limbs and fingers to move (or produce force). At the same time, our somatosensory organs (Pacinian corpuscles, Meissner corpuscles, Ruffini endings, Merkel discs, Golgi tendons, and Muscles Spindles) are constantly sending haptic sensory feedback from the limbs back to the central nervous system through our afferent nerves. This haptic sensory feedback contains information about the current state of the limb (its position and orientation) as well as any external information sensed by the limb, such as the force generated when an object is squeezed, or its weight when lifted. This sensory information is then combined with our internal copy of the efferent command (efferent copy) to provide us with useful knowledge about our actions and the resulting feedback they produce.

It is theorized that afferent sensory information is used by the brain to develop an internal representation of the world (internal model) for use in predictive control during object manipulation tasks [1–3]. When we grasp and lift an object off of a

surface, our grip force is adequately programmed to support, through friction, the load force produced by the weight of the object. During the lifting phase, the grip force and load force increase in parallel until the object just begins to lift off of the surface. The object then rapidly reaches its intended vertical position in a smooth over-damped manner without overshoot [1]. The ratio between grip force and load force are adapted on the basis of the object's friction properties in order to ensure an economically stable grasp with a small safety margin. Throughout every phase of the manipulation task, sensory information is being used to track task progress as well as prediction errors, in order to provide corrective action to the limbs and update the internal models [2].

It is also theorized that the relationship between our volitional commands (provided by efferent copy) and the resulting haptic feedback sensed by our limbs is the basis for haptic perception of an object's mechanical properties. When we check fruit in a market to determine how ripe it is, we squeeze and monitor the resulting deformations. We then compare the relationship between our exploratory action and the resulting feedback to that previously experienced with other fruit, to perceive the ripeness of the fruit we currently hold. The relationship between our action and the resulting feedback represents an invariant property of the fruit. Other invariant properties exist, such as the fruit's shape, surface texture, and weight. Squeezing the fruit is a particular exploratory procedure that we employ to determine softness, and thus ripeness. For other invariant properties, we use particular exploratory procedures such as a lateral motion (for texture), unsupported holding (for weight), and contour following (for shape) [4].

For an individual with an amputated limb, all efferent and afferent signals end abruptly at the most distal part of the residual limb. Prosthetic limbs provide an artificial conduit through which these efferent and afferent pathways can be restored. For upper-limb amputees there are two main types of active prostheses, body-powered prostheses and myoelectric prostheses.

Body-powered prostheses have been around longer, and work by mechanically linking the action of some part of the amputee's body to the action of the prosthetic hand. In most cases this is done with a metal Bowden cable and a shoulder harness. There are two types of prosthetic hands, voluntary-opening and voluntary-closing. In the voluntary-opening hand, the hand is nominally held closed with a spring, and is opened by pulling on the cable through the shoulder harness. In the voluntary-closing hand the opposite is true. The hand is nominally held open by a spring, and is closed by pulling on the cable through the shoulder harness. For both hand

types, the cable provides a mechanical connection between the amputee's shoulder and the prosthetic hand akin to that provided by the tendons that mechanically connect the muscles of the forearm to the fingers of the natural hand. Any action (force or motion) generated by the shoulder that pulls on the cable gets transmitted to the prosthetic hand. Likewise, any action (force or motion) in the prosthetic hand that pulls on the cable gets transmitted to the shoulder. Therefore, this bi-directional control paradigm inherently provides haptic sensory feedback. It is worth noting that this feedback cannot be removed.

In a myoelectric device, the opening/closing action of the prosthetic hand is driven by the electromyographic (EMG) signals derived from the action of certain muscles in the amputee's residual limb. The EMG signal is uni-directional, providing only a command signal to the hand. Thus, myoelectric devices lack the inherent feedback that body-powered devices provide. Amputees must therefore rely even more heavily on other sensory channels such as vision and audition to supplement the lack of haptic feedback.

Recently, there have been major advances in actuator and sensor technologies that have helped bring prosthetic limbs closer to the form and function of the natural limbs they are replacing. In addition, advances in signal processing algorithms and advanced surgical procedures like targeted muscle reinnervation have come even closer to realizing brain-controlled prostheses. While considerable attention has been paid to restoring the efferent command to a prostheses, little work has been done on the afferent side. This means that even with the advanced prosthetic devices currently in development, an amputee is still left without the haptic sensory feedback needed for robust predictive object manipulation strategies, as well as without the ability to perceive objects in the environment by feel alone.

Current investigations hold significant promise for developing methods of interfacing directly to the peripheral efferent and afferent nerves, as well as to the cortical regions of the brain. These technologies, however, are still many years from being fully realized, and will require invasive surgical procedures on top of that required for the amputation itself. What then can be done in the short term for amputees, and in the long term for future amputees that do not want to undergo any additional surgical procedures?

At present, there is no clear indication as to what the best course of action should be. The problem of interfacing a prosthetic limb that has identical form and function as the natural limb it is replacing is decades old. The work of Childress [5–7], Weir [8], Shannon [9, 10], and others [11, 12] has laid the foundation for what has become a

long-term challenge of establishing pathways for both efferent and afferent signals to and from the prosthesis. While the work on establishing robust, high-fidelity efferent pathways has seen major innovations since the early work of Childress and others, significant innovations on afferent pathways are relatively nonexistent.

This is not to suggest that attempts have not been made. Indeed, within the field of haptic feedback, momentum has been gaining on the development of external haptic displays that can provide sufficient afferent haptic feedback to amputees wearing a myoelectric prosthesis [13–20]. There exist various haptic display modalities that communicate information to the user through different tactile channels. These displays provide temporal, spatial, and kinesthetic cues through the application of vibration, force, pressure, stretch, and even electrocutaneous stimulation to the skin. While this body of work has proven that the potential exists for a haptic display to one day non-invasively provide an amputee with afferent information pertaining to the interaction of the prosthesis and the environment, these investigations are based on a trial and error approach to finding the best display, and have failed to establish a working theory or set of design guidelines upon which to build.

Within the field of haptics there are well established subfields that could provide the theoretical basis for the application of haptic display in prosthetics, however these subfields lack the breadth needed to explain the unique interface between an amputee and a prosthesis. Psychophysics for example can explain in detail the limits of our ability to resolve a stimulus in the form of a force [21, 22], vibration [23, 24], or compliance [25, 26] but cannot explain the task-specific utility provided by the stimulus in a prosthesis. Teleoperation provides a thorough foundation for haptic interfaces that connect users to remote or virtual environments [27–30] but cannot explain the intricacies of interfacing a user with partial efferent and afferent pathways (what is left in the residual limb) to an environment that is remote from the perspective of the residual limb, yet remains in close proximity to the rest of the body. Sensory substitution can give a detailed explanation of how effective a prosthetic interface may be at converting afferent sensory information from one sensory modality to another [31–33], yet it cannot explain how it is possible for an amputee to process and interpret the same information through different displays differently, and is often more concerned with the theoretical implications of sensory substitution than its practical application. Even if we look at the field of prosthetics itself, there is little empirical evidence supporting the claim that body-powered prostheses offer advantages over myoelectric prostheses due to the inherent haptic feedback they provide [34–38].

In this dissertation, I have focused my research efforts on efficacy of one haptic

signal that is pertinent to just about every interaction an amputee has between their prosthetic limb and the environment, the force they are gripping with. Giving an amputee knowledge of this force would be beneficial for all amputees regardless of whether their prescribed prosthesis uses a single degree of freedom hand like the Ottobock Greifer, or a more complicated multi-degree of freedom hand like the Touch Bionics i-Limb hand.

It might seem that for grip force any haptic modality would suffice since force can be encoded into another haptic modality, say vibration or pressure. Indeed, there have been numerous studies attempting to render grip force through various types of haptic displays [17, 19, 20, 39, 40] . However, knowledge of the force level alone is usually not enough. Every object that we grab in the world around us has some intrinsic stiffness. Stiffness is encoded in a relationship between force and displacement. We therefore determine stiffness by applying a displacement and comparing the resulting force with our efferent copy of the displacement, or by applying a certain force and comparing the resulting displacement with our efferent copy of the applied force (think back to determining fruit ripeness). Therefore, to accurately measure stiffness, knowledge of the change in force for a given motion is needed. For an amputee wearing a body-powered prosthesis, the measurement of stiffness is possible because the haptic feedback supplied by the cable allows both force and motion to be transmitted to the shoulder. In addition, because all action and feedback occur at the same point of mechanical contact between the shoulder and the harness, mechanical work must be exerted by the shoulder, thus leading to a sense of effort.

Therefore, to determine the best way to haptically display grip force through a prosthesis, it would be worthwhile to functionally compare the utility of grip force feedback for both amputee and able-bodied individuals, to systematically compare the various haptic display modalities proposed for grip force feedback, and to assess the utility of grip force feedback in a body-powered prosthesis through a comparison with a myoelectric prosthesis. These comparisons, however are like comparing apples to oranges, because in each comparison multiple factors are changing simultaneously. What is needed then is a controlled approach involving only one factor changing at a time.

1.1 Dissertation Outline and Contributions

The goal of this dissertation then is to develop the experimental controls necessary to make each of these comparisons more “apples-to-apples” in makeup. In each

chapter, I will present the experimental findings of a systematic hypothesis-driven study featuring a unique experimental control. The majority of this work will feature haptic force feedback that spans an intact joint, which draws upon the principles in operation within a body-powered prosthesis. In a manner similar to the cable and shoulder harness of the body-powered prosthesis, haptic force feedback that spans an intact joint produces an internal force between the limbs connecting the joint. Since the muscles in these limbs can produce a moment across a joint, as well as change length with motion of the joint, both force and motion can be transmitted to the joint. In addition, if the control from the prosthesis comes from action about the joint, force feedback spanning the joint will allow for mechanical work to be exerted by the muscles spanning that joint and thus a sense of effort. This principle will be applied specifically in this dissertation for a trans-radial amputee (an individual with an amputated forearm and an intact elbow) and a myoelectric prosthesis.

In Chapter II, I study the effect of providing grip force feedback (through force display and vibrotactile display) in the control of a myoelectric prosthesis for both amputee and able-bodied participants. Both participant types are inherently different, Therefore, as an experimental control, we attempt to place both participant types on a level playing field by only allowing them to grasp and lift and instrumented object through a custom back-drivable myoelectric prosthetic gripper capable of recording grip force. Both force display and vibrotactile display modalities have been shown to provide utility to an amputee wearing a prosthesis [12, 19, 41, 42], however their utility has not been compared in the same experiment. In addition, these experiments are limited to simple tasks often involving virtual environments or homogeneous participant populations (able-bodied or amputee). Here, we compare *force display* to *vibrotactile display* and *no feedback* in a functional grasp and lift task with both able-bodied and amputee participants. Comparing these two participant populations provides insights into how both groups adjust to a novel prosthesis control paradigm with variable haptic feedback. The instrumented object is capable of recording the load force as well as the distance it has been lifted above a support. In addition, the weight of the instrumented object can be changed without the participant’s knowledge. Force display was provided by a custom exoskeleton worn about the intact or residual elbow. The exoskeleton was capable of producing flexion and extension moments about the elbow proportional to the sensed grip force. Vibrotactile display was provided by a single tactor placed on the upper arm. The amplitude of vibration was then modulated in relation to the sensed grip force. We found that participants gripped the objects differently by weight, that the grip force was nominally coordi-

nated with the load force, and that amputees used a larger grip force at lift-off than able-bodied participants. We also found that force display appears to result in fewer overall slips.

In Chapter III, I compare force display of force to vibrotactile display of force in a stiffness discrimination task. As mentioned above, stiffness is encoded as a change in force with respect to a change in displacement. Therefore, an additional cue for stiffness is mechanical work. When we perceive stiffness with our natural limbs, force, motion¹, and work (or power) are available. This is because the force/motion exchange is colocated at the point of mechanical contact with the object. With a haptic interface, alternatives exist. Not only can the exchange of force and motion be non-colocated (occurring on different body parts), but also the sensory feedback cue (force in this case) can undergo a change in encoding. This is the case for vibrotactile display, which is both non-colocated and involves a change in encoding from force to vibration. When force and motion are non-colocated, a power exchange cannot occur. Therefore, non-colocated force display and vibrotactile display filter power from the invariant stiffness relationship. Any nominal “apples-to-oranges” comparison of colocated force display and vibrotactile display of force involves varying both the encoding of force as well as the availability of a power exchange. This is represented graphically as a comparison between cells 1 and 4 in Table 1.1. In order to make the comparison “apples-to-apples,” comparisons should be made either across rows (involving only changes the encoding of force) or across columns (involving only changes in the availability of a power exchange). To study the impact of both of these changes on manual task performance and psychometric sensitivity, we have created an experimental control corresponding to cell 2 in Table 1.1. This experimental control, non-colocated force display, is an intermediate between colocated force display and vibrotactile display as it allows us to compare the effect of colocated versus non-colocated display without the change in haptic modality. In addition, it allows us to compare the effect of a change in haptic modality without considering the availability of a power exchange. We found that non-colocated force display results in lower stiffness identification accuracy and longer identification times, and that non-colocated display and vibrotactile display result in lower psychometric sensitivity compared to colocated force display. In addition, we found no differences between non-colocated force display and vibrotactile display.

In Chapter IV, I study the utility provided by the force feedback available in a body-powered prosthesis. Body-powered prostheses have anecdotally been consid-

¹here motion refers to displacement or velocity

Table 1.1: Comparison of Force and Vibrotactile Display
 Power Exchange No Power Exchange

Force Displayed as Force	1	2
Force Displayed as Vibration	3	4

ered the gold standard in upper-limb prosthetics due to the inherent force feedback they provide. This claim, however has remained untested. Any nominal “apples-to-oranges” comparison of body-powered and myoelectric prostheses naturally involves a change in control as well as a change in feedback. This is represented graphically as a comparison between cells 1 and 4 in Table 1.2. In order to make the comparisons “apples-to-apples,” comparisons should be made either across rows (involving only changes in the control), or across columns (involving only changes in the availability of force feedback). To study the impact of force feedback (and vision) on the ability to discriminate an object by its stiffness, we have created an experimental control corresponding to cell 2 in Table 1.2. This experimental control, a custom body-powered prosthetic device for able-bodied participants, features modulated force feedback. The device utilizes a cable-driven voluntary-closing prosthetic hand, and a cable-driven exoskeleton to conditionally provide colocated force feedback (control comes from the elbow angle). We found that participants were more accurate with force feedback alone than with vision feedback alone. Participants were also most accurate with both vision and force feedback, and least accurate with no feedback. In all cases with vision, discrimination took a longer duration.

Table 1.2: Comparison of Body-Powered and Myoelectric Prostheses

	Force Feedback	No Force Feedback
Body Action Control	1	2
Myoelectric Control	3	4

The dissertation ends with a summary and discussion of future work in Chapter 5.

1.1.1 Contributions

- Development of an experimental apparatus and protocol that compares amputee and able-bodied participants in the control of a myoelectric prosthesis with grip force feedback in the form of force feedback and vibrotactile feedback.
- Experimental findings demonstrating that even through a prosthesis, both able-bodied and amputee participants scale and coordinate their grip force for the anticipated weight of an object; amputee participants use a larger grip force at object lift-off with force feedback; and force feedback leads to fewer overall object slips.
- Development of a new type of experimental control that allows a comparison with collocated force feedback without a change in haptic modality.
- Experimental findings demonstrating that collocated force feedback results in improved manual task performance (stiffness identification) over non-collocated force feedback, and improved psychometric sensitivity (stiffness discrimination) over non-collocated force feedback and vibrotactile feedback.
- Development of a body-powered prosthesis for use with able-bodied participants that features removable force feedback spanning the elbow joint.
- Experimental findings demonstrating that both vision and force feedback improve task performance (stiffness identification) with a body-powered prosthesis over no vision and no force feedback; force feedback alone provides improved performance (stiffness identification accuracy) over vision alone; vision results in slower performance (stiffness identification timing) over no vision.

CHAPTER II

The Effect of Haptic Feedback on Teleoperated Grasp and Lift Performance for Amputees and Non-amputees

2.1 Introduction

Given recent advances in actuator and sensor technology, upper-limb prosthesis development has seen an explosion in innovation, moving devices closer to the physiological form and function of the natural limbs they are replacing. Unfortunately, the ability to accurately and efficiently control the additional degrees of freedom lags significantly behind. In the intact limb, dexterous control relies on efferent neural pathways carrying user intent to the neuromuscular system and afferent pathways bringing feedback (both anticipated and unanticipated) to the central nervous system (CNS). This sensory information is presumed to be used by the CNS to develop and refine internal models of the limb and the environment for use in dexterous control [2, 3].

For upper-limb amputees, all efferent and afferent pathways end abruptly at the most distal point in the residual limb. Prosthetic limbs can, however, provide an artificial conduit through which these efferent and afferent signals can be partially restored. In terms of interpreting user intent, various approaches exist, including the use of myoelectric signals and the use of motion in other parts of the body (as in body-powered devices). In addition, emerging technologies like targeted muscle reinnervation move closer to detecting user intent directly from the efferent neural command [43, 44]. Vision currently serves as the primary afferent signal. But vision alone cannot provide the information needed for robust and efficient volitional control. What lacks are adequate haptic and proprioceptive afferent pathways to supplement vision and provide feedback regarding a prosthetic device's mechanical interaction

with the environment. Although novel control and feedback technologies are being pursued that can directly interface with the peripheral or the central nervous system, these technologies are still many years from being fully realized [45, 46]. What then can be done in the short term to improve the utility of prosthetic devices?

A number of haptic display technologies can be used to relay sensory feedback to the residual limb from electronic sensors embedded in a prosthetic terminal device. The potential of certain haptic technologies has been explored, including vibrotactile feedback [11, 16–20, 39, 47–50], skin stretch feedback [14, 18], and force feedback [41, 51]. The benefits of haptic feedback in functional tasks have been demonstrated to some extent [12, 41, 42, 52], however only single modalities and homogeneous participant groups have been considered. While these haptic technologies each hold promise, little has been done to compare their utility in a task that is functionally meaningful to an amputee using a prosthesis.

In able-bodied adults, the simple act of grasping and lifting an object is characterized by a remarkable degree of coordination between the forces and motions involved. Individuals maintain grip force in tight proportion to the load force throughout the task, using just enough grip force to prevent slip. Experimental investigations show that the constant of proportionality closely matches the coefficient of friction [3]. Thus there is a parallel increase in grip force and load force in the initial ‘lift-off’ phase of lifting, and a parallel decrease in grip force and load force during the final ‘set-down’ phase. In addition, the grip force predictably scales with object weight. This behavior suggests that the movements involved in task completion are planned, and planning involves the use of internal representations of the object’s weight, shape, and friction properties so that appropriate efferent motor commands are produced and expected sensory afferents are predicted. Actual sensory afferents are then used to monitor task progression and check for errors in the execution of the motor program [1–3].

If able-bodied participants are denied the full suite of sensory afferents available in the natural hand (as with anesthetized digits), they lose the ability to accurately modulate their grip force according to the weight of the object. As a result, they prefer a proportionality constant between grip and load force that is well above the friction coefficient. But grip force control also suffers, such that even with a safety margin in place, a larger number of slips take place [53]. Although similar results have been shown for participants with impaired sensory afferents [54, 55], grasp and lift coordination for amputee participants is still not well understood.

In this study we investigate the ability of both able-bodied and amputee participants to perform a grasp and lift task using a custom prototype prosthetic de-

vice. We attempt to place able-bodied participants on a level playing field with amputees by denying them the mechanoreception, proprioception, and sense of effort that comes from the cutaneous receptors in the hand, as well as the intrinsic and extrinsic muscle/tendons of the hand and arm. In our experiment, grasp and lift takes place through a motorized gripper (terminal device) that can be adapted for either an able-bodied individual or a trans-radial amputee. We also replace physiological/neuromuscular control over grip force with myoelectric control of the gripper, modeled in part after myoelectric control used in commercial prostheses. Specifically, we use proportional myoelectric control, wherein a grip force is produced by the motorized gripper in proportion to the amplitude of an amplified, rectified, and filtered surface electromyographic (EMG) signal derived from muscles in the forearm.

By ‘slaving’ the action of the gripper to the EMG signal from the forearm muscles, our participants essentially perform the grasp and lift task through a teleoperator. In its nominal form, our teleoperated gripper denies grip force sensation to our participants, like a unilateral teleoperator without force reflection. We can, however, conditionally relay the grip force back to our participants through the use of various haptic display devices. Note that our device does not deny the sensation of load force (weight). Since weight is an externally applied force, it is balanced by forces and moments supplied by the participant through the attachments between device and body.

In the present study we compare force feedback to one of the most widely studied modalities for prosthetics, vibrotactile feedback. In our previous work [40, 51], we found that a moment applied at the elbow in proportion to electronically sensed gripper force provides sufficient information to distinguish objects by their stiffness. In subsequent work [56] we compared force feedback coupled in various ways with manual control, finding that force feedback provided at the same interface at which position control is derived supports superior haptic perception. Force feedback is able to support the exchange of mechanical power between user and environment only when it is provided at the same interface as that used for control. This is of course the standard configuration in force-reflecting teleoperators, where it is generally accepted that force feedback aids performance [57–59]. In continuing work we are comparing force feedback to vibrotactile feedback. We are exploring whether force feedback is superior to vibrotactile feedback, especially when the signal being displayed is a force of contact with an object in the environment. Our prior results would suggest that force feedback should out-perform vibrotactile feedback because of its ability to support power exchange between user and environment.

By denying our able-bodied participants the ability to accurately monitor grip force, we expect task performance very similar to our amputee participants. In particular, we should see a lack of appropriate grip force regulation, and an overcompensation in grip force well above what is needed to prevent slip. Restoring this grip force sensation through haptic feedback should improve task performance by diminishing the overcompensating behavior and reducing the amount of task mistakes (object slips). We expect this effect to be stronger for force feedback since the signal being displayed (grip force) is in fact a force and might be more easily interpreted in the force feedback modality than in the vibration feedback modality.

2.2 Methods

2.2.1 Experimental Setup

Our experimental apparatus consisted of a motorized elbow brace, a motorized gripper, a myoelectric sensor and amplifier, a vibrotactile display, and an instrumented object.

The motorized elbow brace was used to provide force feedback in the form of an extension moment about the elbow joint. It consisted of a right-handed Aircast Mayo Clinic Elbow Brace customized with an attached motorized capstan drive (Figure 2.1). The DC motor used in the capstan drive was a Maxon RE 30 (60W), powered by a 24V power supply (TDK-Lambda ZWS150PAF) and H-Bridge amplifier (Advanced Motion Control 12A8). The motor was equipped with a rotary encoder on the motor shaft (Maxon 1024 CPR) and a rotary encoder on the brace shaft (US Digital, 2500 CPR). The motorized brace was capable of delivering 0.15N·m of torque as an extension moment about the elbow. Participants' arms were secured in the elbow brace through four velcro straps. For amputee participants, custom cuffs were used in addition to the velcro straps. The width of the brace could also be adjusted. In operation, the motorized brace produced an extension moment about the elbow proportional to the measured grip force.

The motorized gripper was driven by a DC Motor and capstan drive in a design similar to the motorized brace (Figure 2.2). In addition, the gripper was equipped with a 5kg-capacity beam load cell (Transducer Techniques LSP-5) that measured the grip force. The gripper was capable of delivering 8N of force at the object contact surface. The gripper was hand held about a foam grip for able-bodied participants, and mounted to the distal portion of the motorized elbow brace for amputee participants.

In operation the gripper was position-controlled from EMG signals derived from

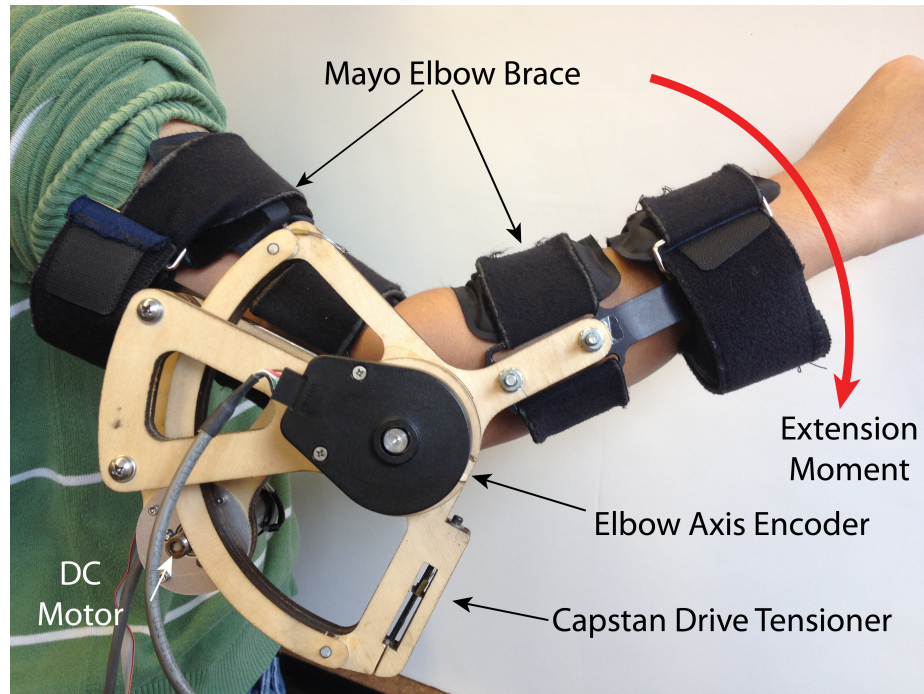


Figure 2.1: Motorized elbow brace with right-handed elbow brace and motorized capstan drive. The brace produced an extension moment about the elbow proportional to force measured by the gripper.

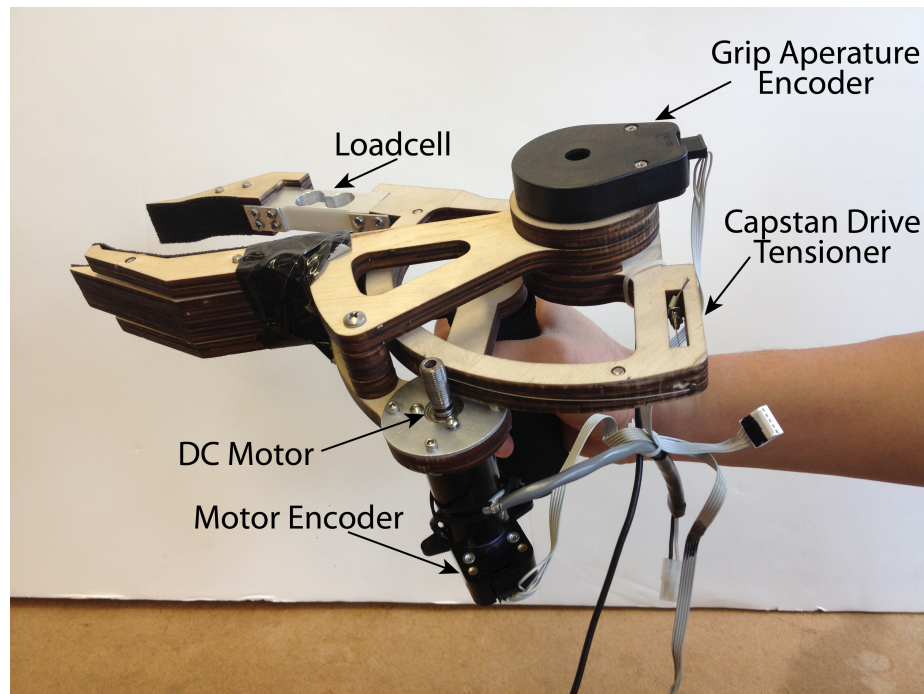


Figure 2.2: Motorized gripper with motorized capstan drive and load cell.

muscles in the forearm. For able-bodied participants these were muscles on the volar aspect of the forearm in the region of the wrist flexor and extrinsic finger flexor muscles. For amputees, these were the muscles in the residual limb usually used for control of a myoelectric prosthesis, as identified by the prosthetist member of the research team.

A custom conditioning circuit provided full-wave rectification, low-pass filtering with a 3.4Hz cutoff frequency, and variable amplification of the raw EMG signal. In addition to the adhesive backing on the electrodes, a compression sleeve was used to keep the electrodes from coming loose during the experiment.

The vibrotactile cue was adapted from Christiansen *et al* [60], and was carefully designed considering human perceptual capabilities and prior psychophysical study results (see Figure 2.3). The vibrotactile display consisted of an Engineering Acoustics Inc. C2 tactor driven through an H-Bridge amplifier (LOGOSOL DC Servo Amplifier LS-5Y-12-DE). The tactor was held in place using an off-the-shelf mp3 player sports arm band. In operation, the tactor’s vibration amplitude T_c was exponentially proportional to the measured grip force and driven according to Equation (2.1) with $T_{camp} = 0.1sec$, $T_{cfreq} = 250Hz$, and $T_{cref} = \frac{|Grip\ Force|}{Maximum\ Grip\ Force}$.

$$T_c = 0.5 \cdot e^{2T_{cref}} \cdot \frac{t}{T_{camp}} \cdot \sin(2\pi T_{cfreq} t) \quad (2.1)$$

The instrumented object was a custom ABS plastic 3D-printed device with a removable drawer for inserting a weight. Rubber grips were placed on the side for grasping, and had a coefficient of friction: $\mu \simeq 1$ (determined experimentally). The object also featured . Two infrared distance sensors (Sharp 2D120X) were affixed to the object to measure vertical position. A 2kg-capacity force plate (AMTI HE6X6-1) was used to measure the vertical load force. A piece of white card stock was attached to the top of the force plate to allow for more accurate position readings from the distance sensors (Figure 2.4).

The entire system was controlled by a Sensoray 626 PCI card installed in a Dell OptiPlex 7010 series desktop running Microsoft Visual C++ 2010 Express Edition. Brain imaging was also undertaken using 32 channel scalp electroencephalography (EEG) and a 16-channel functional near infrared (fNIR) imaging (Figure 2.5). Brain imaging results will not be presented in this paper.

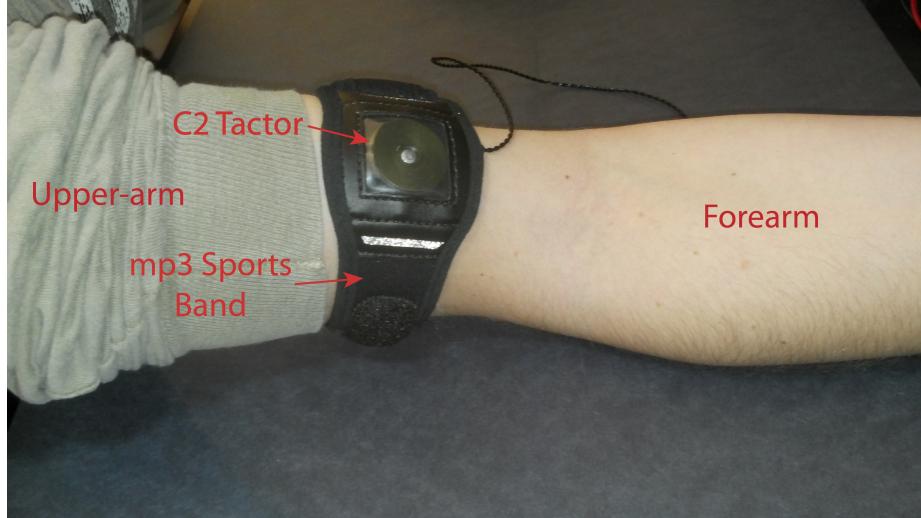


Figure 2.3: C2 tactor inside mp3 sports band.

2.2.2 Experimental Protocol

We tested N=10 male participants, seven able-bodied (mean age 26.6) and three trans-radial amputees (mean age 53.3). Prior to starting the study, each participant was consented according to a protocol approved by the Institutional Review Boards of the University of Michigan, Rice University, University of Houston, and Drexel University. Participants were not compensated, and testing lasted about two hours.

2.2.2.1 Training

Due to the design of the brace, all experimentation involved the right arm. The vibrotactile display was placed on top of the biceps area of the right arm and secured with the velcro sports band. The motorized brace was secured with velcro straps around the upper and lower portions of the right arm, aligning the elbow joint with the brace axis of rotation. The EMG gain was adjusted to ensure the participant's control signal was in the 0-5V range on an oscilloscope. Then the EMG control gains and biases were adjusted so that the participant could independently control the grip force and lifting motion. This was tested by having participants grasp and lift the instrumented object at the maximum weight three successive times. The force feedback gain was adjusted until it was independently recognized by the participant when grasping an object similar in size to the test object. The gain ranged from 1.0-3.5 depending on the participant. For vibrotactile feedback, T_{cref} was set based on the maximum grip force produced when the participant grasped an object similar in size to the test object. The participant was then fitted with the fNIR and EEG

systems.

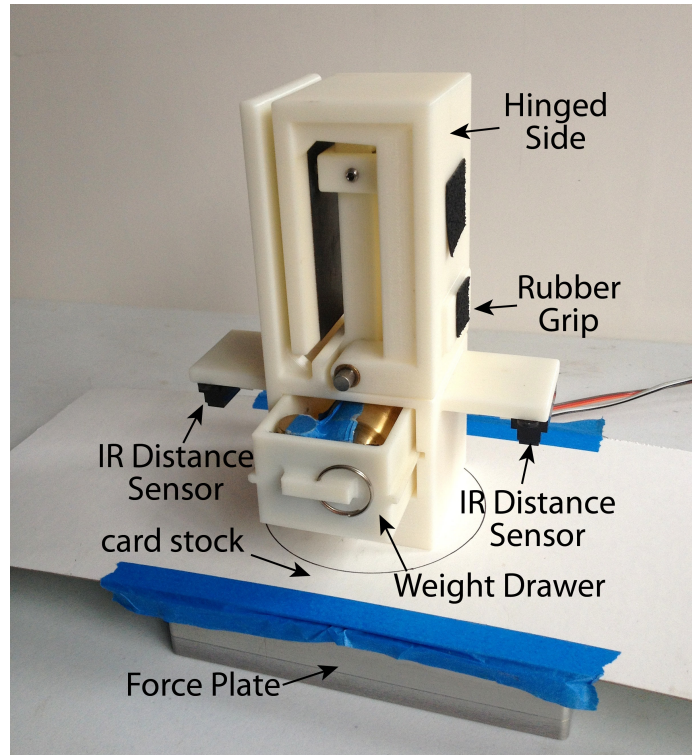


Figure 2.4: Instrumented object with attached distance sensor and removable weight drawer atop a force plate. The card stock and force plate constitute the “table”.

2.2.2.2 Testing

The test consisted of 144 trials broken into four blocks of 36 trials each. There were three conditions being tested: vibrotactile feedback, force feedback, and no feedback. Visual and auditory signals were not blocked during any of the trials. The weight and condition were arranged based on a stratified randomization on two factors (object weight and feedback condition). Two weights were used, 340g (drawer empty) and 590g (250g weight in drawer). During each block, each condition was presented 12 times and each weight was presented 18 times in a stratified random order.

Each trial lasted 10 seconds. For each trial, the participant was instructed to start from a rest position, close and open the gripper, reach, grasp, and lift the instrumented object, then place it back on the force plate. Participants were instructed to grasp the object at the rubber grips and lift it a few inches off the force plate before returning it. After the 10 seconds were up, the tester would remove the object from the force plate and change weights (per schedule) behind a cardboard curtain before replacing



Figure 2.5: Testing setup. (a) Able-bodied participants hold the gripper in hand. (b) Amputee participants wear the gripper attached to the motorized elbow brace. In addition to the motorized elbow brace and gripper, participants are wearing the vibrotactile display, and brain imaging (EEG and fNIR) sensors.

the object on the force plate for the next trial. This was also timed at 10 seconds (for the first participant, 15 seconds were used). The participant was not aware of weight or condition changes prior to grasping and lifting the object. A timer with bell chimes kept track of timing. A break lasting a minimum of three minutes was taken after each block of 36 trials. Prior to starting each block, the control signals and feedback actuators were checked to ensure signal fidelity.

There were a few notable changes in the protocol for amputee participants. Amputees were not required to close the gripper at the beginning of each trial prior to grasping and lifting the object. Also, for amputee participants we only included the first two blocks of trials (1-72), based on results from the able-bodied participants. One amputee (participant 8) was given force feedback in the form of a flexion moment rather than an extension moment because the participant could not feel the extension moment.

Due to complications arising from the brain imaging collection, a few able-bodied participants did not complete all four blocks. All participants completed at least two blocks of the experiment. Four able-bodied participants completed all four blocks, and one completed three blocks.

2.2.3 Metrics

To analyze task performance, assess the utility of haptic feedback, and compare able-bodied participants to amputee participants we examined the coordination between grip and load forces by means of time-domain and phase plots. Phase plots were generated by plotting grip force versus load force for all successful (no-slip) trials. We also examined the grip force just before lift-off for all successful (no-slip) trials. (*GripT-10*) represents the grip force at T=-10% on the scale determined by lift-off (t=0%) and set-down (t=100%). In addition, we examined the effect of object weight (heavy/light), participant type (able-bodied/amputee), and feedback condition (force/vibrotactile/none) on the likelihood of an object to slip while being grasped.

Due to technical difficulties with our data acquisition system, all time-series results only contain the first two blocks (trials 1-72) of data. For our binary slip results all completed trials are analyzed.

2.2.4 Statistical Analysis

Linear mixed models (LMM) were used for the grip force at lift-off (*GripT-10*) using SPSS (v.20) for estimating fixed and random coefficients for the able-bodied and amputee participant groups, separately. Within the model, participants were a random effect while object weight and feedback condition were fixed effects. Trial number was treated as a repeated measure. Bonferroni adjustment were applied to the estimated means to control for Type I errors.

The application of LMM allows for unequal numbers of observations per participant, does not require normality assumptions typically needed in parametric assessments, and is applied in repeated measures assessments [61]. The LMM model was fit by restricted maximum likelihood estimates (REML). The Akaike Information Criterion (AICc), corrected for small sample size, was used for model selection. For each measure, the model with smaller values of the AICc indicated a better fit.

A Generalized Linear Mixed Model (GLiMM) was applied in development of a logistic model of the binary (yes, no), non-normally distributed slip data. The logistic model had a non-independence of measures along with the inclusion of random effects [62]. The probability of a slip occurring on a trial was modeled with participant group (able-bodied and amputee), condition (force feedback, vibrotactile feedback, or no feedback), and object weight (light and heavy) as fixed effects, while participant was a random effect. A binary probability model was applied with the logit link

function and the best covariance type was variance components [62]. Similar to the LMM, AICc was used for model selection. For all tests, a 0.05 significance criterion was applied.

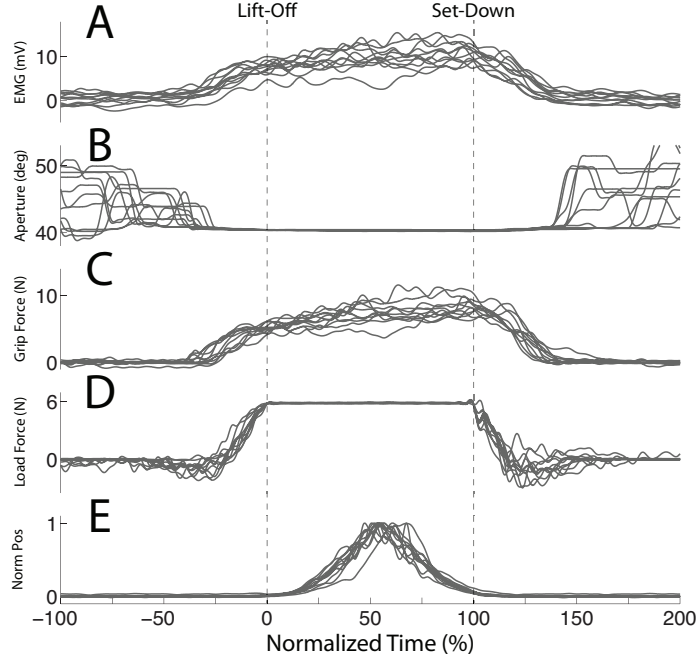


Figure 2.6: Time-domain plots for a representative able-bodied participant: (A) EMG, (B) Gripper Aperture, (C) Grip Force, (D) Load Force, (E) Normalized Object Position. All traces are for successful (no-slip) trials with the heavy object in blocks one and two (trials 1-72). Time has been scaled to object lift-off using a 99% threshold on the maximum load force, and scaled to object set-down using a 98% threshold on the maximum force for each trial.

2.3 Results

All of our participants quickly learned how to operate the proportional myoelectric gripper using an EMG signal derived from the muscles in their forearm. With very little training they became quite proficient at coordinating their grip force with the load force as they lifted the object and set it back down. They also adapted their grip force for the weight of the object.

Figure 2.6 includes EMG, gripper aperture, grip force, load force, and normalized position traces for a representative able-bodied participant. For this particular participant, the 11 trials for the heavy object with no grip force feedback and no object slip are shown. There were no instructions on how high the object was to be lifted off the table. Time has therefore been scaled to object lift-off using a 99% threshold

on the maximum load force, and set-down using a 98% threshold on the maximum force (to account for any contact artifacts) for each trial. Considering only the no-slip trials, the following was observed: gripper aperture followed EMG command until the gripper closed on the object (Figure 2.6A,B); thereafter grip force tracked the EMG signal (Figure 2.6A,C); grip force and load force increased prior to object lift-off and decreased to their initial state after object set-down (Figure 2.6C,D); and object position traces were single peaked (Figure 2.6E). These characteristics held across all participants. In the following, we examine the overall coordination of the grip and load forces, the differences in grip force by object weight and feedback condition, and the likelihood of an object slipping by weight and feedback condition.

2.3.0.1 Phase Plots

Figure 2.7A shows the mean grip force trajectory plotted against the mean load force trajectory for $n=7$ able-bodied and $n=3$ amputee participants for the heavy object. Shaded regions represent the 95% confidence intervals (CI). The dashed line in the figure represents the slip threshold (coefficient of friction, $\mu \simeq 1$). For the able-bodied participants there is an initial increase in grip force at the beginning of lift-off, which precedes the load force increase. The grip force and load force then increase in parallel until the object is lifted off the table. Once the object returns to the table there is a parallel decrease in the grip and load force. In the final portion of set-down, there is a decrease in load force which is followed by a decrease in the grip force. This indicated that able-bodied participants did not completely let go of the object until they were sure it had come to rest on the table. In addition, our able-bodied participants kept their grip force well above the slip threshold (dashed line) on lift-off and set-down. For our amputee participants, the trajectory appears to have more “hysteresis” in it, resulting from a larger grip force on lift-off, and a smaller grip-force on set-down. Also, on set-down, the trajectory dips below the slip threshold and is then followed by a decrease in both grip force and load force that tracks the slip threshold. Note that the object did not slip out of the grasp at this point because contact with the table had already been made. In the final portion of set-down, the sharp decrease in grip force is absent, indicating that amputee participants let go of the object just as it came to rest on the table. Similar trends are found for able-bodied and amputee participants for the light object Figure 2.7B.

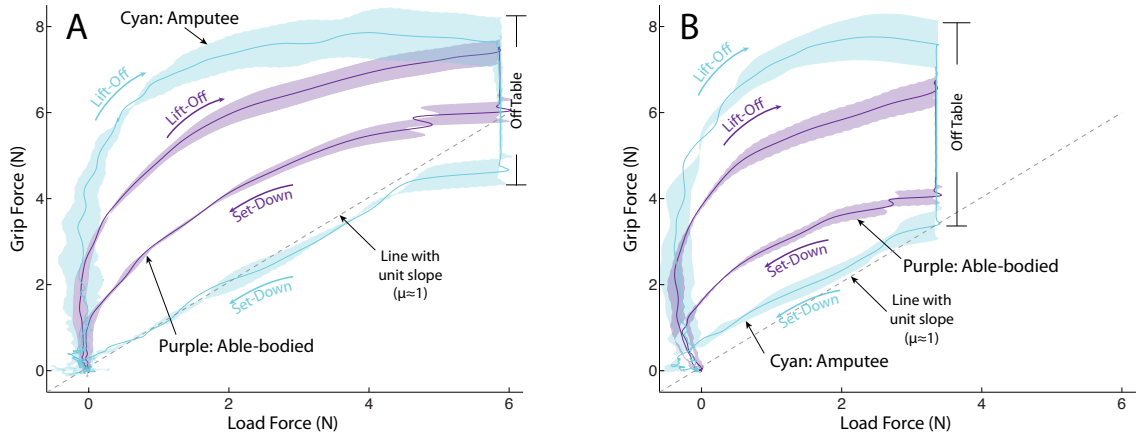


Figure 2.7: Grip force vs. load force trajectory for able-bodied and amputee participants for the (A) Heavy object and (B) Light object. Solid lines represent mean phase trajectory for all successful (no-slip) trials in the first two blocks (trials 1-72). Shaded regions represent the 95% confidence interval of the mean. Purple traces represent able-bodied participants. Cyan traces represent amputee participants. Dashed line represents the slip threshold.

2.3.1 Grip Force by Weight

2.3.1.1 Trajectory

Figure 2.8 shows the mean (with 95% CI) grip force trajectory for all successful (no-slip) trials in the first two blocks (trials 1-72). The mean trajectories have been computed and plotted separately for each participant group (able-bodied (Figure 2.8A) and amputee (Figure 2.8C)). Trajectories are shown in overlay for each object weight (heavy/light). Time has again been scaled to object lift-off and set-down. For both participant groups, there are regions between lift-off and set-down where the 95% CI bands do not overlap for the two weights. This indicates that participants on average used a larger grip force for the heavy object than for the light object. We can also see that the grip force increase begins earlier for the heavy object than for the light object. For able-bodied participants the grip force for the heavy object is greater while the object is just being lifted off the table. For amputee participants, the 95% CI bands overlap in this region indicating that mean grip force was roughly the same for each object weight, though these 95% CI bands seem to separate around time $t = 50\%$.

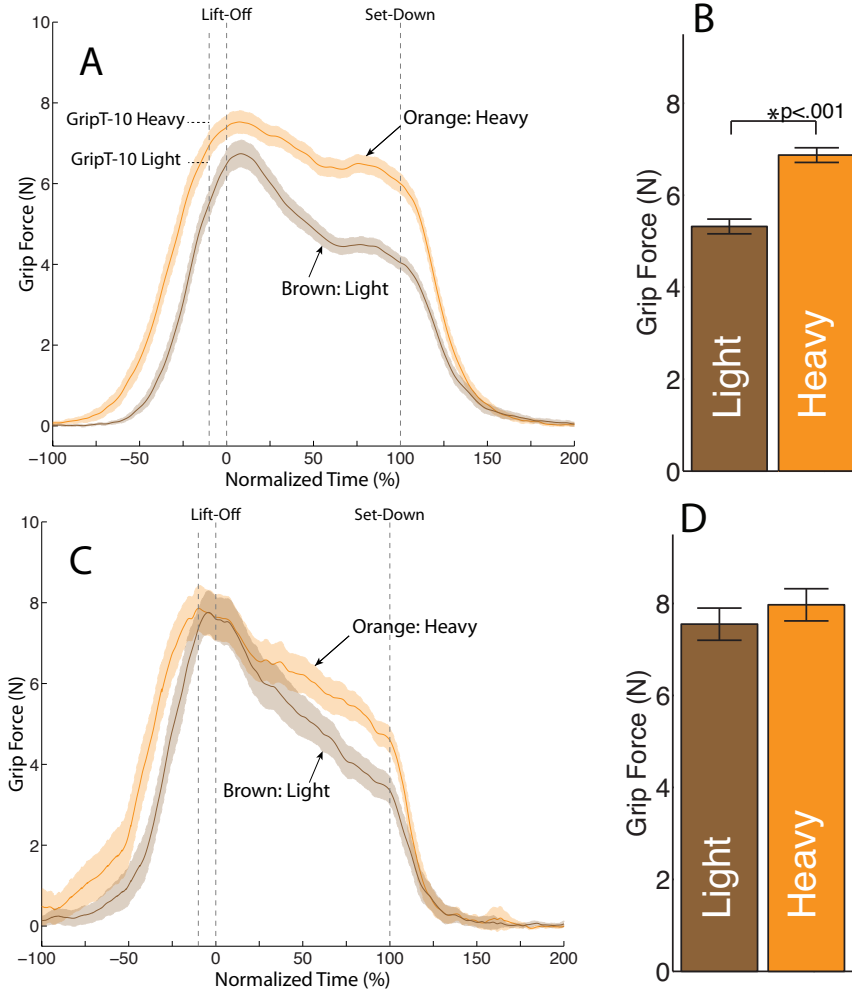


Figure 2.8: Grip force trajectory by object weight: (A) Able-bodied (C) Amputee participant. Solid lines represent the mean of all successful (no-slip) trials in the first two block (trials 1-72). Shading represents the 95% confidence intervals of the mean. Brown traces represent the light object and orange traces represent the heavy object. The mean grip force for each weight just before lift-off *GripT-10* is shown in the accompanying bar plots: (B) Able-bodied, (D) Amputee participants. Error bars represent 1 standard error

2.3.1.2 Grip Force Value Just Before Lift-off

Figure 2.8B shows a bar graph comparing the grip force at lift-off (*GripT-10*) by object weight for the $n=7$ able-bodied participants. Figure 2.8D compares the *GripT-10* values by object weight for the $n=3$ amputee participants. For the able-bodied participants there was a significant fixed effect for object weight ($F_{(1,386.05)} = 92.43, p < .001$). This fixed effect parameter resulted in a significantly smaller grip force for the light object ($\beta = -1.55, SE = 0.16, p < .001$) than the heavy object.

There was no significant difference in $GripT-10$ by weight for the amputee participants at lift-off.

2.3.2 Grip Force by Condition

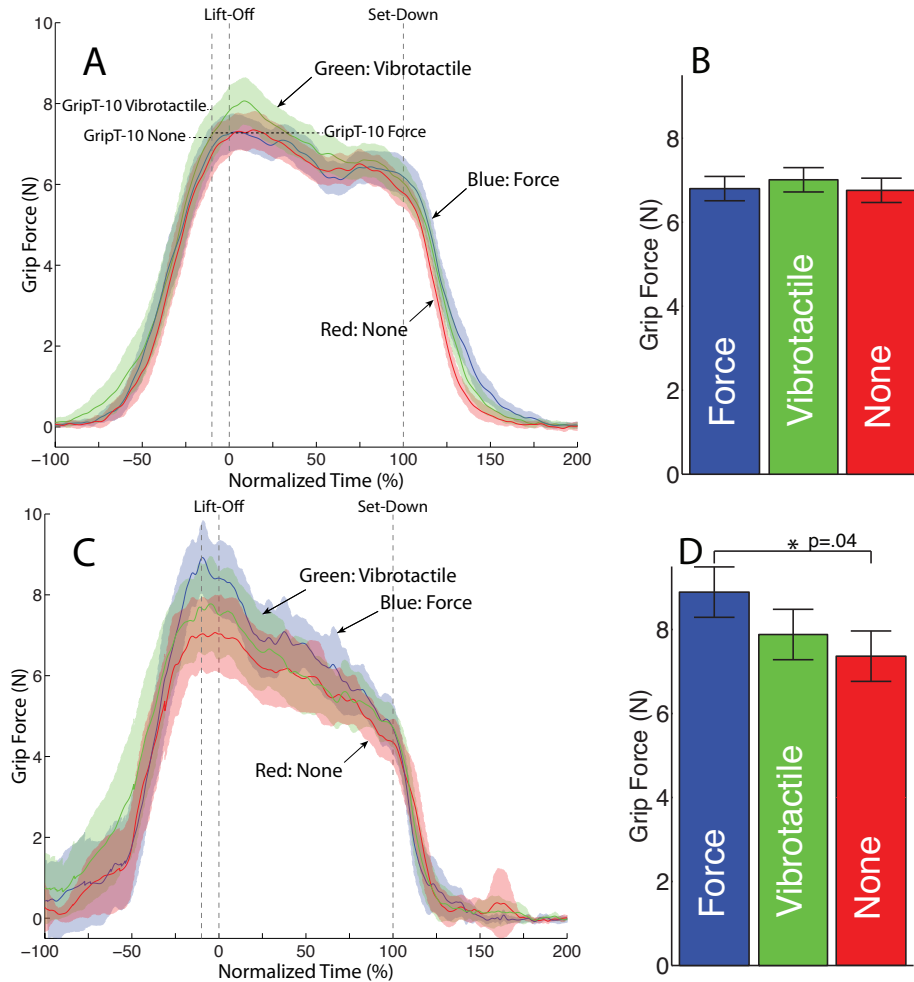


Figure 2.9: Grip force trajectory by feedback condition for the heavy object: (A) Able-bodied (C) Amputee participant. Solid lines represent the mean of all successful (no-slip) trials in the first two block (trials 1-72). Shading represents the 95% confidence intervals of the mean. Blue traces represent force feedback, green traces represent vibrotactile feedback, and red traces represent no feedback. The mean grip force for each condition with the heavy weight just before lift-off $GripT-10$ is shown in the accompanying bar plots: (B) Able-bodied, (D) Amputee participant. Error bars represent 1 standard error.

2.3.2.1 Trajectory

Figure 2.9 shows the mean (with 95% CI) grip force trajectory for all successful (no-slip) trials in the first two blocks (trials 1-72) for the heavy object only. The mean trajectories have been computed and plotted separately for each participant group (able-bodied (Figure 2.9A) and amputee (Figure 2.9C)). Trajectories are shown in overlay for each feedback condition (none, force, vibrotactile). Time has again been scaled to object lift-off and set-down. Overall, the 95% CI bands overlap throughout the grasp and lift task, indicating that feedback condition made little difference on the grip force. However, there are a few time periods, particularly around lift-off where the 95% CI band for one feedback condition is recognizably higher than the other two. For the able-bodied participants this is the vibrotactile condition. For the amputee participants this is the force feedback condition. These same trends hold for the light object as well.

2.3.2.2 Grip Force Value Just Before Lift-Off

GripT-10 was analyzed for the able-bodied (Figure 2.9B) and amputee (Figure 2.9D) participants for each of the three feedback conditions. For the able-bodied participants there were no significant differences by feedback condition. For the amputee participants, there was a significant fixed effect for feedback condition for the heavy object ($F_{(2,61.19)} = 3.36, p = .04$). This fixed effect parameter resulted in a significantly larger grip force for the force feedback condition ($\beta = 1.53, SE = 0.6, p = .04$) than the no feedback condition. There were no other significant differences by feedback condition for the light or heavy object.

2.3.3 Slip by Weight, Condition, and Participant Group

Table 2.1 shows the number of times a gross slip of the object within the gripper was observed, broken down by object weight, participant group, and feedback condition. Pooling the weights, groups, or conditions selectively, we observed more slips for the light object than for the heavy, more slips for the no feedback condition than for force feedback or vibrotactile feedback, and more slips for amputee participants than able-bodied participants. A logistic regression analysis for object slip found a significant fixed effect of object weight ($F_{(1,1069)} = 8.36, p = .004$). This fixed effect parameter resulted in a greater likelihood of slip for the light object ($\beta = 0.47, SE = 0.16, p = .004$) than for the heavy object (Figure 2.10A). There were no significant effects for participant group although it is worth highlighting that am-

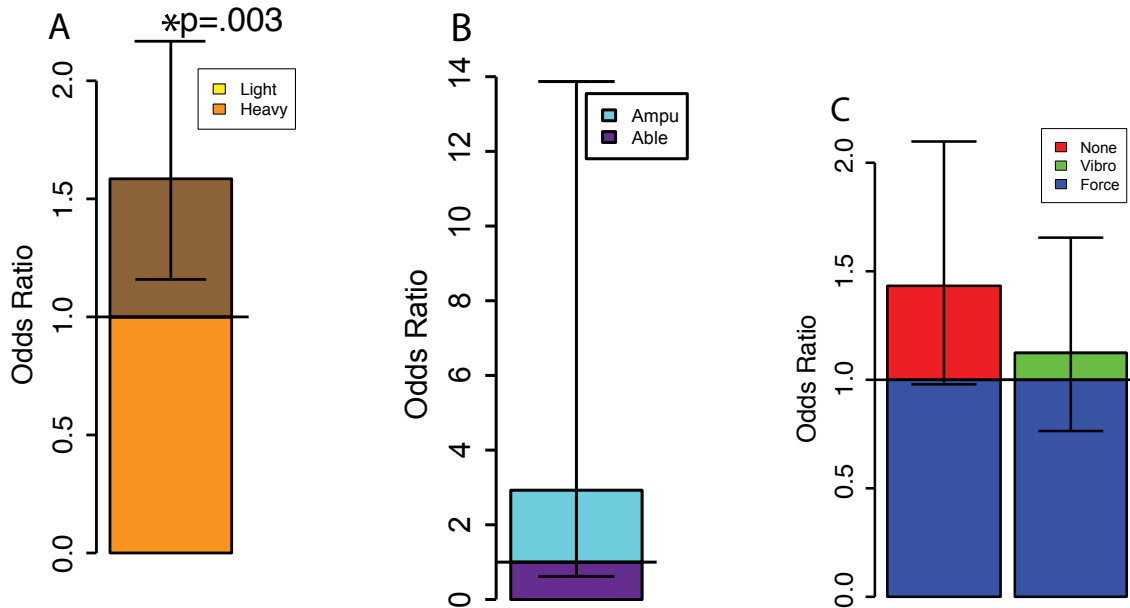


Figure 2.10: Odds ratio for object slip by (A) object weight, (B) participant group, and (C) feedback condition. An odds ratio of or 1.0 represents an equal odds of slipping. Error bars represent the 95% confidence interval.

putees had a higher occurrence of slip than able-bodied participants (Figure 2.10B). Although there were no significant effects for feedback condition, the greater likelihood of slip for no feedback ($\beta_{0.36}, SE = 0.19, p = 0.064$) compared to force feedback is trending towards significance (Figure 2.10C).

2.4 Discussion

In this study we investigated how able-bodied and amputee participants performed a grasp and lift task through a proportional myoelectric gripper that optionally fea-

Table 2.1: Slip Descriptives (#slips/total)

Light Object			
	None	Vibrotactile	Force
Able	39/138 (28.3%)	32/136 (23.5%)	25/138 (18.1%)
Ampu	18/39 (46.2%)	15/41 (36.6%)	14/40 (35.0%)
Heavy Object			
	None	Vibrotactile	Force
Able	21/139 (15.1%)	23/139 (16.5%)	21/140 (15.0%)
Ampu	16/42 (38.1%)	12/41 (29.3%)	16/40 (40.0%)

tured haptic display of grip force. We are ultimately interested in understanding whether and how haptic display can improve dexterous use of a myoelectric prosthesis. Our study was therefore designed to analyze prosthesis performance in light of principles underlying grasp and lift with the natural hand, and in light of prior results on the utility of haptic feedback in teleoperation.

2.4.1 Grip/Load Force Coordination

Our participants coordinated their EMG command and lifting motions to produce a grip force that was roughly scaled to the load force. A perfect unit scaling of grip force to the load force (reflecting the unit-valued coefficient of friction for our gripper/object) would have produced a phase plot along the dashed line in Figure 2.7. Our able-bodied participants produced phase plots significantly above the unit slope line, with a larger scaling on lift-off than on set-down. Evidently our able-bodied participants used a generous margin of safety to prevent slip. Our amputee participants used an even greater safety margin on lift-off, but no safety margin on set-down.

Note, however, that ramp-up of grip force was not complete before load force increased, as the phase plots do indeed bend toward the unit slope line. The existence of at least some simultaneous ramping of grip and load force during lift-off is an indication of coordination that reflects grasp and lift behaviors in the natural hand [1–3, 63–68]. This coordination suggests that our participants were utilizing some form of predictive control to complete the task.

Coordination on lift-off is better for the able-bodied participants than for the amputee participants, as the phase plot for able-bodied participants has lower slope in the lift-off phase. On set-down our able-bodied participants produced a decrease in grip force that paralleled the decrease in load force as a result of the object weight being taken up by the table, with a moderate margin of safety. Our amputee participants did not use a safety margin on set-down and in fact often decreased their grip force below the weight right before the heavy object made contact with the force plate, resulting in a sharp decrease in load force as the weight was first taken up by the table (see Figure 2.7A). Essentially, the amputee participants were occasionally dropping the object on the table from a low height, rather than gently placing it back down.

Grip versus load force phase plots for the grasp and lift task performed with the natural hand typically follow the line with slope set by the coefficient of friction (see, for example, Figure 1B in [1]). As in many motor tasks, adults use an energy-efficient

strategy for grasp and lift, applying just enough grip force to prevent slip without wasting any effort. Though the phase plots for our participants do not follow the line with unit slope, they nevertheless show some evidence of coordination, which is noteworthy given that our device differs so substantially from the natural hand. That our participants used generous safety margins could be due in part to a diminished energetic cost associated with myoelectric control. Engaging the motorized gripper to produce grip force had very little associated energetic cost. It could also be possible that in our brief experiment with many confounding factors, participants opted for task success (no-slip) over energy conservation.

Our able-bodied participants had little to no exposure to myoelectric control, especially for grasp and lift tasks. Our novel control paradigm however did not prevent our participants from quickly learning to operate the gripper with little training. Perhaps our selection of a muscle group for EMG control that is physiologically associated with grip in the natural hand was instrumental for the rapid learning.

Our amputee participants, although each having ample experience with myoelectric prostheses, were not used to our particular myoelectric control paradigm. Instead of mapping the open/close grip rate to the EMG signal from two antagonist muscle groups in the forearm as is commonly done in commercial myoelectric prostheses, we drove the gripper aperture in proportion to an EMG signal derived from only one muscle group in the forearm. This prior experience with a very different control paradigm could have had a negative effect on the performance of our amputees, requiring them to unlearn the control paradigm used for their current prosthesis before learning ours. Perhaps this could explain why in general the grip/load phase for amputees had more “hysteresis.” The larger safety margin on lift-off could be a habitual behavior resulting from expectations appropriate only to their regular prosthesis. The smaller safety margin on set-down could come from inexperience using the same muscle to both open and close the gripper. It is also possible that the smaller safety margin on set-down was due to the involvement in lifting motions of the muscle group used for deriving the EMG signal.

2.4.2 Grip Force Scaling with Object Weight

Our participants also scaled their grip force according to the two levels of maximum load force that resulted from lifting the two object weights. In particular, we saw higher grip force trajectories for the heavy object than for the light (Figure 2.8). This difference was more apparent for able-bodied participants just before lift-off (Figure 2.8B), where the grip force for the heavy object was significantly larger than for the

light object ($p < .001$). Although changes in object weight occurred occasionally and were not made known to participants, we saw very little evidence of within-trial grip force readjustment on the transition trial, as well as very little between-trial adaptation following transitions. The dependence of grip force on object weight even in the early phases of a lift is indicative of a predictive strategy that relied on knowledge of object weight from previous lifts. This dependence was first examined in grasp and lift with the natural hand by Johansson and Westling [1]. For our amputee participants the difference in grip force did not appear until roughly halfway through the lift task. This suggests that perhaps amputee participants were using an anticipatory grip force that was not appropriately programmed for the weight of the object just before lift-off, though it was adequately programmed for the object weight on set-down.

The significant difference by weight in the grip force just before lift-off (*GripT-10*) for able-bodied participants and lack of significant difference for amputee participants might be explained given differences in the way participants from the two groups were fitted with the experimental apparatus. Since our able-bodied participants hand-held the gripper, they were privy, through receptors in their hand, to sensory information regarding object weight as transmitted through the gripper. For amputee participants, the weight had to be transmitted through the brace before it could be sensed. Also, the custom cuffs included a compliant connection between the rigid brace and amputee’s residual limb that could have caused more uncertainty. The weight of our apparatus (brace and gripper) was 2kg, meaning the 250g weight change, though recognizable, could have been masked somewhat by the apparatus, especially for our amputee participants.

2.4.3 Effect of Haptic Feedback on Grip Force

We provided grip force feedback in the form of an amplitude modulated vibration applied to the upper arm (vibrotactile feedback) or an amplitude modulated moment applied at the elbow joint (force feedback). Our results showed that force feedback produced a significantly larger grip force just before lift-off (*GripT-10*) compared to no feedback for our amputee participants ($p = .04$) (Figure 2.9D). This finding suggests that, despite the overall complexity of our setup and task, force feedback did provide some utility to amputee participants. If we liken our myoelectric controlled prosthesis to a teleoperator, we would expect that the addition of haptic feedback would improve task performance, based on work such as that of Wildenbeest *et al* [59], who found that the addition of haptic feedback improved completion times in a teleoperated

assembly task. Similarly, the work of Draper *et al* [57] and Hannaford *et al* [58] showed that force feedback led to reduced errors in teleoperator performance.

It is curious that we saw no significant effects of haptic feedback for our able-bodied participants. The improved levels of coordination and predictive control over our amputee participants have led us to believe that able-bodied participants had more sensory information in general than our amputee participants. Our able-bodied participants hand-held the gripper, and were thus privy to information from the sensory receptors in their hand. In addition, because of their intact hands, contractions of the muscles in their forearm used for EMG control was accompanied by an afferent signal and sense of effort that possibly supported the regulation of grip force and obviated the need for the haptic feedback provided.

Additionally, the strategy preferred by amputees, to increase rather than decrease their grip force compensation with force feedback is surprising. Although counter to our original hypothesis, this strategy could perhaps be explained by considering that the chief aim of our participants was to prevent object slip. Note that slip occurred on 37.4% of the trials for amputees compared to 19.4% for able-bodied participants (Table 2.1). When grip force information was provided, the amputee participants could presumably better monitor their grip force. Instead of using that information to control their grip force to a level just above the force needed to prevent slip as with grasp and lift for the natural hand, they appear to use this knowledge to ensure they were gripping with a sufficient margin of safety while lifting the object. Note that this overcompensation strategy was apparently working to prevent slip, as the object was 1.5 times more likely to slip with no feedback than with force feedback, a result that was trending toward significance (see Figure 2.10C). Also, the diminished energetic cost associated with myoelectric control of the motorized gripper could have contributed to the tendency to increase rather than decrease over compensation with force feedback.

Our chief hypothesis, that force feedback would improve grasp and lift coordination over vibrotactile feedback or no feedback, did not receive particularly strong support from our results. We found only that force feedback led to higher grip force at lift-off than no feedback for our amputee participants. The same result did not hold for our able-bodied participants. We suspect that a driving factor in this outcome is the considerable difference between the experimental setup for able-bodied and amputee participants. A more unbiased approach would have been to deny able-bodied participants the use of their hands, forcing the weight cues to be transmitted through the brace as they were for our amputee participants. This would limit the avail-

ability of afferent signals from the hand and forearm, and possibly make able-bodied participants more dependent on haptic feedback.

2.4.4 Object Slip

The object slipped in least 19% of the trials for our able-bodied participants (Table 2.1), suggesting that they were not always able to suitably modulate grip force with our proportional myoelectric teleoperated gripper. This is likely due to our teleoperated gripper denying our participants the full suite of sensory information that is available in the natural hand. This finding parallels the work of Augurelle *et al* [53], who found that participants with anesthetized digits lack accurate coordination and make more mistakes in a grasp and lift task.

We saw significantly ($p = .003$) more slips for the light than the heavy object (Figure 2.10), which suggests that grip force modulation was more difficult for the light object. Opening the gripper required a relaxation of the muscles generating the EMG signal, and closing the gripper required a contraction of those same muscles. Since neither of our participant groups had extensive training in modulating and maintaining EMG signals between these two extremes (maximum contraction vs maximum relaxation), it is possible that the desire to grip the lighter object with less force was met many times with the inability to maintain that lower force level.

Finally, when pooling participant groups and object weights, we found the object was almost 1.5 times more likely to slip when no feedback was provided than when force feedback was provided, though this result was not statistically significant but trending toward significance.

2.4.5 Final Considerations

While haptic feedback had little effect on the grip force used by able-bodied participants, we found that the conservative strategy used by our amputee participants was amplified with force feedback compared to the no feedback condition. Vibrotactile feedback did not produce the same effect. It is possible that the grip force is more easily interpreted when displayed using force feedback than vibrotactile feedback. In this study we have only begun to explore the role of haptic feedback for a proportional myoelectric gripper. We have only tested one type of force feedback, and one specific type of vibrotactile feedback. Yet our findings suggest that force feedback can be used by amputees using a myoelectric prosthesis to improve performance in the grasp and lift task. While the complexity of our current experimental setup (including the

fNIR and EEG brain imaging equipment) precluded the collection of sufficient data to assess learning, we envision additional studies to assess the role of haptic feedback in the gradual improvement or learning of coordination behaviors.

CHAPTER III

Colocation of Action and Re-action Improves Task Performance and Psychometric Sensitivity

3.1 Introduction

3.1.1 Perception Through Action Response Relationships

When we purchase fruit in a market, we often make selections based on perceived ripeness, determined by squeezing the fruit and feeling its response. In so doing, we become aware the invariant relationship between our exploratory action and the resulting haptic feedback as set by the physical characteristics of the fruit in our hand. We are then able to compare this relationship to prior experience gathered with fruit of differing ripeness. O'Regan and Noë [32] called these invariant relationships between action and sensory feedback *sensorimotor contingencies*. This focus on the relationship between action and response is a drastic shift from a previous research agenda that addressed perception independent of action and has been brought about by the contributions of many authors including Katz [69], Gibson [70], Klatzky and Lederman [4], and others.

Under this framework, perception is a process of recognizing the sensorimotor contingency as an invariant relationship that was previously experienced and given an association. If the sensory modality is changed, perception can still occur as long as the new sensory modality makes the invariant relationship available to the user, and allows a comparison with prior experience. This was demonstrated, for example by the Tactile Visual Sensory Substitution (TVSS) device of Bach-Y-Rita [33], which gave visually impaired individuals a camera to actively explore their environment, and encoded the visual feedback as a tactile display on the individual's back.

It is worth noting here that in addition to the establishment of an invariant relationship between action and sensory feedback, Auvray *et al.* [71] postulated that true

sensory substitution, in which the interface becomes mentally ‘transparent’ to the user, requires distal attribution as well as a recognition of an external space within which the perceived object can be manipulated. Here, we will only focus on the invariant relationship between action and sensory feedback that is presented through an interface.

3.1.2 Haptic Exploration Through an Interface

When we explore fruit or any other object in our environment through an interface, we are reliant upon the interface to transmit our exploratory actions to the object and transmit the resulting feedback to our body in a manner that preserves the invariant relationships governed by the object’s physical properties. For certain interfaces, both transmissions occur without corruption. LaMotte [72] for example found that discriminating softness with a rigid tool was equivalent to that of the natural hand. This implies that the invariant relationship between exploratory action and resulting feedback is preserved with the rigid tool. The percept of softness can therefore be formed through the rigid tool as with the natural hand.

In other cases the actions taken on the interface are not transmitted perfectly to the environment, and the feedback from the environment is not transmitted perfectly to the body. Here, the invariant relationship between exploratory action and resulting feedback that is experienced by the user is different from the environment’s invariant relationship and that of the natural hand. Therefore, the percept that develops may be degraded. Lederman and Klatzky [73] for example found various types of degradation in haptic perception of common objects when manual exploration was performed through rigid and compliant interfaces. This included spatial, temporal, thermal, and kinesthetic perception.

Haptic interfaces that connect users with remote or virtual environments utilize rendering algorithms and devices that often alter the invariant relationship the user experiences between exploratory action and resulting feedback (re-action). This typically occurs when the action and re-action are no longer located (coupled) on the same body site as is the case when the fingers are used to control a robotic hand, and the toe is used to sense force feedback [41]. This also occurs when the re-action is encoded and rendered in a different haptic modality as is the case when force is encoded as vibration [42, 74].

In both the separation of body sites and the change in rendering modality, it is possible for the invariant action/re-action relationship experienced by the user to function in a manner similar to the invariant relationship of the environment,

but it is worth considering whether any information in the environment’s invariant relationship gets filtered by the interface. Besides having an impact on the percept itself, performance may differ and the overall psychometric sensitivity may change. This is particularly important considering that often, decisions pertaining to the interface design are made on the basis of cost and ease of implementation. Using a vibrotactile interface because vibrotaction is considered ‘good enough’ may in fact have serious impacts on the invariant relationship needed to perform a task through the interface.

3.1.3 Haptic Perception of Stiffness Through an Interface

In this paper, we assess the impact of modifying the invariant action/re-action relationship experienced by the user on performance in a manual task, and the impact on psychometric sensitivity. Under three specially designed conditions, we highlight the impact these modified action/re-action relationships have on the perception of a specific object property, stiffness.

Stiffness, (or its inverse, compliance) is encoded in an invariant force/displacement relationship. We perceive stiffness by displacing objects and monitoring the force developed, or through the inverse. It is possible then to argue that all we need to determine stiffness is both force and motion information. From physics, however we understand that force and velocity together express mechanical power ($P = f \cdot v$). Stiffer springs therefore require more power to displace than do more compliant springs. Thus the complete invariant relationship of stiffness may include includes force, motion, and power.

Power can be considered redundant information in the invariant relationship since both force and motion information have to be present as well. With our natural limbs, all action (haptic exploration) and re-action (sensory feedback) are *colocated* (coupled) at the same site on the body. Force, motion, and power are therefore all available when perceiving stiffness.

Through a haptic interface, this is not always the case. Imagine for example that instead of interacting with the interface in a colocated manner with one body part exchanging both force and motion (and therefore power), two separate body parts are used, one for motion input and one for force sensing. Even though there is no change in sensory modality (force from the spring is displayed as force to the user), action and re-action are now *non-colocated* on the body, thereby eliminating the power exchange. Effectively, the invariant stiffness relationship with force, motion, and power is experienced by the user as just force and motion, with power filtered.

Consider now that in addition to the change in body site, the force signal is encoded into another modality, say vibration. Here action and re-action are *non-colocated*, and additionally a sensory substitution has taken place. The sensory receptors that were once excited by force are to be replaced by receptors excited by vibration. To the user, this requires learning a new invariant action/re-action relationship with a new sensory modality involved. Again, power has been filtered due to the non-colocated nature of the display.

Since both the non-colocated force display and vibrotactile display filter power from the invariant stiffness relationship, it might seem redundant to compare both to colocated force display. A comparison of vibrotactile display and colocated force display, however, is more of an “apples to oranges” comparison, involving both a change in action/re-action location (coupling), and a change in re-action encoding. Such “apples to oranges” comparisons are not uncommon [75, 76]. Non-colocated force display however involves only a change in action/re-action location (coupling), and is therefore more of an “apples to apples” comparison to colocated force display.

In both the comparison of colocated force display and non-colocated force display, as well as colocated force display and vibrotactile display, we expect the same result, a degradation in manual task performance and psychometric sensitivity with respect to colocated force display. In what follows, we present the findings of the comparison between colocated and non-colocated force display and colocated and vibrotactile display in two separate experiments. In our first experiment, we compare colocated force display to non-colocated force display in an identification task with three virtual non-linear springs. In our second experiment, we compare colocated force display, non-colocated force display, and vibrotactile display in a psychometric task with two user-adjusted non-linear springs as the stimulus.

3.2 Experiment 1 Methods

3.2.1 Participants

We tested $N=14$ able-bodied participants (ten male, four female; mean age = 21.4 ± 2.9 years). Thirteen participants were right hand dominant. Prior to starting the study, each participant was consented in according to a protocol approved by the University of Michigan Institutional Review Board and given an overview of the study.

3.2.2 Experimental Apparatus

Our testing apparatus consisted of two identical linear voice-coil motors each with a 30mm throw lying parallel in the horizontal plane as shown in Figure 3.1. Each motor was equipped with a linear optical encoder (US Digital EM1-0-500) and driven with a current sourcing amplifier (Advanced Motion Control 12A8). In addition, a 1kg rated beam load cell (Transducer Techniques LSP-1) was mounted to monitor force between the user and each motor carriage. A Dell Precision T3500 Desktop computer with a Sensoray 626 PCI data acquisition card was used for data acquisition and computer control.

A board was placed over the motors so participants could not see the carriages move. Participants interacted with the motors by using a pinch grasp on the loadcell. A hand-rest was provided to assist participants in holding the motor still during one of the experimental conditions (Figure 3.1).

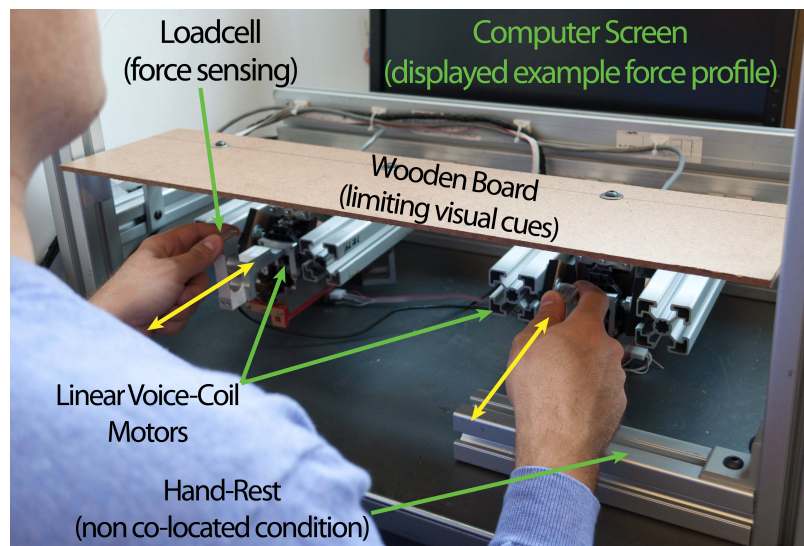


Figure 3.1: Testing Setup showing two linear voice-coil motors with loadcells attached. Yellow arrows indicate axis of motion.

3.2.3 Stimuli

The stimuli were presented in two different conditions. In the collocated condition, the motor held in the right hand was commanded to produce a force as a function of the same motor carriage displacement (see Figure 3.1). Three virtual springs were rendered with the following linear and non-linear constitutive laws:

$$\begin{aligned}
F_1 &= K_1 x_d \\
F_2 &= K_2 \sqrt{x_d} \\
F_3 &= K_3 x_d^2
\end{aligned}
\tag{3.1}$$

where $K_1 = 0.6075 \text{ N/mm}$, $K_2 = 3.0979 \text{ N}/\sqrt{\text{mm}}$, and $K_3 = 0.0234 \text{ N/mm}^2$ respectively, and x_d is the displacement of the right motor carriage in mm .

In the non-colocated condition, the motor held in the right hand was commanded to produce a force as a function of the carriage displacement of the motor held in the left hand (see Figure 3.1). The virtual springs given in Equation 3.1 were rendered with x_d as the displacement of the left motor carriage in mm .

Each spring measured 26mm when fully extended. All three springs produced 0N of force at the resting length and 15.8N when compressed 26mm as shown in Figure 3.2.

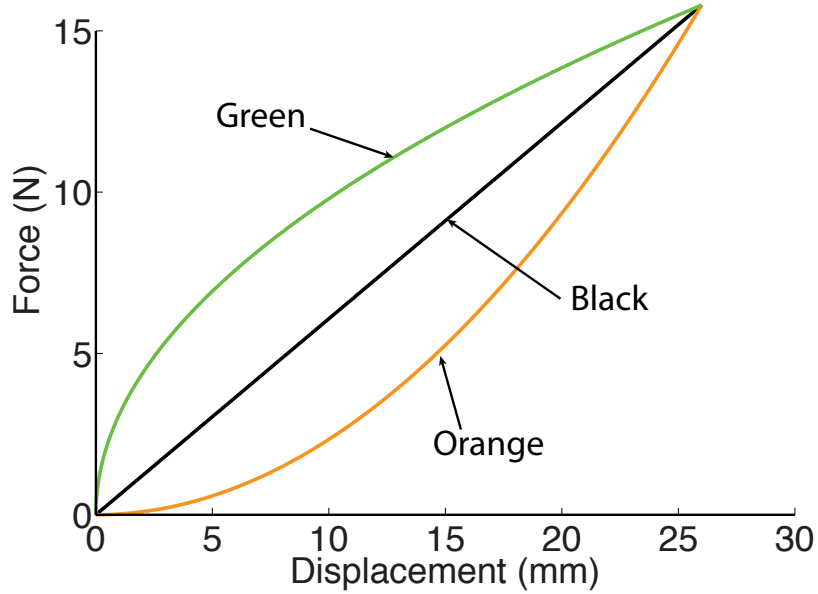


Figure 3.2: Virtual Springs (Black, Orange, Green)

For more details on the apparatus see [56]

3.2.4 Setup and Training

Prior to testing, participants were trained on the two different feedback conditions: colocated and non-colocated. In the non-colocated condition participants were

instructed to hold the motor carriage in the middle of its workspace and use the hand-rest to ground their hand and hold it steady.

During training, a sample force/displacement relationship (Figure 3.3) was displayed on the computer screen, and participants were given an opportunity to explore it in both the colocated and non-colocated conditions. The force-displacement graph, as well as its relationship to the displacements and forces produced by the motors, was explained to the participants. The sample object was only used to familiarize participants with the operation of the motors and was not used in the actual test.

3.2.5 Testing

The three virtual springs used in testing were given a non-descriptive identifier ('black,' 'orange,' and 'green'). Participants were asked to use these names, and were told that the springs might consist of linear and non-linear components. They were not given an opportunity to explore any of the three test springs in either condition, nor were they given any clues as to the association between the three springs and their names prior to beginning the test. They were also not shown any graphs of the springs used in testing. Participants were told that the goal of the experiment was to accurately identify the objects in the shortest time possible in both conditions.

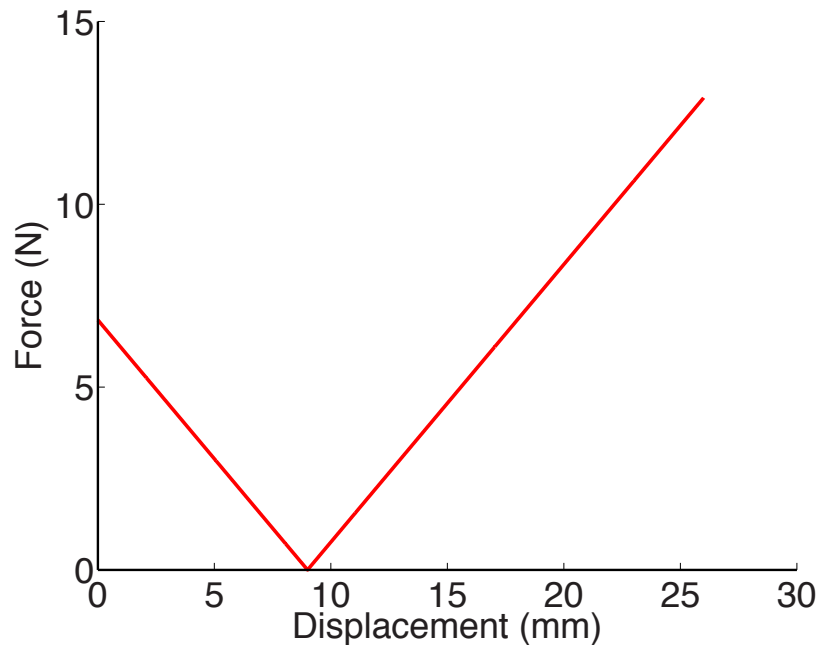


Figure 3.3: Sample force/displacement relationship displayed to participants prior to testing. Used to familiarize participants with the motor operation.

The test consisted of 60 trials with a short break after the first 30 trials were

completed. Each trial alternated between the collocated and non-collocated conditions. During each trial, one virtual spring was presented at random, and the participant was asked to complete a three alternative forced choice identification of the virtual spring presented. Each trial started when the tester verbally announced “begin,” and ended when the participant verbalized their spring choice. Correct answer feedback was provided at the end of each trial. In both conditions, the participant was instructed to explore and probe the object as many times as needed using the entire displacement range. Dwelling or wiggling in any particular region was discouraged. A curtain was used to minimize any visual cues. There were no unique identifying auditory cues available, so the use of noise-canceling headphones was unnecessary. The tester registered the answer on an answer sheet, and time, motor carriage position, and commanded force were recorded by the computer.

3.2.6 Metrics and Data Analysis

The kinematic, kinetic, and performance data was recorded to disk with a 1 kHz sampling rate. Our performance metrics were object identification accuracy (%), trial duration (s), number-of-probes, and probe rate.

Trial duration was measured as the interval from the time the tester announced begin to the time the participant verbalized their object choice.

To measure the number-of-probes, two threshold values were set at 5mm and 21mm within the 26mm length of the spring. Passing both thresholds in one direction as the spring was compressed accumulated a 0.5 (half) probe. Subsequently passing both thresholds in the opposite direction as the spring was released accumulated another 0.5 probe. Passing only one threshold in either direction accumulated 0.25 probe.

3.2.7 Statistical Analysis

All statistical analysis was performed using SPSS (v.19). Descriptive statistics and control charts were used to determine how stable the performance metrics were for each block, as well as whether any participants were outliers. After determining that performance in block two was stable, we compared the effect of our two conditions on the overall mean of each outcome metric for block two using a paired t-test. A sensitivity analysis was also performed for both object identification accuracy and trial duration to assess the effect outliers had on the overall result. A p-value of .05 was used as the threshold to determine statistical significance.

3.3 Results: Experiment 1

In analyzing the results, we found three participants to be outliers from the remaining 11 participants. Overall, these outliers showed no improvements in object identification accuracy or trial duration during the course of the test. Object identification accuracy for all 60 trials was $53\pm 30\%$ for the outlier group and $53\pm 15\%$ for our normal group. The normal group however showed an improvement in accuracy during the first 30 trials that was absent for the outlier group. Trial duration for all 60 trials was 24.2 ± 10.5 s for our outlier group and 5.6 ± 2.2 s for our normal group. The normal group decreased their trial duration during the first 30 trials, whereas the outlier group did not. In what follows, we will analyze in detail the performance of our normal group of participants, and will highlight through a sensitivity analysis the effect of our outliers on both object identification accuracy and trial duration.

3.3.1 Object Identification Accuracy

In terms of identification accuracy (for our normal group of participants), we found that in the collocated condition, the accuracy steadily increased on average from below guessing to well above guessing in the first seven trials. In the non-collocated condition, this steady increase was not present, suggesting that participants encountered more difficulty recognizing the unique force/displacement features with the non-collocated force display as compared to the collocated force display. By the second set of 30 trials, object identification accuracy is mostly stable in both conditions (Figure 3.4A). On average, for the last 30 trials, participants were more accurate in the collocated condition (M=63.64%, SE=7.8%) than in the non-collocated condition (M=52.12%, SE=7.93%), ($t(10) = 4.03$, $p = .003$ see Figure 3.4B). If we include the results of our outliers, participants are still more accurate in the collocated condition (M=64.29%, SE=6.35%) than in the non-collocated condition (M=55.24%, SE=6.65%) ($t(13) = 2.2$, $p = .046$).

3.3.2 Trial Duration

In both conditions (for our normal group of participants), the average trial duration decreased in the first set of 30 trials. This decrease was sustained for more trials in the collocated condition than the non-collocated condition. By the second set of 30 trials, trial duration leveled off for both conditions and remained stable throughout the remainder of the test (Figure 3.5A). The levels at which they leveled off, though, differ by condition. On average, for the last 30 trials, trial duration was

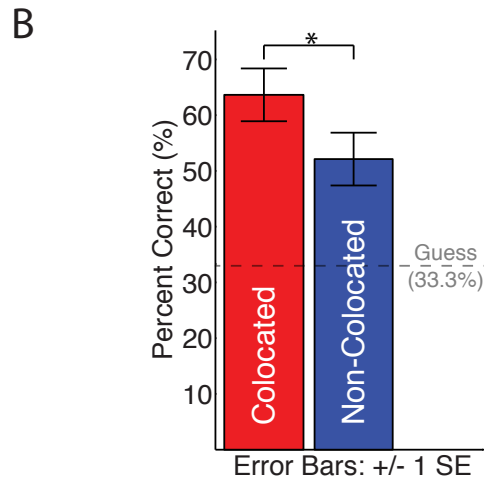
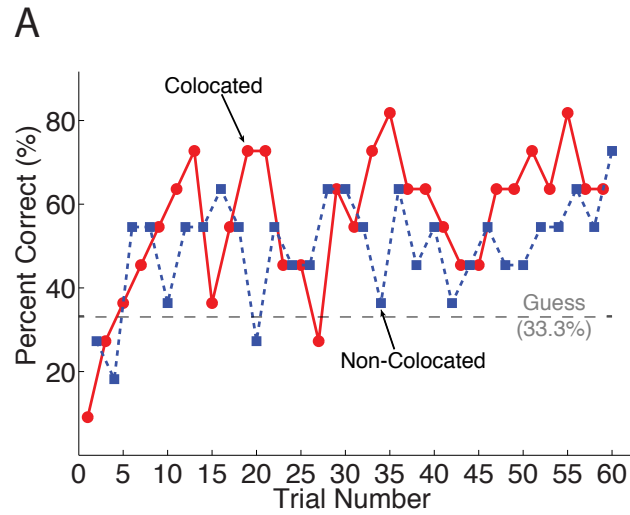


Figure 3.4: Object identification accuracy by feedback condition for the normal group of participants (N=11): (A) Average identification accuracy across participants for trials 1-60. (B) Average identification accuracy for the last 30 trials (31-60). Red traces represent the colocated condition. Blue traces represent the non-colocated condition. Error bars represent 1 standard error.

significantly lower in the colocated condition ($M=6.85s$, $SE=0.63s$) than in the non-colocated condition ($M=8.48s$, $SE=0.77s$), ($t(10) = -3.82$, $p = .002$ see Figure 3.5B). If we include the results of our outliers, trial duration was not significantly lower in the colocated condition ($M=8.88s$, $SE=1.27s$) than in the non-colocated condition ($M=10.82s$, $SE=1.53s$), $t(13) = -1.84$, $p = .088$.

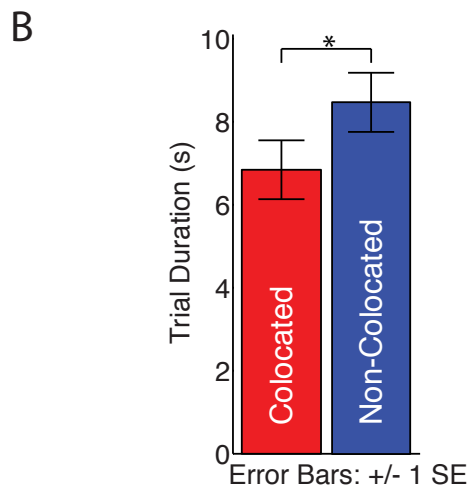
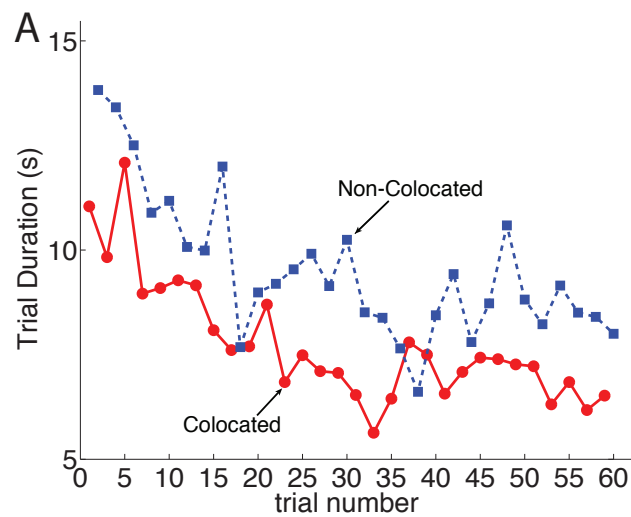


Figure 3.5: Trial duration by feedback condition for all subjects in the normal group (N=11): (A) Average trial duration for trials 1-60. (B) Average trial duration for the last 30 trials (31-60). Red traces represent the colocated condition. Blue traces represent the non-colocated condition. Error bars represent 1 standard error.

3.3.3 Object Exploration

3.3.3.1 Number of Probes

For both conditions, the average number of probes (for the normal group of participants) remained stable for the first 30 trials (Figure 3.6A). For the second set of 30 trials, there was a steady increase in the number of probes in the colocated condition from 1.89 probes to 2.68 probes. The average number of probes for the colocated condition in the second set of 30 trials was 2.24 ± 0.79 . For the non-colocated condition, the number of probes remained stable with an average of 2.72 ± 1.57 probes.

The difference between collocated and non-collocated conditions is not significant.

3.3.3.2 Probe Rate

For the collocated condition, the rate at which participants in the normal group probed the object increased from 0.11 probe/s in trial 1 to 0.31 probe/s in trial 12 (Figure 3.6B). In the non-collocated condition there was a slight increase from 0.21 probe/s to 0.28 probes/s. In the second set of 30 trials, the probe rate was stable with an average of 0.29 ± 0.02 probe/s in the collocated condition and 0.26 ± 0.03 probe/s in the non-collocated condition. The difference in probe rate between the two conditions is not significant.

3.4 Experiment Two: Methods

3.4.1 Participants

We tested $N=10$ able-bodied participants (six males, four females; mean age = 23.7 ± 4.6 years). Only one of these participants participated in the first experiment, but the time-gap between participation was 21 months. Nine of the ten participants were right-hand dominant. Prior to starting the study, each participant was consented according to a protocol approved by the University of Michigan Institutional Review Board and given an overview of the study.

3.4.2 Apparatus and Stimuli

3.4.2.1 Apparatus

Two single-axis linear voice-coil motors provided force feedback. These motors were identical to those described in section 3.2.2 except grips were attached so the motors could be pulled instead of pushed. This was done so that only the fingers of the hand were responsible for displacing the spring. Participants interacted with the motors by placing their palm on the palm-rest, and wrapping their fingers around the grip (see Figure 3.7).

A stimulus adjustment knob (see Figure 3.7) was used to adjust the stimulus intensity level. The knob featured a position indicator along with a scale in order for participants to track their adjustments during the experiment. The scale featured graduation marks, but was unnumbered so that participants had no numerical reference of intensity level between experimental conditions. In addition, a random gain

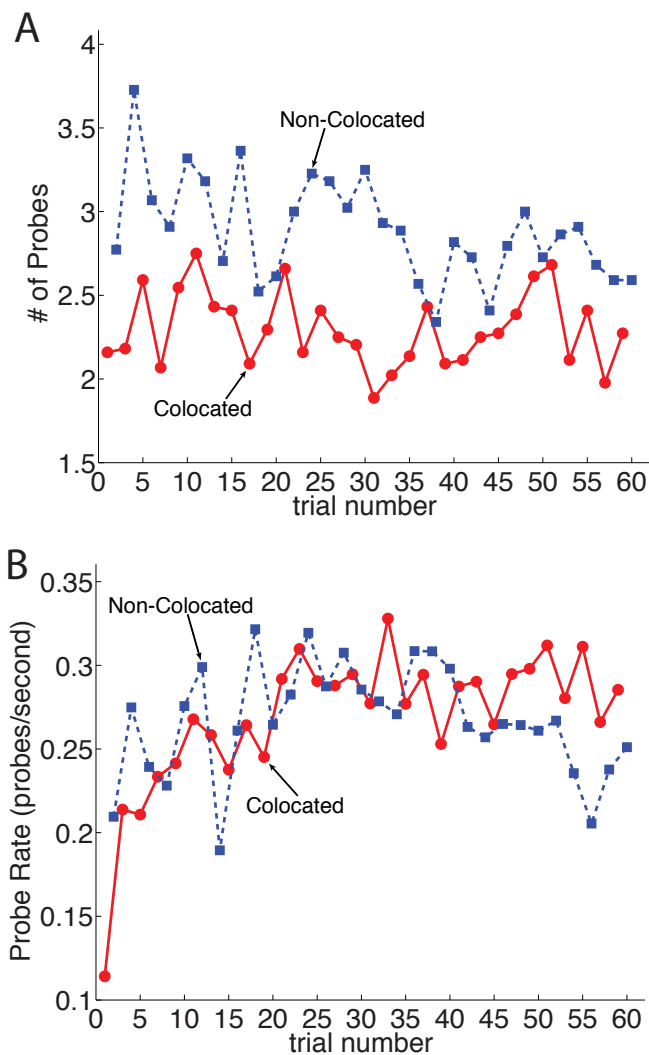


Figure 3.6: Object probe characteristics by feedback condition for all subjects in the normal group: (A) Average number of probes across participants for trials 1-60. (B) Average probe rate for trials 1-60. Red traces represent the collocated condition. Blue traces represent the non-collocated condition.

was used to convert the rotation of the knob to a variation in stimulus intensity. This will be described in more detail in section 3.4.4.

A curtain was placed over the motors so participants could not see the motor movement. Participants interacted with the motors by placing the palm of their hands on the palm rest, and their fingers on the grip (see Figure 3.7).

A small array of vibrotactile actuators (Pololu Shaftless Vibration Motor 10x3.4mm) provided vibrotactile feedback on the volar surface of the forearm (see Figure 3.8). The actuators were driven by an Arduino Mega I/O board and a custom transistor circuit. The tactors operated in the frequency range 0 – 133 Hz . The tactors were

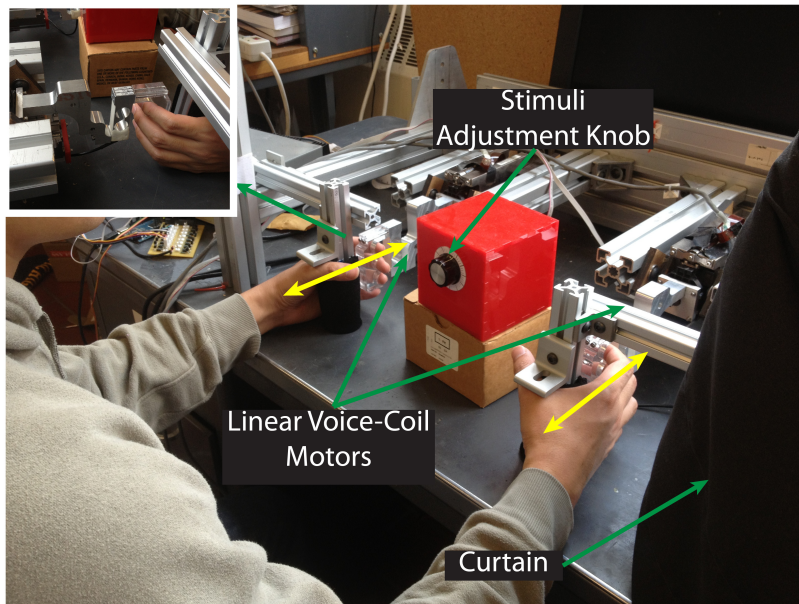


Figure 3.7: Two single-axis linear voice-coil motors lying in the horizontal plane. Yellow arrows indicate axis of motion. A stimuli adjustment knob contains a rotary knob with a position indicator. Inset figure shows grip attached to motor.

evenly distributed along the forearm between the bend in the wrist and the bend in the elbow with a 4 cm space between each tactor. The elastic straps were adjusted so that their circumference was 3 cm less than the circumference of the forearm at each tactor location, to ensure a snug fit. The tactors were attached to the elastic strap with Velcro.

3.4.2.2 Stimuli

The stimuli were presented in three different conditions. In the colocated condition, the motor held in the right hand (see Figure 3.7) was commanded to produce a force as a function of the right motor carriage displacement to render a virtual spring with variable non-linearity according to the following constitutive law:

$$F = A\alpha x_d^2 + B\alpha x_d + Cx_d \quad (3.2)$$

where $A = -3.7e^{-3}$, $B = 0.111$, and $C = 0.667$. The parameter x_d is the displacement of the right motor carriage measured in mm, and the parameter α controls the non-linearity of the spring. (Note that this relationship describes a parabola in Cartesian space with variable vertex $(36.06, \alpha)$, rotated about the angle $\theta = 33.69^\circ$.)

In the non-colocated condition, the motor held in the right hand (see Figure 3.7) was commanded to produce a force as a function of the carriage displacement of the motor held in the left hand to render the virtual spring given in Equation 3.2 with x_d as the displacement of the left motor carriage in mm .

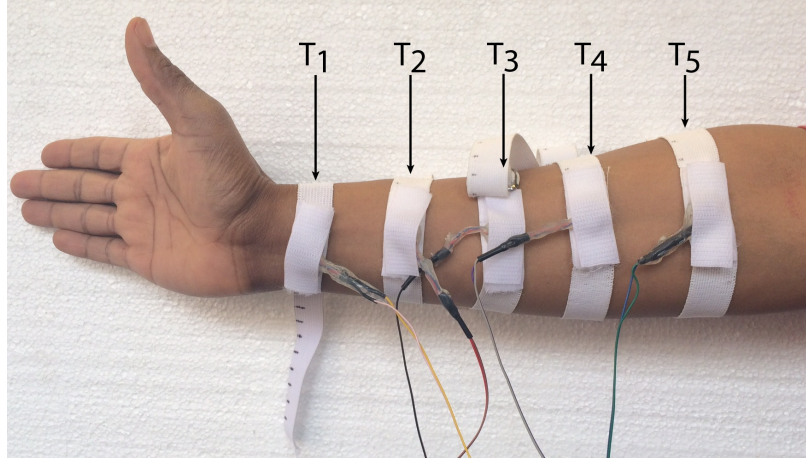


Figure 3.8: Tactile array with five tactors attached to volar surface of the forearm with elastic straps.

In the vibrotactile condition, the five tactors were temporally staggered in their actuation up the forearm as a function of the carriage displacement of the motor held in the right hand to render the virtual spring given in Equation 3.2 with x_d as the displacement of the right motor carriage in mm . Actuation started with the tactor closest to the wrist (T_1) and ended with the tactor closest to the elbow (T_5). The actuation of each tactor ($T_i, i = 1, \dots, 5$) was governed according to the following expression:

$$T_i = Fm_t - (i - 1)s_t, \quad i = 1, \dots, 5 \quad (3.3)$$

where F is the force from the spring given by Equation 3.2, $m_t = 0.75 V/N$, and $s_t = 2.5 V$. Note that the command to the tactors was limited to the voltage range $(0, 5)$.

To determine the relationship between the command to the tactor (T_i) and the output frequency (f), an analysis was conducted with a 3-axis accelerometer (Freescale MMA726). The accelerometer was attached to the surface of the tactor with adhesive, and both were attached to the forearm using the same elastic strap as in the experiment. Command voltages from 0-5 V were sent to the tactor. The resulting empirical relationship was fit by the following expression

$$f = \begin{cases} 0 \text{ Hz} & \text{if } T_i < 1 \text{ V} \\ k_h T_i + b_h \text{ Hz} & \text{if } 1 \text{ V} \leq T_i \leq 5 \text{ V} \end{cases} \quad (3.4)$$

where $k_h = 20.75 \text{ Hz/V}$ and $b_h = 29.67 \text{ Hz}$. Note that at least 1 V needed to be supplied to the tactors to initiate a consistent vibration of $\sim 50 \text{ Hz}$.

A family of virtual springs with different degrees of non-linearity was created by varying the parameter α on the interval $\alpha \in [-6, 6]$ in increments of $.02$, creating a total of 601 different springs. The following boundary conditions were placed on the springs.

$$F = \begin{cases} 20 \text{ N} & \text{if } x_d \geq 30 \text{ mm} \\ 0 \text{ N} & \text{if } x_d \leq 0 \text{ mm} \end{cases} \quad (3.5)$$

For the case $\alpha = 0$ a linear spring is generated. All other springs given by $\pm\alpha$ are symmetric about this linear spring. A few select springs from the set are shown in Figure 3.9. The springs above the linear spring correspond to $+\alpha$ and are ‘softening’ springs. The springs below the linear spring correspond to $-\alpha$ and are ‘hardening’ springs.

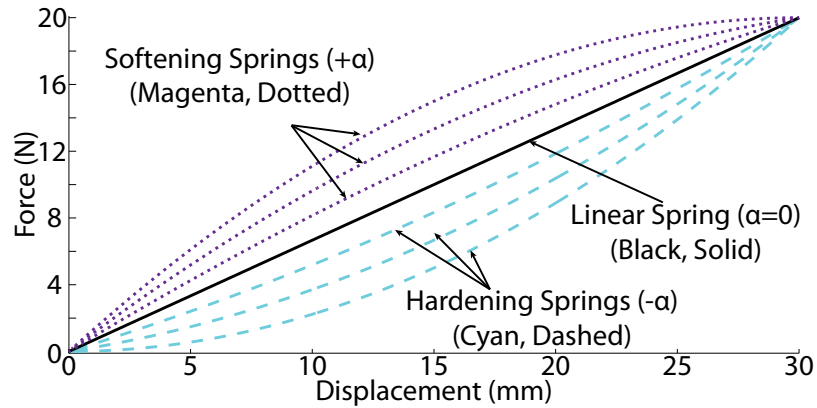


Figure 3.9: Sample virtual springs. Springs each have a parabolic force/displacement relationship. Linear spring (Black, Solid) corresponds to $\alpha = 0$. Springs above the linear spring (Magenta, Dotted) correspond to $+\alpha$ and are ‘softening’ springs. Springs below linear line (Cyan, Dashed) correspond to $-\alpha$ and are ‘hardening’ springs.

3.4.3 Training

Participants were trained on the three different feedback conditions: collocated, non-collocated, and vibrotactile. In the collocated condition participants displaced the

virtual springs with their right hand and the right motor, and the device provided force feedback to the right hand through the right motor. In the non-colocated condition, participants displaced the virtual springs using their left hand and the left motor and force feedback was displayed to their right hand through the right motor. In the vibrotactile condition, participants extended the virtual springs with their right hand and vibrotactile feedback was displayed on their right forearm.

In the training session participants were allowed to feel the linear spring ($\alpha = 0$), a hardening spring ($\alpha = -6$), and a softening spring ($\alpha = 6$) in each condition. The linear spring was presented first in each condition to help familiarize the participant with the given condition. The hardening and softening springs were then presented to the participant in each condition. All three springs were presented alongside a visual aid that showed their force/displacement profiles. Training was considered complete when the participant could correctly identify four random presentations of the springs in each condition without the visual aid.

3.4.4 Testing

Our testing protocol differs from the typical method of adjustments [77]. Rather than starting from a stimulus intensity level well above or below the threshold for each stage, our protocol borrowed from adaptive procedures in that the stimulus intensity for each stage was based on the final intensity of the previous stage. In addition, our protocol was designed to compare two variable stimuli, as opposed to one variable stimuli and one reference stimuli. The intent was to increase the efficiency of the test.

The spring’s non-linearity was controlled through the stimulus adjustment knob. The mapping between the angular displacement of the knob (θ) and the parameter α was governed by the following equation:

$$\alpha = (-6/\theta_n)\theta + 6 \tag{3.6}$$

where the parameter $\theta_n \in [100^\circ, 270^\circ]$ and was randomly selected by the computer at the beginning of each trial in increments of 10° . This was done so that θ was not duplicated in each trial. Clockwise turns of the knob increased θ and decreased α . Counter-clockwise turns of the knob decreased θ and increased α , however θ was limited to non-negative values. If the knob was turned past θ_n , θ would reset to $\theta = 0$ and θ_n would reset to a new randomly selected value. This was done to penalize participants for randomly guessing where the springs were equal ($\theta = \theta_n$, $\alpha = 0$)

In the test, participants were presented with a variable softening spring ($+\alpha$) and a variable hardening spring ($-\alpha$). As they adjusted the knob, they varied the non-linearity of both springs. The goal was to determine the smallest amount of non-linearity they could detect between the two springs in each of the three conditions.

The test consisted of one trial for each of the three conditions, presented at random. In the each trial, there were five stages. In Stages 1, 3, & 5 participants were instructed to adjust the knob clockwise until they could no longer feel the difference between the two springs. In Stages 2 & 4, participants were instructed to adjust the knob counter-clockwise until they could just notice the difference in the the two springs. In each case participants were allowed to adjust in the opposite direction if they felt they adjusted too far.

For Stage 1, the springs started at $\alpha = \pm 6$, the hardening and softening springs presented during training. For Stages 2-5, the starting value of α in each stage corresponded to the final value of α in the previous stage. At the start of each stage, participants were instructed to feel each spring before adjusting α . The spring presentation was controlled by the experimenter and presented to the participant as requested. After each adjustment of α , participants were allowed to feel the hardening and softening spring as many times as needed before making any further adjustments to α . The only requirement was that they felt each spring an equal number of times. After each stage participants were allowed to take a break.

3.4.5 Metrics and Data Analysis

The kinematic and performance data were recorded to disk with a 1 kHz sampling rate. The encoder measurements for the motors were filtered using a 5th order low-pass butterworth filter with a 5Hz cutoff frequency. Subsequently, all data was down-sampled to 500 Hz.

Our metrics consisted of two separate psychometric measures with respect to the non-linear parameter α , as well as the results from a post-test survey administered to each participant.

3.4.5.1 Psychometric Measures

The first measure, the Absolute Threshold (AT), is a measure of the smallest value of non-linearity parameter α that participants could detect in the two stimuli. The second measure, the Separation Threshold (ST) is a measure of the value of the non-linearity parameter required for participants to notice a difference between

the two stimuli. Note, this metric is very similar to the difference threshold found in traditional psychophysics studies. However, we are not comparing our variable stimulus to a fixed reference. In our case, the reference stimulus is also variable, and is determined as the point at which the two stimuli feel equal.

As mentioned in the previous section, the test consisted of five stages for each of the three conditions. In stages 1, 3, & 5, participants were instructed to adjust α until they could no longer feel the difference between the two stimuli. These stages will be referred to as the ‘Equality Stages.’ In stages 2 & 4, participants were instructed to adjust α until they could just notice the difference in the two stimuli. These stages will be referred to as the ‘Difference Stages.’

The Absolute Threshold (AT) for each condition was computed as the mean of the final α value in each of the last four stages. This corresponds to the final value of α at the end of Difference Stage 2 (α_{D2}), Equality Stage 3 (α_{E3}), Difference Stage 4 (α_{D4}), and Equality Stage 5 (α_{E5}), as shown in Equation 3.7 below. The final value of α for Equality Stage 1 (α_{E1}) was excluded from this measurement as it represented an exploratory baseline for each participant.

$$AT = \frac{\alpha_{D2} + \alpha_{E3} + \alpha_{D4} + \alpha_{E5}}{4} \quad (3.7)$$

The Separation Threshold (ST) for each condition was computed as the mean difference between the final value of α for the last two Difference Stages and the last two Equality Stages. This corresponds to the difference between the final value of α in Difference Stage 2 (α_{D2}) and Equality Stage 3 (α_{E3}), as well as between Difference Stage 4 (α_{D4}) and Equality Stage 5 (α_{E5}) as shown in Equation 3.8 below.

$$ST = \frac{(\alpha_{D2} - \alpha_{E3}) + (\alpha_{D4} - \alpha_{E5})}{2} \quad (3.8)$$

3.4.5.2 Post-Test Survey

Our post-test survey represents a qualitative self-assessment of each participant’s perceived performance on the task, as well as a subjective assessment of the three conditions. The survey contained a mix of Likert-based, short-answer, multiple-choice, and ranking questions. The entire survey had 18 questions, and can be found in Appendix A. Only the questions with quantitative responses will be discussed further.

Question 3 asked participants to choose on a scale of 1-7 (1-‘very difficult’ and

7-‘very easy’) how easy/difficult each condition was. Question 10 asked participants to choose on a scale of 1-5 (1-‘strongly disagree’ and 5-‘strongly agree’) how well they agree/disagree with the statement that the colocated condition required more concentration than the non-colocated or vibrotactile conditions. Question 11 was similar to question 10, except that it compared the non-colocated condition to the colocated and vibrotactile conditions. Question 12 was similar to question 11, except it compared the vibrotactile condition to the colocated and non-colocated conditions. Question 15 asked participants on a scale of 1-5 (1-‘strongly disagree’ and 5-‘strongly agree’) how well they agree/disagree with the statement “I would be able to perform the task while holding a conversation” in each of the three conditions. Question 16 asked participants to rank the three conditions in order of preference. In analyzing the results, the various levels of ‘agree’ and ‘disagree’ (i.e. ‘strongly agree’, ‘somewhat agree’, and ‘agree’) were grouped into a single ‘agree’ or ‘disagree’ category, due to the small number of participants. The same was done for the ‘difficult’ and ‘easy’ Likert-based questions.

3.4.6 Statistical Analysis

Linear mixed models (LMM) were used for the Absolute Threshold (AT) and Separation Threshold (ST) using SPSS (v.21) for estimating fixed and random coefficients. Within the model, participants were a random effect while condition was a fixed effect. For the Absolute Threshold (AT), the final value of α in the last four stages is treated as a repeated measure. For the Separation Threshold (ST), the two difference measures are treated as a repeated measure. Bonferroni adjustments were applied to the estimated means to control for Type I errors. A p-value of 0.05 was used as a threshold for significance.

3.5 Results: Experiment 2

Overall, our participants were able to detect smaller differences in the non-linearity of the springs with colocated force display than with non-colocated force display, and smaller differences in the non-linearity of the springs with colocated force display than with vibrotactile display. Participants took on average 9.91 ± 3.49 min and made 18.50 ± 8.44 finite adjustments of α in the colocated condition, 11.78 ± 2.35 min and 15.80 ± 5.35 finite adjustments of α in the non-colocated condition, and 12.52 ± 4.70 min and 15.40 ± 5.93 finite adjustments of α in the vibrotactile condition. As demonstrated by a representative sample participant (see Figure 3.10), 7.56 min and 15

adjustments were taken for the colocated condition, 16.45 min and 17 adjustments were taken for the non-colocated condition, and 9.90 min and 10 adjustments were taken for the vibrotactile condition. The final value of α in each of the five stages is indicated by the solid circles on the traces.

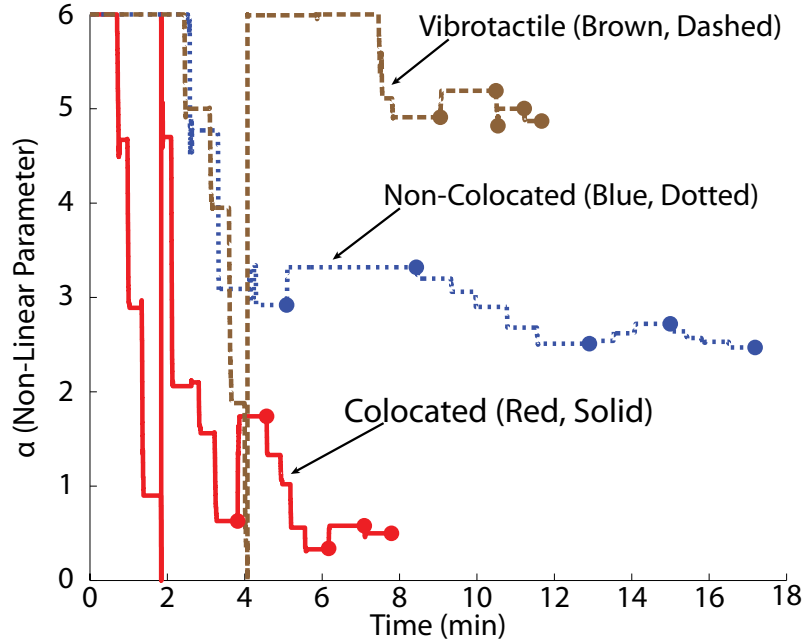


Figure 3.10: Time-domain trajectory of α for a representative participant. Solid red traces represent the colocated condition. Dotted blue traces represent the non-colocated condition. Dashed brown traces represent the vibrotactile condition. Solid circles represent the end of each stage. This particular participant caused a reset of α in both the colocated and vibrotactile conditions by turning past $\alpha = 0, \theta = \theta_n$.

To show the collective results of all participants, the time-domain trajectory of α for each participant at each stage was time-warped to a standardized length. This was accomplished by normalizing the sampled points of the trajectory with respect to the duration of that stage. This was done separately for each condition and each stage for every participant. The resulting trajectories are combined and averaged for all 10 participants as shown in Figure 3.11. In the colocated condition, participants chose on average smaller values of α on all five stages of the experiment, including the three stages aimed at finding the point where the springs felt equal (*Equality Stages*), and the two stages aimed at finding the point where the springs felt noticeably different (*Difference Stages*).

The Absolute Threshold (AT), taken as the mean of the final value of α in the last four stages (α_{D2} , α_{E3} , α_{D4} , and α_{E5}) was significantly smaller in the colocated condition than in the non-colocated condition ($\beta = -.716$, $SE = .271$, $p = .028$)

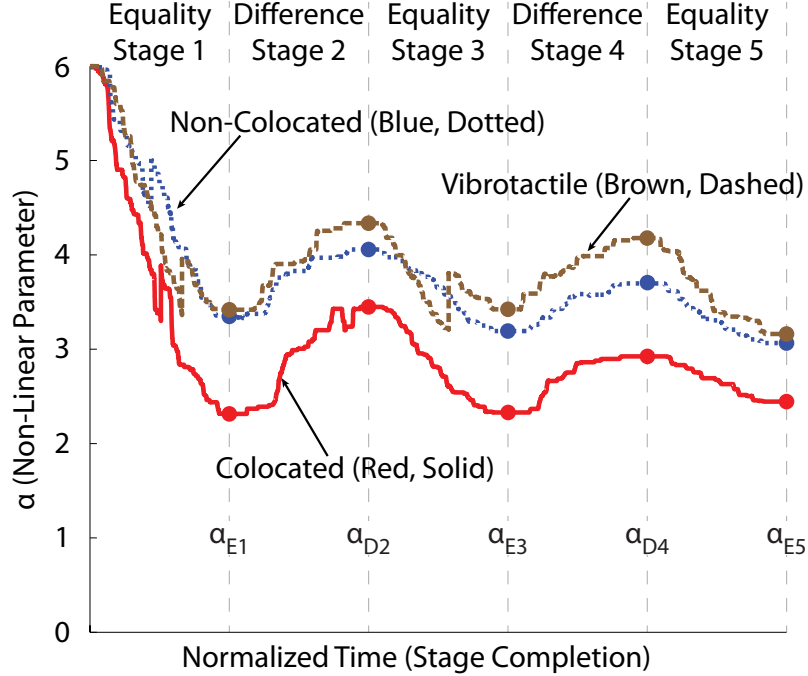


Figure 3.11: Average trajectory of α for all participants in the three conditions. Time has been scaled and normalized to the completion of each stage prior to averaging. Solid red traces represent the colocated condition. Dotted blue traces represent the non-colocated condition. Dashed brown traces represent the vibrotactile condition. Solid circles represent the end of each stage. The large jumps in the trajectory are due to a reset in θ_n or large adjustments by certain participants.

or the vibrotactile condition ($\beta = .988$, $SE = .271$, $p = .001$) (Figure 3.12A). The Separation Threshold (ST), taken as the mean of the difference in the final value of α between the last four stages ($\alpha_{D2} - \alpha_{E3}$ and $\alpha_{D4} - \alpha_{E5}$) was not significantly different for each condition. (Figure 3.12B).

3.5.1 Survey Results

From a qualitative perspective, our participants preferred the colocated condition over the non-colocated condition and the vibrotactile condition (see Table 3.1). The majority of participants found the colocated condition less difficult than the non-colocated or vibrotactile conditions (Question 3). They found that the non-colocated and vibrotactile conditions required more concentration than the colocated condition (Questions 10-12). The majority of participants found that the task was difficult to complete in any condition while distracted (Question 15). Overall the majority of participants ranked the colocated condition first, the vibrotactile condition second, and the non-colocated condition third (Question 16).

Table 3.1: Post-Test Survey Results (# responses)

		Difficult	Neutral	Easy
Question 3	CL	1	7	1
	NCL	6	2	1
	V	7	1	1
		Disagree	Neutral	Agree
Question 10	CL vs. NCL	8	1	1
	CL vs. V	7	1	2
Question 11	NCL vs. CL	3	0	7
	NCL vs. V	5	0	5
Question 12	V vs. CL	3	1	6
	V vs. NCL	4	0	6
Question 15	CL	6	4	0
	NCL	9	1	0
	V	8	1	1
		First	Second	Third
Question 16	CL	7	1	2
	NCL	1	3	6
	V	2	6	2

Colocated (CL), Non-colocated (NCL), Vibrotactile (V).
 Question 3 only contains 9 responses as one participant did not answer. Questions 13 & 14 have been omitted due to conflicts in the answers.



Figure 3.12: Psychometric Measures. (A) Mean Absolute Threshold (AT) for all 10 participants in each of the three conditions. (B) Mean Separation Threshold (ST) for all 10 participants in each of the three conditions. Error bars represent 1 Standard Error.

3.6 Discussion

In this study we have determined that filtering power from an invariant force/motion relationship degrades stiffness discrimination performance and psychometric sensitivity. We have arrived at this conclusion through a comparison of three different haptic displays all designed to interface a user to the same family of virtual non-linear springs. What differs between these three displays is the manner in which the force/motion relationship of a spring is presented to the user. In our colocated force display, the user’s exploratory motion (action) and the spring’s resulting force (re-action) occur on the same hand. The coupled force/motion information of the spring remains coupled through the interface to the user’s hand, thereby allowing a power exchange to occur. In our non-colocated force display, action and re-action occur on separate hands. Although the same force/motion information is available to the user (force in one hand, motion in the other), the coupled force/motion information of the spring gets decoupled through the interface to the user’s two hands, and does not support support for a power exchange. In our vibrotactile display, action comes from the user’s hand, and re-action (the spring’s resulting force) gets encoded as a vibration that is presented on the user’s forearm. The coupled force/motion information of the spring gets transformed to a decoupled force/vibration relationship through the interface, thereby lacking support for a power exchange as well.

The comparison of colocated force display and vibrotactile display can be con-

sidered an “apples to oranges” comparison because it involves both a change in action/re-action coupling (colocated to non-colocated), as well as a change in information encoding. Here, we have introduced the non-colocated force display as a new type of experimental condition that acts as a true control condition. By allowing a comparison of action/re-action coupling without a change in information encoding, an “apples to apples” comparison is now possible.

3.6.1 Task Performance

In our first experiment, participants were able to more accurately identify the three virtual springs ($p = .003$ see Figure 3.4) in the shortest amount of time ($p = .002$ see Figure 3.5) with colocated force display as opposed to non-colocated force display. Leaving out the first set of 30 trials, where learning of the unique force/motion relationship of each spring is taking place, accuracy in the second set of 30 trials was ~64% in the colocated condition and ~52% in the non-colocated condition. In addition, trials lasted ~6.9 s in the colocated condition and ~8.5 s in the non-colocated condition.

Tan *et al* [26] found that when the work cue and terminal force cue were dissociated from the compliance cue, the resolution with which participants could distinguish compliance was poor. In this study, the lack of power exchange in the non-colocated condition is akin to the dissociated work cue in that the work done by both hands is not equal to the work of the spring. The terminal force cue has also been removed as all springs have the same terminal force.

Lederman and Klatzky [73] also found that in addition to decreased object identification accuracy, response time increased when various haptic cues (spatial, temporal, thermal, and kinesthetic) were reduced through constraints on manual exploration. In the same manner, the non-colocated condition reduced the power cue from the force/motion relationship of the spring, resulting in decreased object identification accuracy and increased response time.

It is also worth considering that the non-colocated condition was not performed in isolation (each trial alternated between the colocated and non-colocated conditions). Identification accuracy was better in the colocated condition, so it is possible that experience in the co-located condition helps participants rule out one of the three springs in the non-colocated condition. Participants could very well still be guessing in the non-colocated condition, with the exception that they only have two choices to choose between, thus leading to an accuracy of 50%.

Accuracy in the non-colocated condition was only 12% below the colocated condi-

tion, and trial duration was only 1.4 s slower than the colocated condition. With increased exposure and training, these differences may disappear. Unfortunately, most participants have limited attention spans and patience for complicated interfaces, oftentimes deciding in the first few minutes of use whether a particular interface is useful. In this experiment, participants used each display for ~ 30 min. Given that there were no significant differences between the number of probes (and the probe rate), it is clear that more effort was not given to either condition. Our findings then suggest these differences across condition exist because the colocated condition allows a power exchange to occur and the non-colocated condition does not.

Non-colocated action/re-action coupling has been shown to have detrimental effects outside of human-machine interfaces. In robotics in particular, an extensive body of research exists on the performance effects of having the actuator and sensor non-colocated at the same point on the robot. Significant work by Eppinger and Seering [78] have shown that when the sensor and actuator are located between compliant elements of the robot, the actuator and sensor can vibrate out of phase. This non-colocated actuator sensor architecture introduces dynamic instability, and results in poor performance of robotic force control. In our non-colocated force display, the actuator (left hand) and the sensor (right hand) are located on different sides of the body. Although our identification task has little to do with force control, the performance decline in both situations can be attributed to the lack of colocated coupling between action and re-action.

3.6.2 Psychometric Performance

In our second experiment, participants could detect smaller differences between two non-linear springs with colocated force display than with non-colocated force display ($p = .028$ see Figure 3.12). They were also able to detect smaller differences with colocated force display than with vibrotactile display ($p = .001$ see Figure 3.12). While force discrimination and stiffness/compliance discrimination have been considered in the literature [21, 22, 26, 79], we are not aware of any work that has analyzed discrimination when either action/re-action coupling changes, or when information encoding changes.

Unlike traditional psychophysics experiments that report the just noticeable difference between a variable stimulus and a reference [77], our experiment compared two variable stimuli with equal and opposite non-linearity. Our springs presented a dynamic stimulus that depended on displacement. In addition, they have the same initial and terminal force. We presume that our participants did not use force or

displacement information individually. Therefore, our findings cannot predict exactly the displacement value or force value that participants used to discriminate between the two springs, if one exists at all. Rather, in our experiments participants discriminated between the force/motion relationship of the springs.

In our first experiment we saw task performance differences between the colocated and non-colocated conditions, but it could be argued that these performance differences could be diminished, or disappear with training and more experience. Here, our results point to limitations that are potentially invariant with respect to training and increased exposure. Synthesizing the information from the left and right hands took more time in the first experiment, however we placed no time limitations on participants to perform the task in the second. Identification accuracy performance for non-colocated force display was below that for colocated force display. In this experiment however, participants were able to differentiate between springs that were considerably more linear than the two non-linear springs in experiment one. The maximum force difference between the orange and green spring of the first experiment was 7.46 N , and the maximum force difference between the absolute threshold springs for the non-colocated condition ($\alpha = 3.5$) was 5.83 N . Note that these forces are not within the Just Noticeable Difference (7%) reported for force sensing [21, 22].

Since the same resultant force is presented to the right hand in both force display conditions, discrepancies in force discrimination are not likely causing the differences in sensitivity. Also, we can assume that proprioceptive sensing is equivalent in both hands, and that participants were completely aware of their motion input in both conditions. Since the force/motion information is exactly the same, yet sensitivity does differ by condition, we are left to believe that the only difference is that non-colocated force display lacks the ability to transmit power. This power transfer apparently allows participants to detect smaller differences in the springs.

In our second experiment we also considered the psychometric performance of vibrotactile display. Like force display, vibrotactile display is widely used in haptic interfaces [16, 42, 74, 80–82]. Therefore, we attempted to compare colocated force display to a haptic modality that has more potential use, even if this is an “apples to oranges” comparison. Our findings however were the same as with the “apples to apples” comparison with non-colocated force display; participants could detect smaller non-linear differences in the colocated condition than in the vibrotactile condition.

With vibrotactile display, action/re-action coupling is non-colocated and a change in haptic display modality occurs. It is true that we have only considered one type of vibrotactile display, and that other variations exist that modulate the frequency and

amplitude intensity, the number of factors, the body site location, the waveform, or the vibration patterns [77,80]. In general however, vibration frequency and amplitude discrimination (3-30% and 13-16% respectively) are significantly more variable than force (7%) [77]. Therefore, in addition to the lack of power exchange, information encoding may be responsible for the larger differences seen between the colocated force display and vibrotactile display.

As with the number of probes (and the probe rate) in experiment one, the lack of significant differences in the separation threshold between the three conditions suggest that participants were not turning the knob at random given that θ_n was different for each condition for each participant. Apparently there existed a certain amount of non-linearity that participants needed in order to feel comfortable that the two springs were in fact different. This difference did not seem to be effected by the type of display.

3.6.3 Haptic Display Considerations

Overall our findings suggest that task performance and psychometric sensitivity are degraded when power is filtered from the force/motion relationship of stiffness, as is the case with non-colocated force display and vibrotactile display. Although power is redundant information in the force/motion relationship for stiffness, its absence appears to have an effect. Perhaps this is because the power transfer allowed by colocated force display aligns well with the user's prior experience with their natural limbs. In addition, this power exchange couples the dynamics of the spring to the dynamics of the participant's limb. Due to this dynamic coupling, participants could be performing a system identification experiment on the springs since the dynamics of their limbs are already known via the proprioceptive and kinesthetic senses.

In a previous study from our lab [40], we found there to be no difference between the colocated and non-colocated conditions. This finding was consistent with results by Cholewiak *et al* [79] and Tan *et al* [26], who found that the terminal force can be used to determine the compliance of an object in the absence of work cues. Since our springs in that study were linear leaf springs, participants could ignore the work cues altogether and utilize only the terminal force cues. In our current experiments, we eliminated the terminal force cues by creating virtual springs with the same terminal force (and same initial force). What we did change however was the force-displacement (work) profile of each spring.

Performing the non-colocated force condition accurately required holding the right hand as still as possible to only sense the force induced by the motion in the left

hand. A few participants mentioned having difficulty sensing force in the right hand because of the motion induced by the force. Still, over half of our participants in the first experiment reported that the colocated condition was easier overall than the non-colocated. In the second experiment our qualitative results tell a very similar story, with participants favoring the colocated condition to the non-colocated and vibrotactile conditions.

Although most participants reported their right hand as their dominant hand, the current protocol in either experiment does not take into account handedness. To balance the protocol, participants should be tested with the motors switched in the two force display conditions and the motor and forearm switched in the vibrotactile display condition. It might also be worthwhile to compare the results of our second experiment with results from other psychometric procedures.

Demonstrating that both changes in action/re-action coupling as well as changes in information encoding (via changes in haptic modality) from the environment to the user should have an impact on the design of haptic interfaces. All haptic displays are not created equal. Therefore, those displays which have the potential to filter information pertaining to the invariant relationships within the environment should be avoided. Perhaps the best evidence of this can be seen in the utilization of haptic feedback in upper-limb prosthetic devices. Those haptic displays which give the amputee full access to the information contained within invariant relationships explored by the prosthetic limb, such as colocated force display, will align with the amputee's prior experience with their natural limb, and will result in better overall performance. For an amputee, that means giving them the ability to perform tasks often taken for granted, such as knowing how hard to squeeze a child's hand while crossing a busy intersection, choosing a ripe fruit in a market, or finding their reading glasses in a dark room.

CHAPTER IV

[Characterizing the Gold Standard:] Assessing the Impact of Vision and Force Feedback in a Body-Powered Prosthesis

4.1 Introduction

When an individual loses a upper-limb due to amputation, not only motor function but sensory function is lost as well. Restoring full function with an artificial limb requires closed-loop and anticipatory control, both of which depend on sensory feedback from the point of interaction with the environment. Closed-loop control is only possible when pathways for both the efferent and afferent nerves are established between the amputee and the prosthesis. In this manner, a prosthesis provides an interface between the amputee's residual limb and the environment, similar to the manner in which a teleoperator interfaces a human user to a remote environment.

Looking at teleoperators and prostheses more generally, their evolutionary paths follow similar trajectories. Indeed, the original teleoperators developed by Goertz [27, 28, 83, 84] featured mechanical linkages between the manual control interface operated by the user (the 'master') and the end-effector handling the radioactive material (the 'slave'). The advantage of these mechanical linkages was that they provided inherent force-reflection between the master and the slave side of the device. Any forces generated by the operator were transmitted to the slave side of the device. Likewise, any force sensed on the slave side of the device (hitting a rigid object for example) were transmitted to the operator through the master.

In a similar manner, body-powered prostheses feature a mechanical linkage between the shoulder harness and the terminal device. This mechanical linkage, nominally provided through a Bowden cable, provides inherent force-reflection between the shoulder harness and the terminal device. It is worth making the distinction here

that the type of force-reflection in a body-powered prosthesis depends on the type of terminal device. For voluntary-opening terminal devices, a spring nominally holds the device closed. Pulling on the cable through the shoulder harness opens the device. Therefore, the only forces that get transmitted from the terminal device to the amputee's shoulder are those that act to resist the device from opening, usually just the spring force. For voluntary-closing devices, a spring nominally holds the device open. Pulling on the cable through the shoulder harness closes the device. Therefore, the only forces that get transmitted from the terminal device to the amputee's shoulder are those that resist the device closing. This includes the spring force, as well as a force produced by any object in the grip of the terminal device.

In the next stage of teleoperator evolution, the mechanical linkage between the master and slave was replaced by a motorized slave. These unilateral teleoperators allowed the operator and master to be physically located further from the slave. In addition, motorizing the slave device allowed for less cumbersome mechanical linkages between the master and slave, as well as more degrees of freedom. Despite these benefits, these teleoperators lacked the inherent force-reflection available in the mechanical teleoperators. This lack of force-reflection has detrimental effects on the operator's ability to perform tasks with the teleoperator [57–59].

In a similar evolutionary step, the terminal device of the body-powered prosthesis has been motorized. Instead of relying on a cable and shoulder harness to control the terminal device, electromyographic signals, generated from contraction of the muscles are used. These myoelectric prostheses allow the user to control both opening and closing of the terminal device, as well as more degrees of freedom in the terminal device. In addition, embedding myoelectric sensors in the prosthetic cuff and the use of small highly geared motors allows for the development of limbs that look more like their natural counterparts. Like the unilateral teleoperators, myoelectric prostheses lack the inherent force-reflection available with body-powered prostheses, forcing amputees to rely even more on vision and audition to supplement the lack of force. As it turns out, the deficit caused by this lack of force-reflection has yet to be empirically quantified.

The lack of force-reflection in unilateral teleoperation, and the associated decrement in performance promoted the development of bilateral teleoperators. Bilateral teleoperators feature both a motorized slave and a motorized master [28]. Using a variety of control architectures including position-position control and position-force control [85], these teleoperators are capable of providing force-reflection between slave and master similar to their original mechanical version.

For myoelectric prostheses, evolution has taken a path divergent from that of teleoperation. While teleoperation has shifted focus to feedback (the field of haptic feedback has its origins in teleoperation), prosthetics has shifted focus to control. This change in focus, however, is not without merit. It is readily apparent that the interface between the amputee and prosthesis requires a great deal of referral in the sense of control. Whereas the human operator controls the teleoperator with their hand(s) on the master, amputees control their prosthesis through a body part other than the hand (i.e. the shoulder) or muscles in the residual limb. Control from the shoulder or a muscle in the residual limb involves compromises such as limited degrees of freedom in the device. Therefore, recent research on upper-limb prosthetics has focused on more advanced control techniques, including targeted muscle reinnervation [43] and myoelectric pattern recognition algorithms [86]. In addition, advancements in sensors and actuators have led to the development of multi-degree of freedom limbs that feature almost as many articulations as the human hand.

Despite the benefits of advanced control techniques, these advanced myoelectric prostheses are still analogous to the unilateral teleoperator. Without adequate force reflection, amputees are still reliant upon vision and audition for sensory feedback. The desire for increased feedback in myoelectric devices and less reliance on vision is well established in the amputee community [34,35]. If the master side of the prosthesis was motorized to provide force-reflection, would amputees have the additional utility they desire? This question cannot be answered by comparing current myoelectric and body-powered prosthetics, as there are too many differences including the manner in which control is derived (shoulder articulation as opposed to EMG).

To begin answering this question we have developed a mock prosthesis to be worn by able-bodied individuals that features removable force-reflection. By design our prosthesis resembles a body-powered prosthesis. The action of the terminal device is linked to the action of a body part through a Bowden cable; here the elbow is used instead of the shoulder. In other ways our prosthesis resembles a myoelectric prosthesis. Rather than directly connecting the terminal device to the user through the Bowden cable, the user's elbow angle is measured by an electronic encoder, and used to drive a linear actuator that is connected to the terminal device through a Bowden cable. Unlike myoelectric or body-powered prostheses, our mock prosthesis features a force transducer in series with the cable-drive terminal device. The forces measured by this transducer are displayed to the user through a separate linear actuator and elbow exoskeleton connected by a Bowden cable. In teleoperator language, our mock prosthesis is a bilateral force-reflecting teleoperator with a motorized master and a

motorized slave. By changing the control architecture from position-force to position only, our device quickly becomes a unilateral non force-reflecting teleoperator. Note that both the control and the force feedback are referred from and to the elbow joint.

In this study, we have undertaken an experiment to assess the impact of both vision and force feedback in the control of an upper-limb prosthesis. Using able-bodied individuals, we have conducted an experiment that compares participant’s ability to distinguish between a set of objects based on their stiffness in four separate conditions with and without vision, and with and without force feedback. Experiments with our new mock prosthesis will allow us to quantify the benefits of force feedback using a properly controlled experiment that removes the inherent differences between myoelectric and body-powered prostheses.

4.2 Methods

4.2.1 Participants

We tested $n=10$ able-bodied participants (seven male, three female; mean age = 24.3 ± 2.9 years). Prior to starting the study, each participant was consented according to a protocol approved by the University of Michigan Institutional Review Board (IRB) and provided with an overview of the study.

4.2.2 Experimental Apparatus

Our experimental apparatus consisted of two linear actuator drives, a custom mock prosthesis, and a custom cable-driven elbow brace. A Dell Precision T3500 Desktop computer with a Sensoray 626 PCI data acquisition card was used for data acquisition and computer control.

Both linear actuator drives featured a Maxon RE65 rotary motor and a linear ballscrew with a 20 *mm* lead (see Figure 4.1). Each motor was equipped with a rotary optical encoder (US Digital EM1-1-1024) and driven with a current sourcing amplifier (Advanced Motion Control 12A8). A 10-kg rated beam load cell (Transducer Techniques LSP-10) was attached to the ball nut of each ball screw screw through a custom ABS 3D printed carriage. The carriage was attached to linear slides so that it could move freely with the ball nut. Two limit switches were placed along the length of the ballscrew to limit the actuator’s range of motion. Each actuator drive provided pulling-based actuation for a Bowden cable. The cable housing was mounted at the end of the ballscrew to a cable housing support structure, and the cable was attached

to the loadcell through an attachment plate.

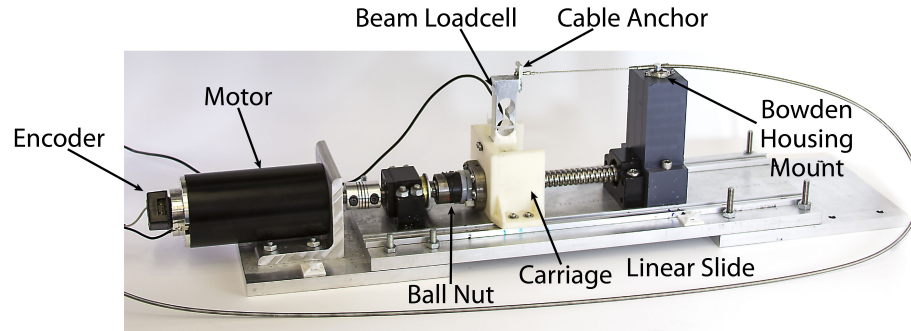


Figure 4.1: Linear actuator drive featuring rotational motor, encoder, ballscrew, beam loadcell carriage, loadcell carriage, Bowden cable anchor and housing mount, and linear slide. In operation, the motor, ballscrew, and carriage tracked a desired position to generate no force on cable, or produced a pulling force on the cable.

The mock prosthesis (see Figure 4.2) consisted of a thermoplastic shell mated with a Hosmer Quick Disconnect Wrist - USMC style and voluntary-closing terminal device (TRS Grip 2S), which was nominally held open by an internal torsional spring. The prosthesis was designed to mate to the right arm of an able-bodied participant. The thermoplastic shell was fabricated by casting the forearm and hand of a healthy subject with their hand in a closed (fist) position. The cast was digitized using an Ohio WillowWood Omega Tracer Scanner where the overall diameter of the model increased by 15 mm to accommodate larger sized forearms. The digitized model was fabricated on a Milltronics 4-axis mill using an ISO technologies 4.0 density foam blank as the carving medium. A 3/16 AIN Plastic co-poly thermoplastic sheet was then vacuum-formed over the foam model to create the thermoplastic shell. Royal Knit prosthetic socks were worn over the participant's arm to create a tight and comfortable fit of the thermoplastic shell. The Bowden cable housing attached to the housing attachment, and the cable attached to the mounted terminal device. In operation, pulling on the cable closed the terminal device.

The cable-driven exoskeleton consisted of two ABS 3D printed halves (upper and lower) that were connected about two separate concentric rotational axes on either side (see Figure 4.3). One of the axes was fixed to the lower half of the exoskeleton, and a rotary optical encoder (US Digital EM1-1-1250) was mounted to the axis to measure angular position. Custom thermoplastic cuffs (available in three different sizes) were attached to each half and featured velcro straps as well as foam padding. The housing of the Bowden cable attached to the housing support structure on the upper half, and the cable itself attached to the lower half through a cable attachment

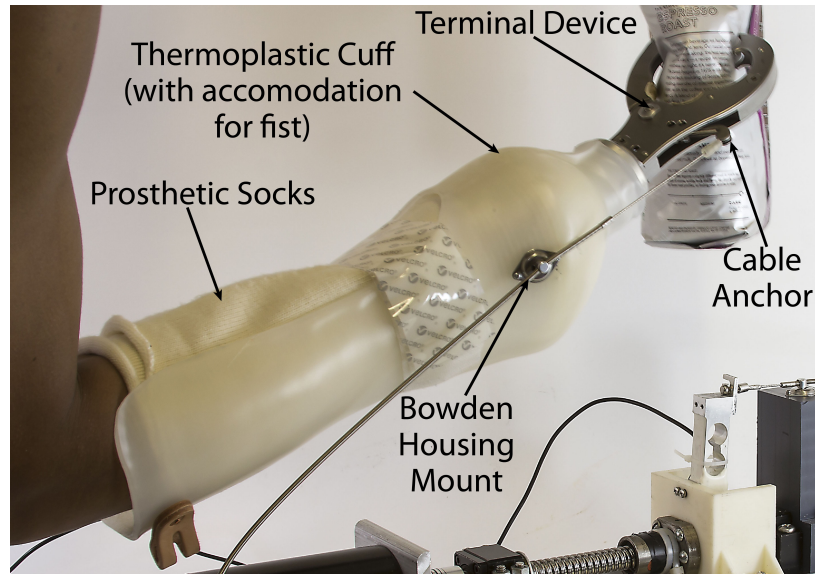


Figure 4.2: Mock prosthesis featuring a thermoplastic shell with accommodations for the fist of an able-bodied participant, a voluntary-closing terminal device, and anchor and mount points for a Bowden cable and housing. To ensure a snug fit, participants were required to wear prosthetic socks. In operation, pulling on the cable closed the terminal device.

swivel. The exoskeleton was fit to the left arm of an able-bodied participant with the axis of rotation of the elbow joint concentric with the exoskeleton axis of rotation. Velcro straps were used to secure the exoskeleton to the upper and lower portion of the participant's arm. In operation, pulling on the cable caused the exoskeleton to produce an extension moment about the elbow.

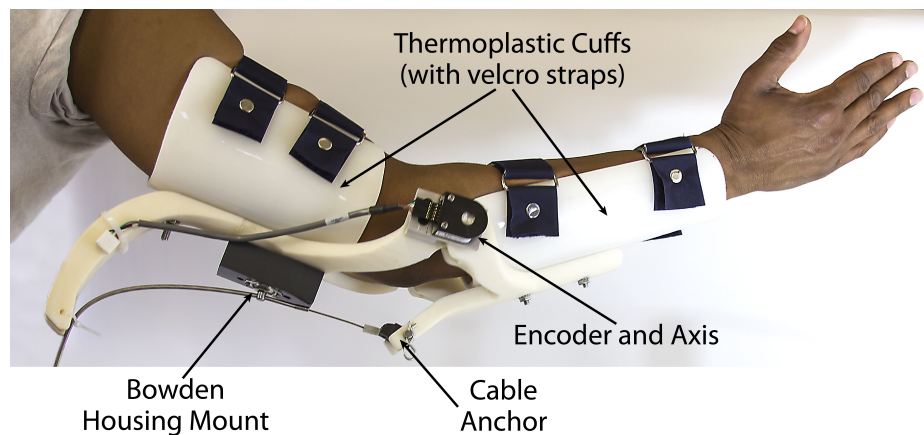


Figure 4.3: Cable-driven exoskeleton featuring an encoder and thermoplastic cuffs with velcro straps, and anchor and mount for Bowden cable and housing. In operation, pulling on the cable would produce an extension moment about the elbow.

Together, the individual elements of our experimental apparatus created a body-powered prosthesis that could be used with able-bodied participants (see Figure 4.4). This body-powered prosthesis differs from a traditional body-powered prosthesis in that the participant’s arm (as opposed to a shoulder through a shoulder harness) is used for control. In addition, haptic (force) feedback can be removed. This is possible because the user is connected to the prosthesis through the two separate actuators. One actuator is mechanically linked through a Bowden cable to the cable-driven prosthesis (prosthesis actuator), and the other is mechanically linked via a separate cable to the cable-driven exoskeleton.

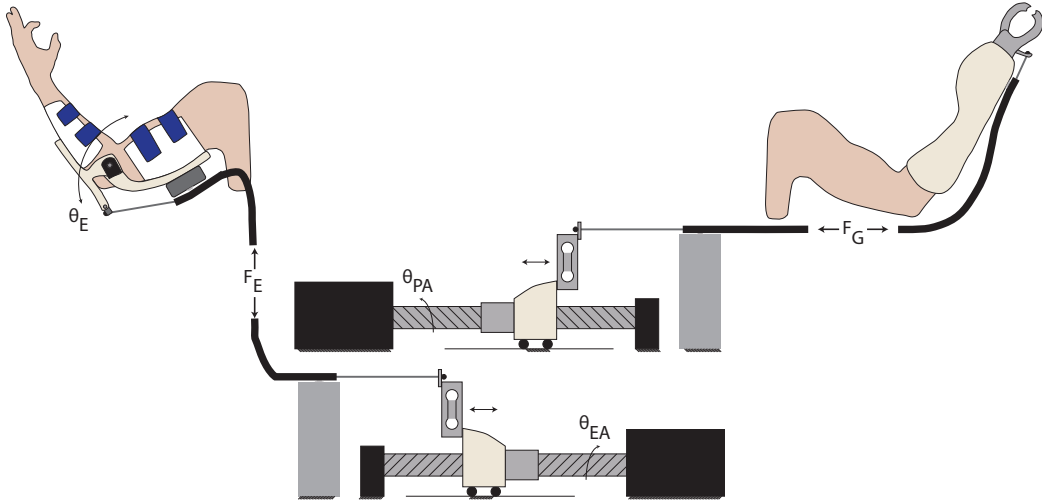


Figure 4.4: Schematic of mock body-powered prosthesis for able-bodied participants.

Both linear actuators were controlled through a proportional-derivative controller (see Figure 4.5). The control law for the exoskeleton actuator u_{EA} with force feedback ‘off’ and force feedback ‘on’ is shown in Equations 4.1, 4.2, respectively, with $K_p = 2.0$, $K_d = .06$, and $K_F = 2.0$. The angular position of the exoskeleton is θ_E , θ_{EA} is the angular position of the exoskeleton actuator motor, and F_G is the force measured by the loadcell on the prosthesis actuator. Parameter K_{EA} scales the exoskeleton position to that of the exoskeleton actuator motor, and is determined through a calibration routine described in Section 4.2.4 below.

The control law for the prosthesis actuator u_{PA} is shown in Equation 4.3, with $K_p = 2.0$ and $K_d = .06$. The angular position of the exoskeleton is θ_E , and θ_{PA} is the angular position of the prosthesis actuator motor. Parameter K_{PA} scales the exoskeleton position to that of the prosthesis actuator motor, and is determined through a calibration routine described in Section 4.2.4 below.

When force feedback was turned off, the body-powered device operated like a uni-

lateral position controlled teleoperator. The position of the exoskeleton was mapped to the position of the prosthesis actuator motor, and controlled actuation of the terminal device. Any forces sensed by the terminal device F_G however were not displayed to the participant. The exoskeleton actuator tracked the position of the exoskeleton to minimize the device impedance. When force feedback was turned on, the body-powered device operated like a bi-lateral position-force teleoperator. The position of the exoskeleton was mapped to the position of the prosthesis actuator motor, and controlled actuation of the terminal device. Any forces sensed by the terminal device F_G were displayed to the user through the exoskeleton and the exoskeleton actuator.

$$u_{EA} = (K_p + K_d s)[K_{EA}\theta_E - \theta_{EA}] \quad (\text{Force Feedback 'off'}) \quad (4.1)$$

$$u_{EA} = (K_p + K_d s)[K_{EA}\theta_E - \theta_{EA}] + K_F F_G \quad (\text{Force Feedback 'on'}) \quad (4.2)$$

$$u_{PA} = (K_p + K_d s)[K_{PA}\theta_E - \theta_{PA}] \quad (4.3)$$

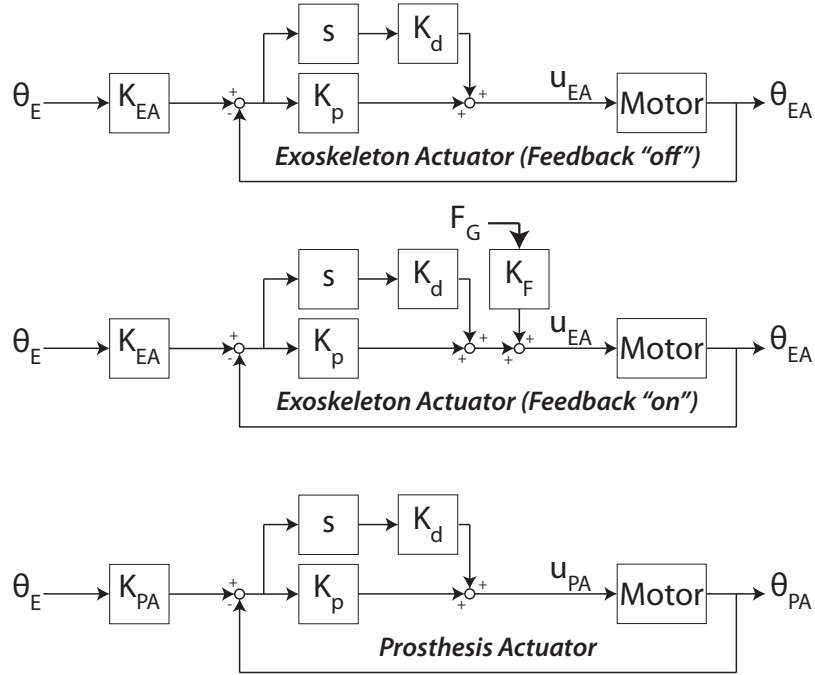


Figure 4.5: Block diagrams of exoskeleton actuator with force feedback on and off, and prosthesis actuator.

4.2.3 Stimuli

Our stimuli consisted of foam blocks (Temper Foam® R-Lite™ Foam Blocks) in three different stiffnesses: extra-soft, soft, and medium (see Figure 4.6). In the experiment they were referred to as ‘soft,’ ‘medium,’ and ‘hard,’ respectively. The blocks were covered with black athletic socks to hide their unique color descriptors.

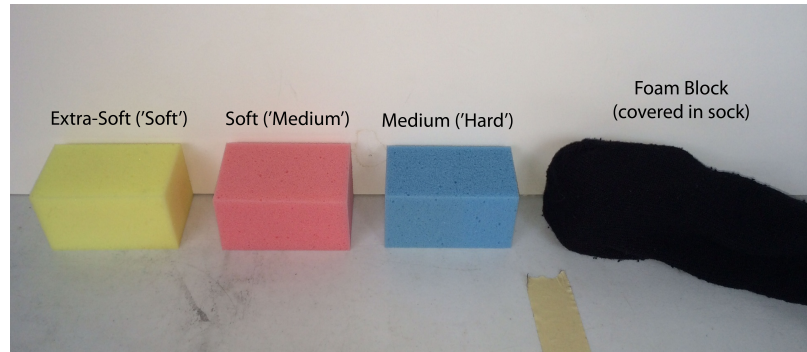


Figure 4.6: Foam testing blocks in three different stiffnesses. The names in quotes are the identifiers used during testing. Black athletic socks were used to hide the color of the blocks.

4.2.4 Setup and Training

Participants sat on a stool facing the table where the experiment would take place. The appropriate size cuffs were attached to the exoskeleton and the exoskeleton was mated to the left arm of the participant with the exoskeleton’s axis of rotation in-line with the participant’s elbow axis. Additional padding was used to ensure the velcro straps did not pinch the participant’s skin. The participant’s right arm was placed inside two Royal Knit prosthetic socks (#3 and #5), and their arm was placed inside the custom prosthesis. Participants were then instructed to make a loose fist with their right hand to ensure the prosthesis stayed on.

A calibration routine was run to scale the range of motion of each actuator to the range of motion of the participant’s arm. For the prosthesis actuator, the gain K_{PA} was tuned such that when the participant’s arm was fully extended, the terminal device was open and when the arm was fully flexed, the terminal device was closed. For the exoskeleton actuator, the gain K_{EA} was tuned so that the loadcell carriage (and cable) moved in-sync with the participant’s arm. The participant was made aware of the fact that if they moved their arm too fast, the motor would not be able to keep up, and they would feel the actuator’s impedance through the exoskeleton. The participants were also told that the blocks were made of memory foam.

Prior to testing, the participant was given an opportunity to experience the four experimental conditions: both vision and force feedback, vision feedback alone, force feedback alone, and feedback. In each condition they were allowed to feel a test block. This test block was a foam block similar to the stimuli blocks, except it had a higher stiffness than all three test blocks.

4.2.5 Testing

Participants were not given an opportunity to feel the three test blocks with their hand or through the device prior to beginning the test. Participants were told that the goal of the experiment was to accurately identify and sort the blocks.

The test consisted of five trials for each condition. The trial order was randomized into five sets of four, with each set containing a randomized order of the four experimental conditions. In each trial, the experimenter randomly selected eight blocks from a group of 12 (four blocks of each stiffness). The blocks were then presented one at a time to the participant. For each block presentation, participants started from a rest position (terminal device resting on the edge of the table). When the experimenter announced ‘begin,’ the participant was instructed to approach the block from the front, as opposed to the top, to avoid any stiffness cues associated with displacing the block with respect to the table. Participants were allowed to squeeze the block through the teleoperated cable as many times as desired while the block rested on the table in a specified location. Participants were also allowed to squeeze any portion of the block they chose, and could request that the experimenter rotate the block. Participants were then asked to sort each block in a corresponding bin ‘soft,’ ‘medium,’ or ‘hard’ (see Figure 4.7). After picking the block up, participants were not allowed to place it back down on the table to squeeze it again. Participants were also not allowed to move the blocks once they were placed in the bin.

The no vision trials were special. The prosthesis was held in a specified location, and the terminal device was shielded from the participant’s view by a poster-board curtain. When the participant announced begin, participants were allowed to squeeze the foam block while it was held by the experimenter, and then verbalize their choice as to which block it was. The experimenter would then place the object in the corresponding bin on their behalf (see Figure 4.8). After verbalizing their bin choice, participants were not allowed to change.

After each trial, the experimenter would verbally identify the blocks in each bin as a means of correct answer feedback. This was also recorded by the experimenter. Short breaks (~2 min) were taken between trials, and participants were made aware



Figure 4.7: Testing setup for trials with vision feedback.



Figure 4.8: Testing setup for trials without vision feedback.

of the condition before starting the trial. Noise-canceling headphones were not used so that verbal instructions could be understood clearly. In addition, the auditory cues provided by the actuators were thought to be consistent with the auditory cues available in current prostheses, especially myoelectric prostheses.

4.2.6 Metrics and Data Analysis

The kinematic, kinetic, and performance data was recorded to disk with a 1 kHz sampling rate. Our performance metrics were the object identification accuracy (%), object identification duration (s), number-of-probes, and probe rate (probe/s).

Object identification accuracy was computed as an overall accuracy for each group of eight blocks (i.e. the percentage of blocks in the correct bin).

Object identification duration was measured as the time in milliseconds from the time the tester announced ‘begin’ to the time the participant placed the block in a bin (vision trials) or verbalized their bin choice (no vision trials).

To measure the number-of-probes, two threshold values were set at 80mm and 120mm on the gripper actuator. Passing both thresholds in one direction as the terminal device closed accumulated a 0.5 (half) probe. Subsequently, passing both thresholds in the opposite direction as the terminal device opened accumulated another 0.5 probe. Passing only one threshold in either direction accumulated 0.25 probe. The probe rate was taken as the number-of-probes divided by the object identification duration for each block.

4.2.6.1 Statistical Analyses

All statistical analyses were performed using SPSS (v.21). Linear models were used to assess the effect of condition, controlling for trial order on both object identification accuracy and object identification duration. For identification accuracy, an ordinary least squares regression model was used. Bonferroni adjustments were applied to the estimated means to control for Type I errors. Mixed models were used for the object identification duration, the number-of-probes, and the probe rate because of the strong amount of within -subject correlation. Within the model, participants were a random effect, condition was a fixed effect, and object exploration order was a covariate. Bonferroni adjustments were applied to the estimated means to control for Type I errors. A p-value of 0.05 was used as the threshold for significance for all analyses.

4.3 Results

We found one participant to be an outlier from the remaining nine participants. Overall, this participant appeared to struggle with the operation of the device, and kept expressing confusion as to what cues were important. This participant also seemed to lack the concentration needed to perform the experiment. The participant mentioned feeling ‘drowsy’ on several occasions, but never requested to withdraw from the study. Since the experiment posed no medical risk to the participant, this participant was not asked to withdraw by the study coordinator. In analyzing this participants’s results we found trends inconsistent with the remaining participants.

Our analysis will therefore focus on the results of our remaining nine participants.

With feedback off, both the exoskeleton actuator and the prosthesis actuator tracked the position of the exoskeleton with excellent accuracy (see Figure 4.9). In addition, the load measured by the loadcell on the prosthesis actuator was not displayed to the user through the exoskeleton actuator. With feedback on, the tracking accuracy of the exoskeleton actuator was affected by the additional load from prosthesis actuator loadcell (see Figure 4.10). Here both the loadcell on the prosthesis actuator and the loadcell on the exoskeleton actuator measured a load from squeezing the foam block.

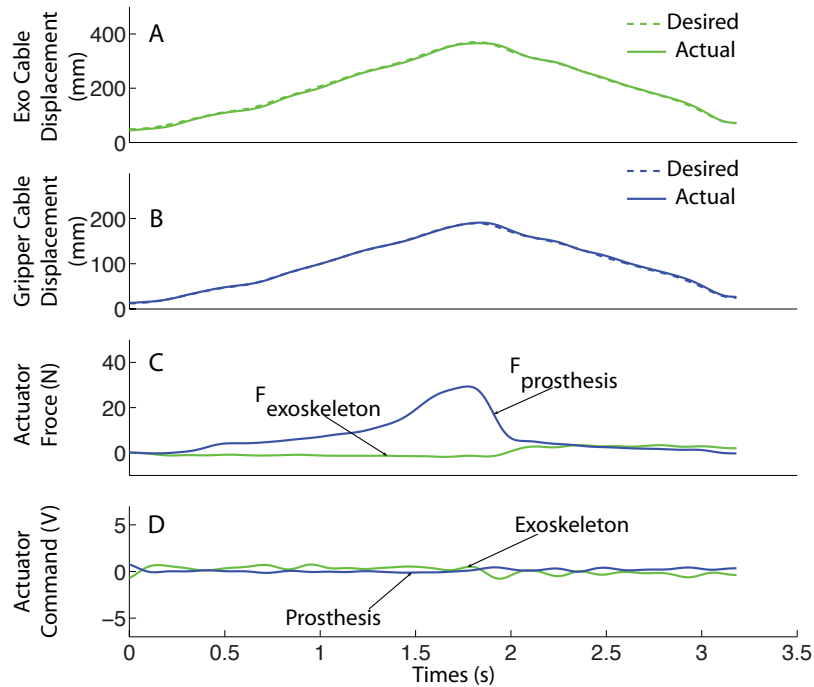


Figure 4.9: Exoskeleton actuator and prosthesis actuator kinematics with force feedback ‘off’ for a sample probe of a medium foam block: (A) Exoskeleton actuator cable displacement, (B) Prosthesis actuator cable displacement, (C) Exoskeleton actuator and prosthesis actuator loadcells, (D) Exoskeleton actuator and prosthesis actuator command voltage. Green traces refer to the exoskeleton actuator. Blue traces refer to the prosthesis actuator. Dashed traces represent the desired position as commanded by the exoskeleton.

As described in Section 4.2.3, our stimuli were memory foam blocks with three different stiffnesses. With feedback off, the prosthesis actuator loadcell and encoder measured the force/displacement relationship of each block. As demonstrated by the sample traces in Figure 4.11A, three distinct stiffnesses were measured by the prosthesis actuator. These stiffnesses however were not displayed to the exoskeleton

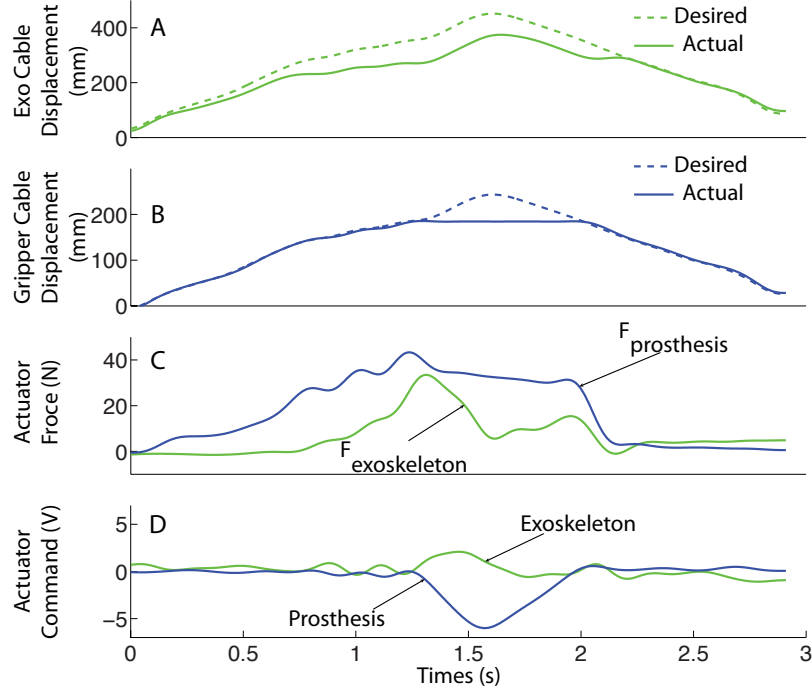


Figure 4.10: Exoskeleton actuator and prosthesis actuator kinematics with force feedback ‘on’ for a sample probe of a medium foam block: (A) Exoskeleton actuator cable displacement, (B) Prosthesis actuator cable displacement, (C) Exoskeleton actuator and prosthesis actuator loadcells, (D) Exoskeleton actuator and prosthesis actuator command voltage. Green traces refer to the exoskeleton actuator. Blue traces refer to the prosthesis actuator. Dashed traces represent the desired position as commanded by the exoskeleton.

(see Figure 4.11B). Note that these traces were colored in post-processing based on the presentation order of each block. The hysteresis in the stiffness traces is due to the memory foam material.

With feedback on, both the prosthesis actuator loadcell and encoder as well as the exoskeleton actuator loadcell and encoder capture the stiffness of the block. The sample traces in Figure 4.12 are very similar to the traces for the prosthesis actuator with no feedback with the exception that the stiffness traces are not as smooth for the medium and hard blocks. For the exoskeleton actuator (see Figure 4.12), the traces do not resemble a typical stiffness profile. However, the traces do fall into three distinct groupings based on the stiffness of each block.

4.3.1 Object Identification Accuracy

In terms of identification accuracy, participants were most accurate with both vision and force feedback ($M = 68.1\%$, $SE = 2.5\%$), followed by force feedback alone

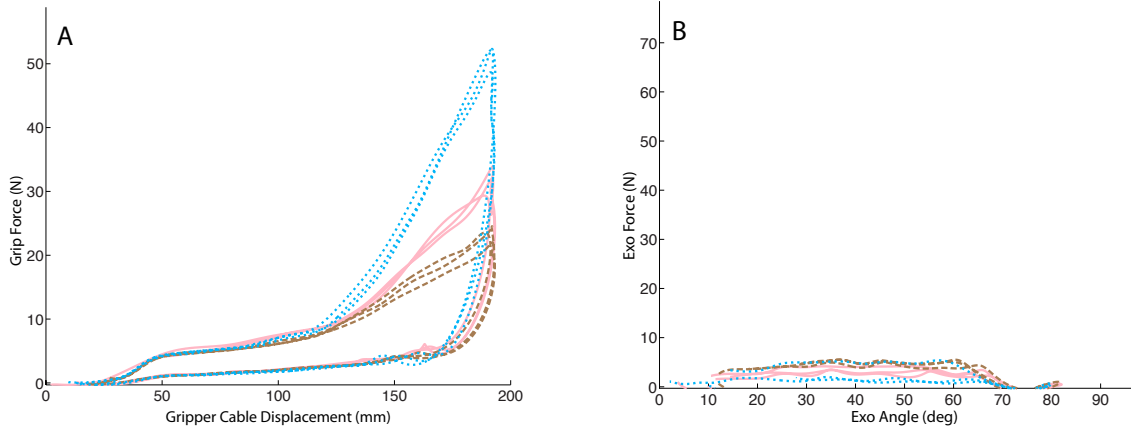


Figure 4.11: Sample stiffness (force/displacement) profiles generated by the (A) Prosthesis actuator and (B) exoskeleton actuator, with force feedback ‘off.’ Blue dotted traces refer to the ‘hard’ block. Pink solid traces refer to the ‘medium’ block. Yellow dashed traces refer to the ‘soft’ block.

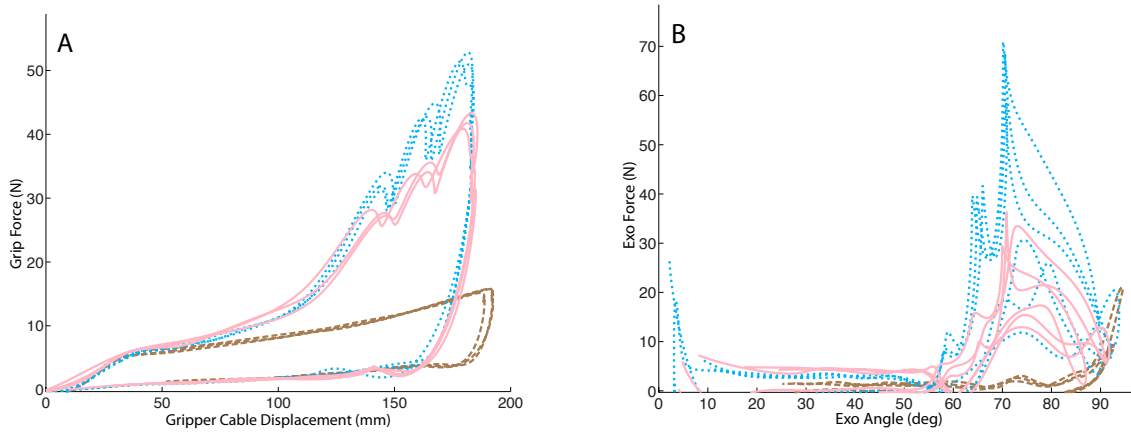


Figure 4.12: Sample stiffness (force/displacement) profiles generated by the (A) Prosthesis actuator and (B) exoskeleton actuator, with force feedback ‘on.’ Blue dotted traces refer to the ‘hard’ block. Pink solid traces refer to the ‘medium’ block. Yellow dashed traces refer to the ‘soft’ block.

($M = 56.4\%$, $SE = 2.5\%$), followed by vision feedback alone ($M = 44.4\%$, $SE = 2.5\%$), followed by no feedback ($M = 30.8\%$, $SE = 2.5\%$), as shown in Figure 4.13.

Participants were significantly more accurate with both vision and force feedback than with vision feedback alone ($\beta = 23.7\%$, $SE = 3.5\%$, $p < .001$). Participants were significantly more accurate with both vision and force feedback than force feedback alone ($\beta = 11.6\%$, $SE = 3.5\%$, $p = .007$). Participants were more accurate with both vision and force feedback than no feedback ($\beta = 37.3\%$, $SE = 3.5\%$, $p < .001$).

In terms of force feedback alone, participants were significantly more accurate than vision feedback alone ($\beta = 12.0\%$, $SE = 3.5\%$, $p = .005$). Participants were

also significantly more accurate with force feedback alone than no feedback ($\beta = 25.6\%$, $SE = 3.5\%$, $p < .001$). In terms of vision feedback alone, participants were more accurate than no feedback ($\beta = 13.6\%$, $SE = 3.5\%$, $p = .001$).

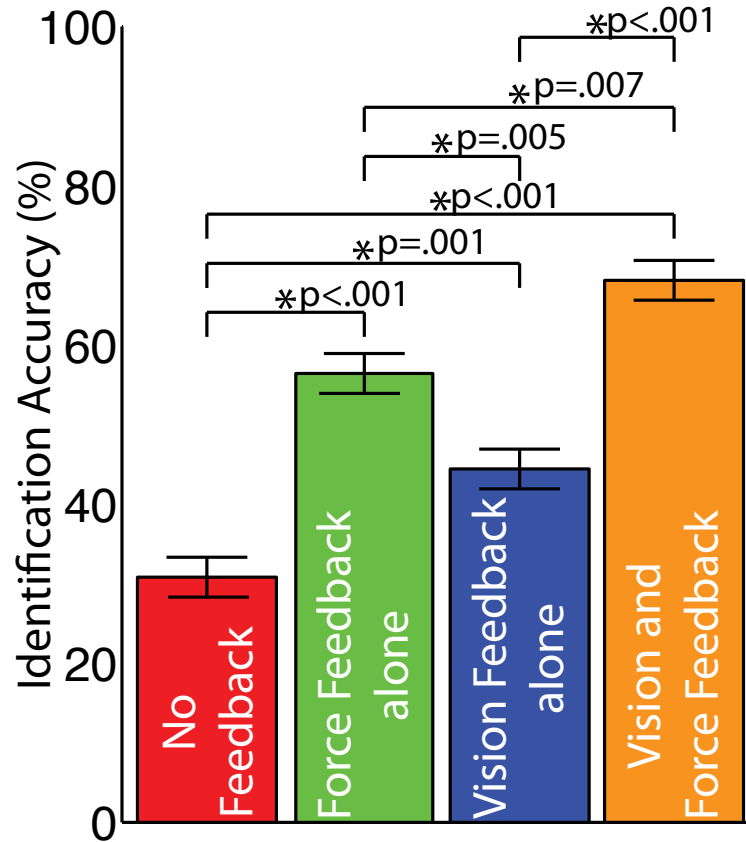


Figure 4.13: Average identification accuracy for all nine normal participants in all five trials of the four conditions. Error bars represent 1 standard error.

Since eight blocks were presented for each trial in each condition, the learning that occurs with the first few blocks is washed out with an overall accuracy for each group of eight trials. In addition, because the experimenter was unaware of the object type until after the trial, individual identification performance for each block was not possible.

4.3.2 Object Identification Duration

The duration of each object exploration was recorded as the time from the moment the experimenter announced “begin” to the time the participant placed the foam block in a bin (vision trials) or verbalized their bin choice (no vision trials). Partici-

participants took the longest amount of time with vision feedback alone ($M = 7.62s$, $SE = .18s$), followed by both vision and force feedback ($M = 7.47s$, $SE = .18s$), followed by force feedback alone ($M = 6.00s$, $SE = .18s$), followed by no feedback ($M = 5.55s$, $SE = .18s$) as shown in Figure 4.14. In terms of differences between conditions, participants were significantly faster with force feedback alone than vision feedback alone ($\beta = -1.56s$, $SE = .18s$, $p < .001$). Participants were also significantly faster with force feedback alone than both vision and force feedback ($\beta = -1.38s$, $SE = .18s$, $p < .001$). Participants were significantly faster with no feedback than vision feedback alone ($\beta = -2.04s$, $SE = .18s$, $p < .001$) and both vision and force feedback ($\beta = -1.86s$, $SE = .18s$, $p < .001$). Participants were also faster with no feedback than force feedback alone, although this difference is not quite significant ($\beta = -.48s$, $SE = .18s$, $p = .051$). All other differences are not significant.

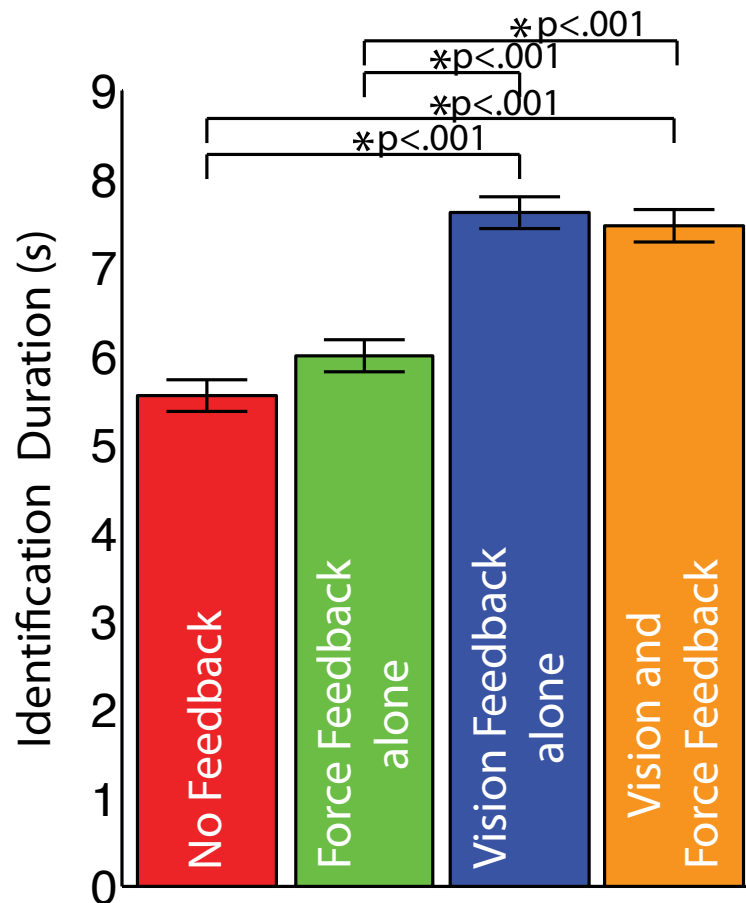


Figure 4.14: Average identification duration for all nine normal participants in all five trials of the four conditions. Note that the first object exploration for each condition is excluded. Error bars represent 1 standard error.

Since trial duration was recorded for every object exploration, some learning did occur. This learning however was complete by the end of the first trial. The trial duration results therefore do not include the first trial for each condition.

4.3.3 Object Exploration

4.3.3.1 Number of Probes

Participants probed the blocks a different number of times for each condition. Participants used the most number of probes for vision feedback alone ($M = 1.408$, $SE = .048$), followed by both vision feedback and force feedback ($M = 1.498$, $SE = .049$), followed by force feedback alone ($M = 1.414$, $SE = .048$), followed by no feedback ($M = 1.408$, $SE = .048$). In terms of differences between conditions, participants used significantly more probes with vision feedback alone than no feedback ($\beta = .147$, $SE = .043$, $p = .003$). Participants also used significantly more probes with vision feedback alone than and force feedback alone ($\beta = .143$, $SE = .043$, $p = .005$). As with object identification duration, the first trial for each condition is not included in the analysis.

4.3.3.2 Probe Rate

Participants also probed the blocks at different rates by condition. Participants used the fastest rate with no feedback ($M = .290$ probe/s, $SE = .005$ probe/s), followed by force feedback alone ($M = .267$ probe/s, $SE = .005$ probe/s), followed by vision feedback alone ($M = .205$ probe/s, $SE = .005$ probe/s), followed by both vision feedback and force feedback ($M = .201$ probe/s, $SE = .005$ probe/s). In terms of differences between conditions, participants used a significantly faster probe rate with no feedback than with force feedback alone ($\beta = .024$ probe/s, $SE = .005$ probe/s, $p < .001$). Participants used a significantly faster probe rate with no feedback than with vision feedback alone ($\beta = .084$ probe/s, $SE = .005$ probe/s, $p < .001$). Participants used a significantly faster probe rate with no feedback than both vision feedback and force feedback ($\beta = .087$ probe/s, $SE = .005$ probe/s, $p < .001$). Participants used a significantly faster probe rate with force feedback alone than with vision feedback alone ($\beta = .059$ probe/s, $SE = .005$ probe/s, $p < .001$). Participants also used a significantly faster probe rate with force feedback alone than both vision feedback and force feedback ($\beta = .062$ probe/s, $SE = .005$ probe/s, $p < .001$). As with object identification duration, the first trial for each condition is not included in the analysis.

4.4 Discussion

In this study, we have found that force feedback alone provides greater utility to able-bodied individuals wearing a mock prosthesis than vision feedback alone. We have arrived at this conclusion through a simple experiment involving a body-powered prosthesis that is capable of being worn by an able-bodied individual, and features force feedback that can be conditionally removed. In four separate conditions, we evaluated our participants' ability to discriminate objects based on their stiffness with both vision feedback and force feedback, force feedback alone, vision feedback alone, and no feedback. Vision was controlled with a simple curtain. Haptic feedback however was controlled through the device itself. The prosthesis can be considered a teleoperator, with the master on the participant's left arm and the slave worn on the participant's right arm. With feedback 'off,' the prosthesis resembled a unilateral teleoperator with position control. With feedback 'on,' the prosthesis resembled a bilateral force reflecting teleoperator with a position-force control architecture. Rather than using a shoulder harness like a traditional trans-radial body-powered prostheses, our device coupled the terminal device of the prosthesis to a prototype cable-driven exoskeleton worn about the elbow. The manner in which it operates is still consistent with traditional body-powered devices when feedback is on, in that action at the elbow joint is mechanically linked through a cable to the action of the terminal device.

Overall, participants were more accurate at identifying the foam blocks with force feedback alone than with vision feedback alone ($p = .005$, see Figure 4.13). They were also able to identify the foam blocks in the shortest amount of time with force feedback alone than with vision feedback alone ($p < .001$, see Figure 4.14). Object identification accuracy was $\sim 56\%$ with force feedback alone and $\sim 44\%$ with vision feedback alone. In addition object identification duration was ~ 6.0 s with force feedback alone and ~ 7.6 s with vision feedback alone.

The combination of vision feedback and force feedback resulted in improved identification accuracy over vision feedback alone or force feedback alone ($p < .001$ and $p = .007$ respectively, see Figure 4.13). Both vision and force feedback resulted in the greatest identification accuracy $\sim 68\%$, but this appeared to come at the cost of timing, resulting in a duration of ~ 7.5 s. This was not significantly different from vision feedback alone, but was significantly slower than no force feedback alone ($p < .001$, see Figure 4.14).

As might be expected with no feedback, identification accuracy was $\sim 31\%$ near

the 33% expected for guessing. At the other end of the spectrum, no feedback had the shortest duration ~ 5.6 s. Evidently participants did not bother to explore the block in detail, and just guessed.

In addition, participants explored the foam blocks differently. In particular, with force feedback alone, participants used a smaller number of probes ($p = .005$) and a faster probe rate ($p < .001$) than vision feedback alone. Participants also used a significantly faster probe rate with force feedback alone than with both vision feedback and force feedback ($p < .001$). Although the number of probes are relatively close, due in part to the large number of single probe explorations, the differences highlight the propensity of a particular display to have more than one probe.

Although our results only directly address an able-bodied individual wearing a mock prosthesis, they have significant implications in prosthetics. Each of our four conditions resembles a situation that an amputee may face. The vision feedback with force feedback condition as mentioned above resembles the operation of a body-powered prosthesis where amputees have access to both visual operation of their prosthesis as well as haptic grip force feedback. Note that this is more consistent for a body-powered prosthesis featuring a voluntary-closing terminal device than a voluntary-opening terminal device, but the underlying principle remains unchanged. The condition with vision feedback alone resembles the operation of a standard myoelectric prosthesis. The obvious exception being that the efferent command came from action about the elbow joint as opposed to the myoelectric signal generated from the muscles that span the joint. Even still, because the muscles that span the joint are attached to the skeletal structure, participants could detect a sense of effort. This may not be possible with all trans-radial amputations where the myoelectric signal is taken from muscles in the residual forearm. In addition, our particular style of terminal device allowed for better visual information than some traditional myoelectric terminal devices. Our force feedback alone condition resembles the operation of a body-powered device in the absence of vision. The lack of vision could result from working in a dimly lit or dark room, or could result from working in an environment in which vision is altogether obscured, such as a pants pocket. The no feedback condition then resembles the operation of a myoelectric device in the absence of vision. As with both types of prostheses, auditory feedback was available in all four conditions in the form of the motor and ballscrew movement, but participants may not have had enough experience with the device to correlate the auditory feedback with the visual and/or haptic feedback. The foam blocks also produced no discernible auditory signatures.

The differences seen in our experiment are consistent with findings in the teleoperator literature. Haptic feedback has been demonstrated to improve teleoperator performance over vision alone. Indeed, Wildenbeest *et al* [59] found that haptic feedback improved completion times in a teleoperated assembly task. In addition, Draper *et al* [57] and Hannaford *et al* [58] showed that force feedback, led to reduced errors in teleoperator performance.

Although there are no studies assessing teleoperator performance in the absence of vision, the identification performance decline with vision alone is consistent with the literature on the visual estimation of stiffness [87]. Even though visual estimation can be performed, the measurement has high variability, and depends heavily upon the ability to discriminate object deformations under common forcing conditions. Given that our objects are made of memory foam, it is quite possible that the hysteresis in the stiffness relationship made visual estimation more difficult.

To generate the conditions needed for visual estimation of stiffness, participants apparently had to probe at a slower rate. The probe rate with vision feedback alone was significantly slower than force feedback alone. Likewise, the probe rate with both vision feedback and force feedback was significantly slower than force feedback alone. Perhaps this is why conditions with vision took longer than the force feedback alone condition. The faster time with vision feedback and force feedback over vision feedback alone, although not significant, could be attributed to the confirmation provided by the faster, more accurate haptic feedback.

While it may be possible that with increased experience and exposure, accuracy with vision feedback alone may improve, and duration decrease, the same is true for the other conditions, except perhaps the no feedback condition. Anecdotally however, it is well known amongst prosthetists that an amputee's decision as to which type of prosthesis they prefer is often made in the first 10-15 minutes of use, and depends heavily on how successful they were at using the prosthesis during that period. Testing in this experiment lasted about an hour, meaning each participant spent ~15min in each condition. Although many factors such as cost, the amputation cause, and the aesthetics of the device affect the final decision as to which prosthesis technology to choose, amputees still desire increased feedback and less reliance on vision [34,35]. Our results demonstrate the impact the addition of force feedback can have in providing a decreased reliance on vision.

It could be possible that performance in the vision feedback alone condition could be improved if the foam blocks had linear stiffness profiles without hysteresis. Unfortunately, this is more of an experimentally contrived condition than a real-world

occurrence. In addition, it could be argued that the sock covering the foam block masked some of the visual information, but the same could be argued about the dynamics available in our force feedback apparatus.

In this study we have taken able-bodied participants and effectively made them trans-radial amputees. Since they have had no prior experience with a body-powered prosthesis, we were able to see the effect both vision and haptic feedback in a prosthesis without the influence of prior experience. Our findings support the theory touted in the orthotics and prosthetics community that body-powered devices are the ‘gold standard’ due to their inherent haptic force feedback. In addition, these findings suggest that performance improvements could be achieved by adding grip force feedback in the control of a myoelectric device.

APPENDIX

APPENDIX A

Chapter III Post-Test Survey

JND_Survey

Q1 Subject ID#

Q2 Where any of the conditions more easy or difficult than the others?

- Yes (1)
- No (2)

Q3 Please select how easy or difficult each condition was.

	Very Difficult (1)	Difficult (2)	Somewhat Difficult (3)	Neutral (4)	Somewhat Easy (5)	Easy (6)	Very Easy (7)
Colocated (1)	<input type="radio"/>	<input type="radio"/>	<input type="radio"/>	<input type="radio"/>	<input type="radio"/>	<input type="radio"/>	<input type="radio"/>
Non-colocated (2)	<input type="radio"/>	<input type="radio"/>	<input type="radio"/>	<input type="radio"/>	<input type="radio"/>	<input type="radio"/>	<input type="radio"/>
Vibrotactile (3)	<input type="radio"/>	<input type="radio"/>	<input type="radio"/>	<input type="radio"/>	<input type="radio"/>	<input type="radio"/>	<input type="radio"/>

Q4 Why do you think some of the conditions were easy and others were difficult?

Q5 Did you use the same strategy for each of the three conditions?

- Yes (1)
- No (2)

Q6 What overall strategy did you use, and why?

Q7 What strategy did you use for the colocated condition, and why?

Q8 What strategy did you use for the non-colocated condition, and why?

Q9 What strategy did you use for the vibrotactile condition, and why?

Q10 Please rank how well you agree or disagree with the following statement in each condition: The colocated condition required more concentration than the...

	Strongly Disagree (1)	Disagree (2)	Neither Agree nor Disagree (3)	Agree (4)	Strongly Agree (5)
Non-colocated condition (1)	<input type="radio"/>	<input type="radio"/>	<input type="radio"/>	<input type="radio"/>	<input type="radio"/>
Vibrotactile condition (2)	<input type="radio"/>	<input type="radio"/>	<input type="radio"/>	<input type="radio"/>	<input type="radio"/>

Q11 Please rank how well you agree or disagree with the following statement in each condition: The non-colocated condition required more concentration than the...

	Strongly Disagree (1)	Disagree (2)	Neither Agree nor Disagree (3)	Agree (4)	Strongly Agree (5)
Colocated condition (1)	<input type="radio"/>	<input type="radio"/>	<input type="radio"/>	<input type="radio"/>	<input type="radio"/>
Vibrotactile condition (2)	<input type="radio"/>	<input type="radio"/>	<input type="radio"/>	<input type="radio"/>	<input type="radio"/>

Q12 Please rank how well you agree or disagree with the following statement in each condition: The vibrotactile condition required more concentration than the...

	Strongly Disagree (1)	Disagree (2)	Neither Agree nor Disagree (3)	Agree (4)	Strongly Agree (5)
Colocated condition (1)	<input type="radio"/>	<input type="radio"/>	<input type="radio"/>	<input type="radio"/>	<input type="radio"/>
Vibrotactile condition (2)	<input type="radio"/>	<input type="radio"/>	<input type="radio"/>	<input type="radio"/>	<input type="radio"/>

Q13 Please rank how well you agree or disagree with the following statement in each condition: I would be able to perform the task just as well in a crowded store.

	Strongly Disagree (1)	Disagree (2)	Neither Agree nor Disagree (3)	Agree (4)	Strongly Agree (5)
Colocated condition (1)	<input type="radio"/>	<input type="radio"/>	<input type="radio"/>	<input type="radio"/>	<input type="radio"/>
Non-colocated condition (2)	<input type="radio"/>	<input type="radio"/>	<input type="radio"/>	<input type="radio"/>	<input type="radio"/>
Vibrotactile condition (3)	<input type="radio"/>	<input type="radio"/>	<input type="radio"/>	<input type="radio"/>	<input type="radio"/>

Q14 Please rank how well you agree or disagree with the following statement in each condition: I would be able to perform the task just as well in a crowded store.

	Strongly Disagree (1)	Disagree (2)	Neither Agree nor Disagree (3)	Agree (4)	Strongly Agree (5)
Colocated condition (1)	<input type="radio"/>	<input type="radio"/>	<input type="radio"/>	<input type="radio"/>	<input type="radio"/>
Non-colocated condition (2)	<input type="radio"/>	<input type="radio"/>	<input type="radio"/>	<input type="radio"/>	<input type="radio"/>
Vibrotactile condition (3)	<input type="radio"/>	<input type="radio"/>	<input type="radio"/>	<input type="radio"/>	<input type="radio"/>

Q15 Please rank how well you agree or disagree with the following statement in each condition: I would be able to perform the task just as well while holding a conversation.

	Strongly Disagree (1)	Disagree (2)	Neither Agree nor Disagree (3)	Agree (4)	Strongly Agree (5)
Colocated condition (1)	<input type="radio"/>	<input type="radio"/>	<input type="radio"/>	<input type="radio"/>	<input type="radio"/>
Non-colocated condition (2)	<input type="radio"/>	<input type="radio"/>	<input type="radio"/>	<input type="radio"/>	<input type="radio"/>
Vibrotactile condition (3)	<input type="radio"/>	<input type="radio"/>	<input type="radio"/>	<input type="radio"/>	<input type="radio"/>

Q16 Please rank the three conditions in order of preference

_____ Colocated (1)

_____ Non-colocated (2)

_____ Vibrotactile (3)

Q17 Is there anything else you would like us to know about your experience as a participant?

Yes (1)

No (2)

Q18 Final comments

BIBLIOGRAPHY

BIBLIOGRAPHY

- [1] R. Johansson and G. Westling, “Coordinated isometric muscle commands adequately and erroneously programmed for the weight during lifting task with precision grip,” *Experimental Brain Research*, pp. 59–71, 1988.
- [2] J. R. Flanagan, M. C. Bowman, and R. S. Johansson, “Control strategies in object manipulation tasks.” *Current opinion in neurobiology*, vol. 16, no. 6, pp. 650–9, Dec. 2006.
- [3] J. R. Flanagan and a. M. Wing, “The role of internal models in motion planning and control: evidence from grip force adjustments during movements of hand-held loads.” *The Journal of Neuroscience*, vol. 17, no. 4, pp. 1519–28, Feb. 1997.
- [4] S. J. Lederman and R. L. Klatzky, “Extracting object properties through haptic exploration.” *Acta psychologica*, vol. 84, no. 1, pp. 29–40, Oct. 1993.
- [5] D. S. Childress, “Closed-loop control in prosthetic systems: historical perspective.” *Annals of Biomedical Engineering*, vol. 8, no. 4-6, pp. 293–303, Jan. 1980.
- [6] J. a. Doubler and D. S. Childress, “Design and evaluation of a prosthesis control system based on the concept of extended physiological proprioception.” *Journal of Rehabilitation Research and Development*, vol. 21, no. 1, pp. 19–31, May 1984.
- [7] J. Doubler and D. Childress, “An Analysis of Extended Physiological Proprioception as a Prosthesis-Control Technique,” *Journal of Rehabilitation Research and Development*, vol. 21, no. 1, pp. 5–18, 1984.
- [8] R. F. Weir, C. W. Heckathorne, and D. S. Childress, “Cineplasty as a control input for externally powered prosthetic components.” *Journal of Rehabilitation Research and Development*, vol. 38, no. 4, pp. 357–63, 2001.
- [9] G. Shannon, “A comparison of alternative means of providing sensory feedback on upper limb prostheses,” *Medical and biological engineering*, vol. 14, no. 3, pp. 289–294, Jan. 1976.
- [10] G. F. Shannon, “A myoelectrically-controlled prosthesis with sensory feedback.” *Medical and Biological Engineering*, vol. 17, no. 1, pp. 73–80, Jan. 1979.

- [11] P. E. Patterson and J. a. Katz, “Design and evaluation of a sensory feedback system that provides grasping pressure in a myoelectric hand,” *Journal of Rehabilitation Research and Development*, vol. 29, no. 1, pp. 1–8, Jan. 1992.
- [12] S. G. Meek, S. C. Jacobsen, and P. P. Goulding, “Extended physiologic taction: design and evaluation of a proportional force feedback system.” *Journal of Rehabilitation Research and Development*, vol. 26, no. 3, pp. 53–62, Jan. 1989.
- [13] A. Blank, A. M. Okamura, and K. J. Kuchenbecker, “Identifying the role of proprioception in upper-limb prosthesis control,” *ACM Transactions on Applied Perception*, vol. 7, no. 3, pp. 1–23, Jun. 2010.
- [14] J. Wheeler, K. Bark, J. Savall, and M. Cutkosky, “Investigation of Rotational Skin Stretch for Proprioceptive Feedback With Application to Myoelectric Systems,” *IEEE Transactions on Neural Systems and Rehabilitation Engineering*, vol. 18, no. 1, pp. 58–66, Feb. 2010.
- [15] R. R. Riso, “Strategies for providing upper extremity amputees with tactile and hand position feedback—moving closer to the bionic arm.” *Technology and Health Care*, vol. 7, no. 6, pp. 401–9, Jan. 1999.
- [16] M. D’Alonzo, C. Cipriani, and M. C. Carrozza, “Vibrotactile sensory substitution in multi-fingered hand prostheses: Evaluation studies,” in *2011 IEEE International Conference on Rehabilitation Robotics (ICORR)*. IEEE, Jul. 2011, pp. 1–6.
- [17] A. Chatterjee, P. Chaubey, J. Martin, and N. V. Thakor, “Quantifying Prosthesis Control Improvements Using a Vibrotactile Representation of Grip Force,” in *2008 IEEE Region 5 Conference*. IEEE, Apr. 2008, pp. 1–5.
- [18] K. Kim and J. E. Colgate, “Haptic feedback enhances grip force control of sEMG-controlled prosthetic hands in targeted reinnervation amputees.” *IEEE Transactions on Neural Systems and Rehabilitation Engineering*, vol. 20, no. 6, pp. 798–805, Nov. 2012.
- [19] H. Witteveen, F. Luft, J. Rietman, and P. Veltink, “Stiffness feedback for myoelectric forearm prostheses using vibrotactile stimulation,” *IEEE Transactions on Neural Systems and Rehabilitation Engineering*, vol. 22, no. 1, pp. 53 – 61, Jun. 2014.
- [20] E. Rombokas, C. E. Stepp, C. Chang, M. Malhotra, and Y. Matsuoka, “Vibrotactile sensory substitution for electromyographic control of object manipulation.” *IEEE Transactions on Biomedical Engineering*, vol. 60, no. 8, pp. 2226–32, Aug. 2013.
- [21] X. Pang, H. Tan, and N. Durlach, “Manual discrimination of force using active finger motion,” *Attention, Perception, & Psychophysics*, vol. 49, no. 6, pp. 531–540, 1991.

- [22] L. A. Jones, “Matching forces: constant errors and differential thresholds,” *Perception*, vol. 18, no. 5, pp. 681–687, 1989.
- [23] D. A. Mahns, N. M. Perkins, V. Sahai, L. Robinson, and M. J. Rowe, “Vibrotactile frequency discrimination in human hairy skin.” *Journal of Neurophysiology*, vol. 95, no. 3, pp. 1442–50, Mar. 2006.
- [24] O. Franzén and J. Nordmark, “Vibrotactile frequency discrimination,” *Perception & Psychophysics*, vol. 17, no. 5, pp. 480–484, Sep. 1975.
- [25] W. M. Bergmann Tiest and A. Kappers, “Cues for haptic perception of compliance,” *IEEE Transactions on Haptics*, vol. 2, no. 4, pp. 189–199, 2009.
- [26] H. Tan and N. Durlach, “Manual Discrimination of compliance using pinch grasp: The roles of force and work cues,” *Perception & Psychophysics*, vol. 57, no. 4, pp. 531–540, 1995.
- [27] R. C. Goertz, “Mechanical master-slave manipulator,” *Nucleonics*, vol. 12, no. 11, pp. 45–46, 1954.
- [28] ———, “A force-reflecting positional servomechanism,” *Nucleonics*, vol. 10, no. 11, pp. 43–45, 1952.
- [29] R. Daniel and P. McAree, “Fundamental Limits of Performance for Force Reflecting Teleoperation,” *The International Journal of Robotics Research*, vol. 17, no. 8, pp. 811–830, Aug. 1998.
- [30] F. Tendick, M. Downes, T. Goktekin, M. C. Cavusoglu, D. Feygin, X. Wu, R. Eyal, M. Hegarty, and L. W. Way, “A Virtual Environment Testbed for Training Laparoscopic Surgical Skills,” *Presence: Teleoperators and Virtual Environments*, vol. 9, no. 3, pp. 236–255, Jun. 2000.
- [31] Y. Visell, “Interacting with Computers Tactile sensory substitution : Models for enaction in HCI,” *Interacting with Computers*, vol. 21, pp. 38–53, 2009.
- [32] J. K. O’Regan and A. Noë, “A sensorimotor account of vision and visual consciousness.” *The Behavioral and Brain Sciences*, vol. 24, no. 5, pp. 939–73; discussion 973–1031, Oct. 2001.
- [33] P. Bach-y Rita, C. Collins, and F. Saunders, “Vision substitution by tactile image projection,” *Nature*, vol. 221, pp. 963–964, 1969.
- [34] E. a. Biddiss and T. T. Chau, “Upper limb prosthesis use and abandonment: a survey of the last 25 years.” *Prosthetics and orthotics international*, vol. 31, no. 3, pp. 236–57, Sep. 2007.
- [35] D. Atkins, D. C. Heard, and W. H. Donovan, “Epidemiologic overview of individuals with upper-limb loss and their reported research priorities,” *Journal of Prosthetics and Orthotics*, vol. 8, no. 1, pp. 1–11, 1996.

- [36] T. W. Wright, a. D. Hagen, and M. B. Wood, “Prosthetic usage in major upper extremity amputations.” *The Journal of hand surgery*, vol. 20, no. 4, pp. 619–22, Jul. 1995.
- [37] S. G. Millstein, H. Heger, and G. a. Hunter, “Prosthetic use in adult upper limb amputees: a comparison of the body powered and electrically powered prostheses.” *Prosthetics and Orthotics International*, vol. 10, no. 1, pp. 27–34, Apr. 1986.
- [38] L. V. McFarland, S. L. H. Winkler, A. W. Heinemann, M. Jones, and A. Esquenazi, “Unilateral upper-limb loss: Satisfaction and prosthetic-device use in veterans and servicemembers from Vietnam and OIF/OEF conflicts,” *The Journal of Rehabilitation Research and Development*, vol. 47, no. 4, pp. 299–316, 2010.
- [39] C. Cipriani, M. D’Alonzo, and M. C. Carrozza, “A miniature vibrotactile sensory substitution device for multifingered hand prosthetics.” *IEEE Transactions on Biomedical Engineering*, vol. 59, no. 2, pp. 400–8, Feb. 2012.
- [40] J. D. Brown and R. B. Gillespie, “The effect of force/motion coupling on motor and cognitive performance,” in *2011 IEEE World Haptics Conference (WHC)*. IEEE, Jun. 2011, pp. 197–202.
- [41] A. Panarese, B. B. Edin, F. Vecchi, M. C. Carrozza, and R. S. Johansson, “Humans Can Integrate Force Feedback to Toes in Their Sensorimotor Control of a Robotic Hand,” *IEEE Transactions on Neural Systems and Rehabilitation Engineering*, vol. 17, no. 6, pp. 560–567, Dec. 2009.
- [42] I. Saunders and S. Vijayakumar, “The role of feed-forward and feedback processes for closed-loop prosthesis control.” *Journal of Neuroengineering and Rehabilitation*, vol. 8, no. 1, p. 60, Jan. 2011.
- [43] T. A. Kuiken, G. Li, B. A. Lock, R. D. Lipschutz, L. A. Miller, K. A. Stubblefield, and K. B. Englehart, “Targeted muscle reinnervation for real-time myoelectric control of multifunction artificial arms.” *Journal of the American Medical Association*, vol. 301, no. 6, pp. 619–28, Feb. 2009.
- [44] K. Ohnishi, R. F. Weir, and T. A. Kuiken, “Neural machine interfaces for controlling multifunctional powered upper-limb prostheses.” *Expert Review of Medical Devices*, vol. 4, no. 1, pp. 43–53, Jan. 2007.
- [45] A. Abbott, “Neuroprosthetics: in search of the sixth sense,” *Nature*, vol. 442, no. 7099, pp. 125–127, Jul. 2006.
- [46] A. B. Schwartz, X. T. Cui, D. J. Weber, and D. W. Moran, “Brain-controlled interfaces: movement restoration with neural prosthetics,” *Neuron*, vol. 52, no. 1, pp. 205–220, Oct. 2006.

- [47] M. Zafar and C. L. Van Doren, “Effectiveness of supplemental grasp-force feedback in the presence of vision.” *Medical & Biological Engineering & Computing*, vol. 38, no. 3, pp. 267–74, May 2000.
- [48] D. Damian, A. Arita, H. Martinez, and R. Pfeifer, “Slip speed feedback for grip force control.” *IEEE Transactions on Biomedical Engineering*, vol. 59, no. 8, pp. 2200–10, Aug. 2012.
- [49] A. Chatterjee, V. Aggarwal, A. Ramos, S. Acharya, and N. V. Thakor, “A brain-computer interface with vibrotactile biofeedback for haptic information.” *Journal of Neuroengineering and Rehabilitation*, vol. 4, p. 40, Jan. 2007.
- [50] C. Antfolk, C. Cipriani, M. C. Carrozza, C. Balkenius, A. Björkman, G. Lundborg, B. Rosén, and F. Sebelius, “Transfer of tactile input from an artificial hand to the forearm: experiments in amputees and able-bodied volunteers.” *Disability and Rehabilitation: Assistive Technology*, vol. 8, no. 3, pp. 249–54, May 2013.
- [51] R. B. Gillespie, J. L. Contreras-Vidal, P. A. Shewokis, M. K. O’Malley, J. D. Brown, H. Agashe, R. Gentili, and A. Davis, “Toward improved sensorimotor integration and learning using upper-limb prosthetic devices,” in *Engineering in Medicine and Biology Society (EMBC), 2010 Annual International Conference of the IEEE*. IEEE, Sep. 2010, pp. 5077–5080.
- [52] P. J. Kyberd, N. Mustapha, F. Carnegie, and P. H. Chappell, “A clinical experience with a hierarchically controlled myoelectric hand prosthesis with vibro-tactile feedback,” *Prosthetics and Orthotics International*, vol. 17, no. 1, pp. 56–64, Apr. 1993.
- [53] A.-S. Augurelle, A. M. Smith, T. Lejeune, and J.-L. Thonnard, “Importance of cutaneous feedback in maintaining a secure grip during manipulation of hand-held objects.” *Journal of Neurophysiology*, vol. 89, no. 2, pp. 665–71, Feb. 2003.
- [54] D. A. Nowak, S. Glasauer, and J. Hermsdorfer, “How predictive is grip force control in the complete absence of somatosensory feedback?” *Brain*, vol. 127, no. Pt 1, pp. 182–92, Jan. 2004.
- [55] D. A. Nowak and J. Hermsdörfer, “Predictive and reactive control of grasping forces: on the role of the basal ganglia and sensory feedback.” *Experimental Brain Research*, vol. 173, no. 4, pp. 650–60, Sep. 2006.
- [56] J. D. Brown, R. B. Gillespie, D. Gardner, and E. a. Gansallo, “Co-location of force and action improves identification of force-displacement features,” *2012 IEEE Haptics Symposium*, pp. 187–193, Mar. 2012.
- [57] J. Draper, W. Moore, J. Herndon, and B. Weil, “Effects of force reflection on servomanipulator task performance,” in *International Topical Meeting on Remote Systems and Robotics in Hostile Environments*, 1986.

- [58] B. Hannaford and L. Wood, "Performance Evaluation of a Six-Axis Generalized Force-Reflecting Teleoperator," *IEEE Transactions on Systems, Man, and Cybernetics*, vol. 21, no. 3, pp. 620–633, 1991.
- [59] J. G. Wildenbeest, D. A. Abbink, C. J. Heemskerk, F. C. van der Helm, and H. Boessenkool, "The Impact of Haptic Feedback Quality on the Performance of Teleoperated Assembly Tasks," *IEEE Transactions on Haptics*, vol. 6, no. 2, pp. 242–252, Apr. 2013.
- [60] R. Christiansen, J. L. Contreras-Vidal, R. B. Gillespie, P. A. Shewokis, and M. K. O'Malley, "Vibrotactile feedback of pose error enhances myoelectric control of a prosthetic hand," in *2013 IEEE World Haptics Conference*. IEEE, Apr. 2013, pp. 531–536.
- [61] R. Baayen, D. Davidson, and D. Bates, "Mixed-effects modeling with crossed random effects for subjects and items," *Journal of Memory and Language*, vol. 59, no. 4, pp. 390–412, 2008.
- [62] S. Kachman, "An introduction to generalized linear mixed models," in *Proceedings of a symposium at the organizational meeting for a NCR coordinating committee on Implementation Strategies for National Beef Cattle Evaluation*, Athens, 2000, pp. 59–73.
- [63] P. Jenmalm and R. S. Johansson, "Visual and Somatosensory Information about Object Shape Control Manipulative Fingertip Forces," *The Journal of Neuroscience*, vol. 17, no. 11, pp. 4486–4499, Jun. 1997.
- [64] R. S. Johansson and J. R. Flanagan, "Coding and use of tactile signals from the fingertips in object manipulation tasks." *Nature Reviews: Neuroscience*, vol. 10, no. 5, pp. 345–59, May 2009.
- [65] R. Johansson and K. Cole, "Sensory-motor coordination during grasping and manipulative actions," *Current Opinion in Neurobiology*, vol. 2, no. 6, pp. 815–823, 1992.
- [66] R. Johansson and G. Westling, "Programmed and triggered actions to rapid load changes during precision grip," *Experimental Brain Research*, vol. 71, no. 1, pp. 72–86, 1988.
- [67] I. Salimi and I. Hollender, "Specificity of Internal Representations Underlying Grasping," *Journal of Neurophysiology*, vol. 84, pp. 2390–2397, 2000.
- [68] D. Wolpert and J. Flanagan, "Motor prediction," *Current Biology*, vol. 11, no. 18, pp. 729–732, 2001.
- [69] D. Katz, *The World of Touch*. Psychology Press, 1989.
- [70] J. J. Gibson, "Observations on active touch." *Psychological Review*, vol. 69, no. 6, pp. 477–91, Nov. 1962.

- [71] M. Auvray and S. Hanne-ton, “There is something out there: distal attribution in sensory substitution, twenty years later,” *Journal of Integrative Neuroscience*, vol. 4, no. 4, pp. 505–521, 2005.
- [72] R. LaMotte, “Softness discrimination with a tool,” *Journal of Neurophysiology*, vol. 83, pp. 1777–1786, 2000.
- [73] S. J. Lederman and R. L. Klatzky, “Haptic identification of common objects: effects of constraining the manual exploration process.” *Perception & Psychophysics*, vol. 66, no. 4, pp. 618–28, May 2004.
- [74] T. Debus, T.-j. Jang, P. Dupont, and R. Howe, “Multi-Channel Vibrotactile Display for Teleoperated Assembly,” *International Journal of Control, Automation, and Systems*, vol. 2, no. 3, pp. 390–397, 2004.
- [75] K. Bark and J. Wheeler, “Comparison of skin stretch and vibrotactile stimulation for feedback of proprioceptive information,” in *2008 IEEE Symposium on Haptic Interfaces for Virtual Environment and Teleoperator Systems*. IEEE, Mar. 2008, pp. 71–78.
- [76] Z. F. Quek, S. B. Schorr, I. Nisky, W. R. Provancher, and A. M. Okamura, “Sensory substitution using 3-degree-of-freedom tangential and normal skin deformation feedback,” in *2014 IEEE Haptics Symposium*. Ieee, Feb. 2014, pp. 27–33.
- [77] L. A. Jones, S. Member, and H. Z. Tan, “Application of Psychophysical Techniques to Haptic Research,” *IEEE Transactions on Haptics*, vol. 6, no. 3, pp. 268–284, 2013.
- [78] S. Eppinger and W. Seering, “Three Dynamic Problems in Robot Force Control,” in *1989 IEEE International Conference on Robotics and Automation*, 1989, pp. 392–397.
- [79] S. Cholewiak, H. Tan, and D. Ebert, “Haptic identification of stiffness and force magnitude,” in *2008 IEEE Symposium on Haptic Interfaces for Virtual Environment and Teleoperator Systems*, vol. 83, 2008, pp. 87 – 91.
- [80] L. A. Jones, J. Kunkel, and E. Piatieski, “Vibrotactile pattern recognition on the arm and back,” *Perception*, vol. 38, no. 1, pp. 52–68, 2009.
- [81] H. Yao and V. Hayward, “An experiment on length perception with a virtual rolling stone,” in *2006 Proceedings of Eurohaptics*, 2006, pp. 325–330.
- [82] J. Romano and K. Kuchenbecker, “Creating realistic virtual textures from contact acceleration data,” *IEEE Transactions on Haptics*, vol. 5, no. 2, pp. 109–119, 2012.
- [83] R. C. Goertz, “Fundamentals of general purpose remote manipulators,” *Nucleonics*, vol. 10, no. 11, pp. 36–42, 1952.

- [84] R. C. Goertz and W. M. Thompson, “Electronically controlled manipulator,” *Nucleonics*, vol. 12, no. 11, pp. 46–47, 1954.
- [85] G. Niemeyer, C. Preusche, and G. Hirzinger, “Telerobotics,” in *Springer Handbook of Robotics*, B. Siciliano and O. Khatib, Eds. Springer Berlin Heidelberg, 2008, ch. 31, pp. 741–757.
- [86] A. B. Ajiboye and R. F. F. Weir, “A heuristic fuzzy logic approach to EMG pattern recognition for multifunctional prosthesis control.” *IEEE Transactions on Neural Systems and Rehabilitation Engineering*, vol. 13, no. 3, pp. 280–91, Sep. 2005.
- [87] K. Drewing, A. Ramisch, and F. Bayer, “Haptic, visual and visuo-haptic softness judgments for objects with deformable surfaces,” in *Third Joint Eurohaptics Conference and Symposium on Haptic Interfaces for Virtual Environment and Teleoperator Systems*, 2009, pp. 640 – 645.